

Optimizing reaction and transport fluxes in temperature gradient-driven chemical reaction-diffusion systems

Mohammed Loukili

Institut de Recherche de l'École Navale, EA 3634, IRENav, Brest, France

Ludovic Jullien

*CPCV, Département de chimie, École normale supérieure, PSL University,
Sorbonne Université, CNRS, 24, rue Lhomond, 75005 Paris, France*

Guillaume Baffou

Institut Fresnel, CNRS, Aix Marseille University, Centrale Med, 13013 Marseille, France

Raphaël Plasson*

Avignon University, INRAE, UMR408 SQPOV, 84000 Avignon, France

(Dated: February 25, 2025)

Temperature gradients represent energy sources that can be harvested to generate steady reaction or transport fluxes. Technological developments could lead to the transfer of free energy from heat sources and sinks to chemical systems for the purpose of extraction, thermal batteries, or nonequilibrium synthesis.

We present a theoretical study of 1D chemical systems subjected to temperature gradients, for sustaining nonequilibrium chemical fluxes. A complete theoretical framework describes the behavior of the system induced by various temperature profiles. An exact mathematical derivation was established for a simple two-compartment model and was generalized to arbitrary reaction-diffusion systems based on numerical models. An experimental system was eventually scaled and tuned to optimize either nonequilibrium chemical transport or reaction.

The relevant parameters for this description were identified; they focused on the system symmetry for chemical reaction and transport. Nonequilibrium thermodynamic approaches lead to a description analogous to electric circuits. Temperature gradients lead to the onset of a steady chemical force, which maintains steady reaction-diffusion fluxes moderated by chemical resistance. The system activity was then assessed using the entropy production rate as a measure of its dissipated power.

The chemical characteristics of the system can be tuned for general optimization of the nonequilibrium state or for the specific optimization of either transport or reaction processes. The shape of the temperature gradient can be tailored to precisely control the spatial localization of active processes, targeting either precise spatial localization or propagation over large areas. The resulting temperature-driven chemical system can in turn be used to drive secondary processes into either nonequilibrium reaction fluxes or concentration gradients.

Keywords: Free energy transduction, coupled reactions, reaction-diffusion, steady state, temperature gradient, thermodynamics of nonequilibrium, chemical fluxes, entropy rate.

I. INTRODUCTION

The logic of preparative chemistry is in sharp contrast with the one of biochemical systems. The former focuses primarily on multistep synthesis, with the objective of producing pure compounds in optimal yield through individually optimized reactions. In living cells, the reactions are also grouped in sets. However, they occur in cycles, like the Krebs and Calvin cycles, where reactants and products are not distinguished from each other, but simultaneously coexist in non-equilibrium steady states. Hence, although sharing a same common canon of reactivity, a cell operates differently than a chemical reactor seeking maximal yields. What advantages does this mode of operation afford?

Thermodynamics fixes the final composition in which a reactive system reaches equilibrium under chemical and physical constraints. In practice, it governs the realization of multiple chemical reactions of academic and industrial

interest, as well as the elementary steps of most separation processes, such as distillation or chromatography. In contrast, kinetics drives the trajectory of the evolution of a reactive system. It also governs the dynamic behavior of the latter when sustained in an nonequilibrium steady state, which can exhibit much richer phenomena (e.g. oscillations, waves, patterns, and chaos) than in the equilibrium state. In particular, such nonequilibrium steady states are encountered in living biological matter, where they control its dynamics [1, 2] and lead to the propagation of a sustained energy flux throughout metabolism by exploiting free energy transduction [3–5].

The dynamic behavior of the nonequilibrium steady states is theoretically understood [6–8]. In contrast, the issue of steadily sustaining an nonequilibrium reactive state has received much less attention and remains a major challenge [9]. In practice, its realization requires either introducing constraints to prevent the effective relaxation of the reactive processes towards equilibrium [10–12], or steadily applying a periodic excitation on the reactive system. [13] We previously demonstrated the relevance of the first approach by frustrating the relaxation

* raphael.plasson@univ-avignon.fr

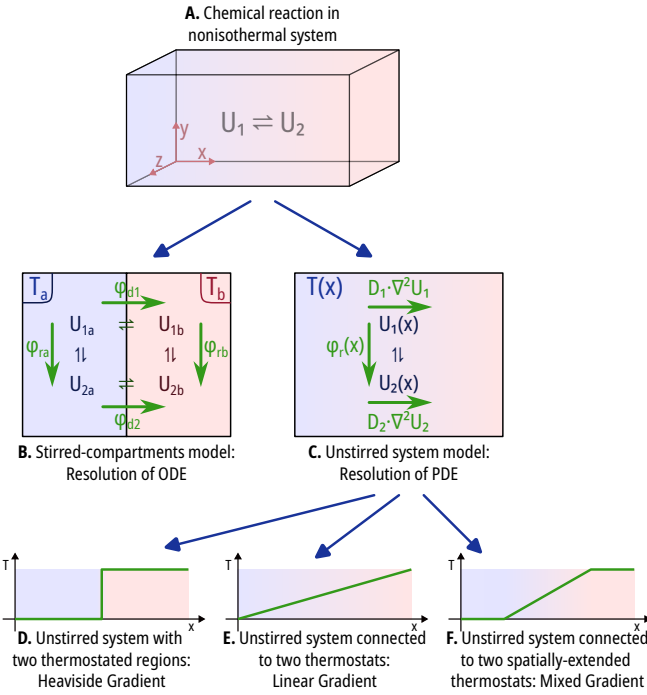


FIG. 1. Description of the chemical system. **A**, general representation; **B**, two-compartment model; **C**, unstirred model; **D-F**, applied temperature gradient profiles.

of reactive processes by the interference of molecular motion [14, 15], a strategy to generate reaction-diffusion cycles that are thought to establish spatial gradients of signaling activities in living cells [16, 17]. However, the efficiency of this first approach has not been theoretically analyzed, and is the object of the present manuscript.

In our previous work [14, 15], we used light as an energy source to maintain a reactive system in a nonequilibrium state. In the present study, we favored a more general approach and adopted the application of a temperature gradient. Despite its chemical relevance, the behavior of reactive media in contact with two thermostats at different temperatures has included glorious names (including Nernst [18], Dirac [19], Prigogine [20, 21]). Several papers have been published since then, but have been mainly concerned with the gas phase and the question of how a chemical reaction that occurs in a system modifies its thermal conductivity [22–30]. Recently, heat flow has been applied to generate proton gradients and pH oscillations in microscale aqueous solutions [31, 32]. In the latter works, the reactive system was often assumed to be at chemical equilibrium within the temperature gradient.

In this paper, we level off this assumption, which has been predicted to generate attractive behavior such as dissipation-driven selection of states in nonequilibrium chemical networks [33], or emergent thermophoretic behavior in chemical reaction systems [34]. We investigate the behavior of an active chemical system submitted to a nonequilibrium force, induced by an externally imposed temperature gradient. The primary objective is to determine the optimal characteristics and conditions that will lead to maximizing an internal nonequilibrium reaction-diffusion flux within the system. This consists in a simple chemical reaction subjected to an inhomogeneous field

of temperature. The associated temperature gradient directly generates a large entropy production by heat diffusion; the aim is to redirect a maximal part of this source of nonequilibrium to chemical processes.

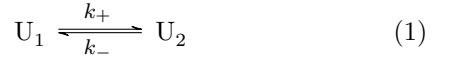
In this context, the temperature gradient-induced steady chemical force and the resulting steady chemical flux must both be maximized, with the ultimate objective of maximizing the entropy rate produced specifically by this internally sustained cyclic process. This objective was further refined by recognizing that the focus might entail optimizing either the transport process or the reaction process on their own, or balancing both processes. To achieve this optimization, we benefited from a fruitful analogy between entropy production by a chemical reaction and the ohm dissipated power by electrical resistors.

We then identified the conditions for the spatial localization or delocalization of nonequilibrium activity, emphasizing the important role of the system scaling and of the shape of the temperature gradient. Finally, we assessed the possibility of propagating this primary energy transfer from the heat sources and sinks to secondary athermic reaction or transport processes.

II. RESULTS AND DISCUSSION

A. Chemical model

The studied chemical system was reduced to experiencing a single isomerization reaction



where the rate constants k_+ and k_- are linked to the thermodynamic constant K with

$$K = \frac{k_+}{k_-} \quad (2)$$

This represents a generic reaction, in its simplest form. It can be easily extended to more complex mechanisms, as detailed further, namely for the description of second-order reactions or more complex mechanisms.

This chemical reaction was driven in a steady nonequilibrium state by an imposed temperature gradient (see Fig. 1). We studied different configurations embodied by various temperature profiles associated with different experimental setups, leading to the study of theoretical models with increasing complexities.

Using thermodynamic and Arrhenius relationships, the variation in the constants with temperature can be expressed as:

$$K = K^\infty e^{-\frac{\Delta_r H_0}{RT}} \quad (3a)$$

$$k_+ = k_+^\infty e^{-\frac{E_{a,+}}{RT}} \quad (3b)$$

$$k_- = k_-^\infty e^{-\frac{E_{a,-}}{RT}} \quad (3c)$$

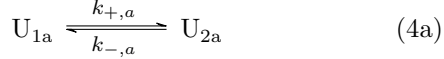
with

$$\Delta_r H_0 = E_{a,+} - E_{a,-} \quad (3d)$$

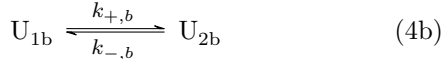
B. Chemical response to a temperature gradient between two homogeneous compartments

The general behavior of a reaction driven by temperature gradients was first characterized in the limits of two compartments, each of which was homogeneous in temperature and concentration. This corresponds to two stirred systems; each compartment A/B is connected to the other by chemical exchange with the reaction rate constant $k_{d,i}$ for each compound of concentration c_i :

Compartment A :



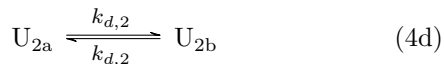
Compartment B :



Diffusion of U_1 :



Diffusion of U_2 :



1. Parameters

Identifying the relevant parameters for the description of the system is a critical step. We focused on describing the system in general terms by assessing the global symmetry or asymmetry of the parameters, as this leads to a description of the system behavior in the simplest mathematical terms.

The general properties of the system are described based on its characteristic dimensions: concentration c_0 (corresponding to the total concentration), temperature T_0 (corresponding to the median system temperature) and time t_0 . All subsequent system parameters were nondimensionalized using these characteristic parameters (see Table I). This leads to:

$$K = K_0 e^{\frac{\Delta_r H_0}{RT_0} \left(\frac{T-T_0}{T} \right)} \quad (5a)$$

$$k_+ = k_{+,0} e^{\frac{E_{a,+}}{RT_0} \left(\frac{T-T_0}{T} \right)} \quad (5b)$$

$$k_- = k_{-,0} e^{\frac{E_{a,-}}{RT_0} \left(\frac{T-T_0}{T} \right)} \quad (5c)$$

with $K_0 = K(T_0)$, $k_{+,0} = k_+(T_0)$, $k_{-,0} = k_-(T_0)$.

This is then nondimensionalized as:

$$\bar{k}_+ = \kappa \rho e^{\beta(1-\gamma) \frac{\theta}{\theta+1}} \quad (6a)$$

$$\bar{k}_- = \kappa^{-1} \rho e^{\beta(1+\gamma) \frac{\theta}{\theta+1}} \quad (6b)$$

$$K = \kappa^2 e^{2\beta\gamma \frac{\theta}{\theta+1}} \quad (6c)$$

$$\eta = 2\beta\gamma \quad (6d)$$

$$\varepsilon_+ = \beta(1-\gamma) \quad (6e)$$

$$\varepsilon_- = \beta(1+\gamma) \quad (6f)$$

The diffusion is modeled as a first-order exchange reaction between two compartments as a function of the geometric mean of the exchange kinetic constant δ :

$$\delta_1 = \lambda\delta \quad (7a)$$

$$\delta_2 = \lambda^{-1}\delta \quad (7b)$$

The system can then be reduced to a set of ordinary differential equations with a set of nondimensionalized parameters:

$$\frac{du_{1a}}{d\bar{t}} = \lambda^{-1}\delta(-u_{1a} + u_{1b}) - \bar{k}_{+,a}u_{1a} + \bar{k}_{-,a}u_{2a} \quad (8a)$$

$$= -\varphi_{d1} - \varphi_{ra} \quad (8b)$$

$$\frac{du_{1b}}{d\bar{t}} = \lambda^{-1}\delta(u_{1a} - u_{1b}) - \bar{k}_{+,b}u_{1b} + \bar{k}_{-,b}u_{2b} \quad (8c)$$

$$= +\varphi_{d1} - \varphi_{rb} \quad (8d)$$

$$\frac{du_{2a}}{d\bar{t}} = \lambda\delta(-u_{2a} + u_{2b}) + \bar{k}_{+,a}u_{1a} - \bar{k}_{-,a}u_{2a} \quad (8e)$$

$$= -\varphi_{d2} + \varphi_{ra} \quad (8f)$$

$$\frac{du_{2b}}{d\bar{t}} = \lambda\delta(u_{2a} - u_{2b}) + \bar{k}_{+,b}u_{1b} - \bar{k}_{-,b}u_{2b} \quad (8g)$$

$$= +\varphi_{d2} + \varphi_{rb} \quad (8h)$$

The system is thus described in the nondimensionalized concentrations $u_{i,j}$ of compound i in compartment j , relative temperature deviation θ , and time \bar{t} . Each compartment is thermostated at temperature $\theta_a = -\theta_g$ and $\theta_b = +\theta_g$, with $\theta_g \in [0, 1]$; the limit cases correspond, respectively, to a uniform temperature T_0 and a temperature gradient from 0 K to $2T_0$; the median temperature is T_0 in all situations. The initial concentration is 1 in each compartment, i.e.:

$$u_{1a}(0) + u_{2a}(0) = u_{1b}(0) + u_{2b}(0) = 1 \quad (9)$$

Analytical solutions for the resulting steady state were obtained. A second-order Taylor development as a function of the temperature gradient θ_g leads to simpler but more informative solutions (see Appendix C for details).

The resulting system behavior in the steady state was then characterized in terms of three dimensionless parameters: chemical force α , chemical flux φ , and entropic production σ , which can be expressed as:

$$\sigma = \alpha\varphi \quad (10)$$

2. Parameter description

The chemical reaction characteristics can be described using the following parameters:

- ρ is the geometric mean of the nondimensionalized kinetic constants at $\theta = 0$ (i.e. T_0), which reports the global reaction rate,
- κ is the square root of the thermodynamic constant at T_0 , which reports the reaction asymmetry between the forward and backward reactions, with $\kappa = 1$ for $u_1 = u_2$ at equilibrium at T_0 ,
- β is the arithmetic mean of activation energies, which reports the average activation energy,

	Description	Dimensionalized Unit	Nondimensionalized
Characteristic dimensions	Concentration	c_i	$u_i = c_i/c_0$
	Length	x	$\bar{x} = x/l_0$
	Temperature	T	$\theta = (T - T_0)/T_0$
	Diffusion constant	D_i	$d_i = D_i/D_0$
	Time	t	$\bar{t} = t/t_0$ (with $t_0 = l_0^2/D_0$)
Chemical characteristics	Reaction rate constant	k_{\pm}	$\bar{k}_{\pm} = k_{\pm}t_0$
	Exchange rate constant	$k_{d,i}$	$\delta_i = k_{d,i}t_0$
	Activation energy	$E_{a,\pm}$	$\varepsilon_{\pm} = E_{a,\pm}/RT_0$
	Reaction enthalpy	$\Delta_r H_0$	$\eta = \Delta_r H_0/RT_0$
Primary parameters	Equilibrium constant		$\kappa = \sqrt{\bar{k}_{+,0}/\bar{k}_{-,0}}$
	Exchange ratio		$\lambda = \sqrt{\delta_2/\delta_1} = \sqrt{d_2/d_1}$
	Mean kinetic rate		$\rho = \sqrt{\bar{k}_{+,0}\bar{k}_{-,0}}$
	Mean exchange rate		$\delta = \sqrt{\delta_1\delta_2}$
	Mean diffusion constant		$d = \sqrt{d_1d_2}$
	Average activation energy		$\beta = (\varepsilon_+ + \varepsilon_-)/2$
	Energy profile asymmetry		$\gamma = (\varepsilon_+ - \varepsilon_-)/(\varepsilon_+ + \varepsilon_-)$
Secondary parameters	Gradient intensity		$\theta_g : \theta \in [-\theta_g, +\theta_g]$
	Reaction asymmetry		$\kappa' = 2\kappa/(1 + \kappa^2)$
Steady state characteristics	Exchange asymmetry		$\lambda' = 2\kappa\lambda/(1 + \kappa^2\lambda^2)$
	Chemical force	\mathcal{A}/T	$\alpha = \mathcal{A}/RT = \ln K/Q$
	Chemical flux	ϕ	$\varphi = \phi t_0/c_0$
	Diffusion flux	J_i	$j_i = d_i \partial u_i / \partial \bar{x}$
	Rate of entropy production	\dot{S}	$\sigma = \dot{S} t_0 / R c_0$

TABLE I. Dimensionalized and nondimensionalized parameters, classified as characteristic dimensions, chemical characteristics, primary parameters (control parameters for the description of a given system), secondary parameters (used for the simplification of the final equations), and steady state characteristics (describing the resulting steady dynamic properties of the system). $R = 8.314 \text{ J.mol}^{-1}.\text{K}^{-1}$.

- γ , which reports the asymmetry of the activation energy profile (see Fig. S3 in SI for a graphical representation).

Similarly, the characteristics of the chemical exchanges can be described in terms of:

- δ is the geometric mean of the exchange rate constants, which reports the global exchange rate between the two compartments,
- λ is the squared root of the exchange rate constant, which reports the asymmetry between the exchange rate of the two compounds (see Eqs. (7)).
- κ and λ can be combined into two secondary parameters κ' and λ' , leading to simpler mathematical representations. They represent the reaction and exchange asymmetry, respectively, with a maximal value of 1 for a perfectly symmetric process and 0 for a process totally displaced in a given direction.

3. Establishment of a nonequilibrium steady state

The difference in temperature implies a difference in the equilibrium constant in each compartment. Thus, a temperature gradient necessarily leads to a frustrated state, which is characterized by the impossibility of simultaneously reaching chemical equilibrium in each compartment (which would imply that each compound coexists at different concentrations in both compartments) and the

transport equilibrium between each compartment (which would imply identical concentrations for each compound in both compartments).

This results in a nonequilibrium state, whose distance from equilibrium can be quantified by the chemical force α , as the sum of the chemical forces of each chemical reaction in each compartment and the chemical forces of each chemical exchange between the two compartments. It can then be expressed for low values of θ_g (see Eqs. (C8)-(C9)) as:

$$\alpha = 2\eta\theta_g \quad (11)$$

In all cases, a steady chemical force is thus sustained by the temperature gradient. It is proportional to the intensity of the gradient θ_g and the enthalpy of the reaction η and does not depend on the other parameters.

In response to this non-zero chemical force, a circular reaction-diffusion flux is established. Chemical reaction fluxes are processed in opposite directions in each compartment, compensated by the continuous exchange of each compound in the opposite direction (see Fig. 2A). By analogy to electric circuits, α can be interpreted as the potential difference and φ as the intensity. These are expressed as (see Eqs. (C17) and (C20)):

$$\varphi = \frac{\alpha}{R_{\text{tot}}} \quad (12)$$

In the case of the linear regime, characterized by low

values of θ_g , this chemical resistance can be expressed as:

$$R_{\text{tot}} = \frac{4}{\kappa'} \left(\frac{1}{\rho} + \frac{1}{\lambda' \delta} \right) \quad (13)$$

It is decomposed as the sum of two terms: the first one is directly linked to the chemical reaction (term in $1/\rho$), and the second one to the chemical exchanges (term in $1/\lambda' \delta$). Outside the linear regime, for large values of θ_g , this chemical resistance will not be constant and may depend on the chemical force.

4. Process Distribution

This steady nonequilibrium reaction-diffusion flux leads to a continuous dissipative process characterized by σ , as an analog of electric power dissipation [35] according to Eq. (10). The corresponding chemical entropy production taps on the important thermal entropy production by heat diffusion generated by the temperature gradient (Fig. 2B and appendix B). The energy extracted from the temperature gradient is dissipated differently in each process (see Fig. 2C), and can be decomposed as a sum of terms specific to each process, according to each chemical resistance as (see Eqs. (C4)-(C6)):

$$\sigma = \sum_i \sigma_i = \sum_i R_i \varphi^2 \quad (14)$$

$$R_{\text{tot}} = \sum_i R_i \quad (15)$$

a. Reactions and exchanges The full entropy production σ is first dispatched between the reaction term σ_r and the exchange term σ_d :

$$\sigma_r = \frac{\lambda' \delta}{\lambda' \delta + \rho} \sigma \quad ; \quad \sigma_d = \frac{\rho}{\lambda' \delta + \rho} \sigma \quad (16)$$

with

$$R_r = \frac{4}{\kappa' \rho} \quad ; \quad R_d = \frac{4}{\kappa' \lambda' \delta} \quad (17)$$

and

$$\sigma = \frac{\lambda' \delta \rho}{\lambda' \delta + \rho} \kappa' \cdot \eta^2 \theta_g^2 \quad (18)$$

Two limit regimes are observed:

- If $\lambda' \delta \gg \rho$, then $\sigma \approx \sigma_r$; this is the case for a fast exchange system. Both compartments are in equilibrium with each other, and most of the dissipative process is directed to the chemical reactions within each compartment.
- If $\lambda' \delta \ll \rho$, then $\sigma \approx \sigma_d$; this is the case for a fast-reaction system. Chemical equilibrium is observed in each separate compartment, and most of the dissipative process is directed to the chemical exchanges between compartments.

In the intermediate regime $\rho \sim \lambda' \delta$, both the chemical reaction and the transport are actively processed.

b. Reaction balance between the compartments The reaction entropy production is decomposed in each compartment as:

$$\sigma_{ra} = \frac{1 + \varepsilon \theta_g}{2} \sigma_r \quad (19)$$

$$\sigma_{rb} = \frac{1 - \varepsilon \theta_g}{2} \sigma_r \quad (20)$$

The parameter ε (see Eqs. (C13)) comes down to an apparent activation energy for the full system, varying from ε_+ to ε_- through the average β value, depending on the global symmetry of the system: it tends to β when $\kappa \lambda \sim 1$, to $\beta(1 - \gamma) = \varepsilon_+$ when $\kappa \lambda \gg 1$, and to $\beta(1 + \gamma) = \varepsilon_-$ when $\kappa \lambda \ll 1$.

Qualitative changes are observed as functions of $\varepsilon \theta_g$. When $\varepsilon \theta_g \ll 1$, the dissipation due to the chemical reaction is equally shared between both compartments as $\sigma_{ra} \approx \sigma_{rb}$. This dissipation is asymmetric for higher values of $\varepsilon \theta_g$, increasing the dissipation in the colder compartment and reducing it by the same value in the warmer compartment.

This asymmetry originates from the slowing of the chemical reaction in the cold compartment. The chemical flux φ is necessarily of the same intensity in each compartment to guarantee a steady state; this implies an increase in the chemical force α in the cold compartment due to a less efficient chemical relaxation toward equilibrium and its decrease in the warm compartment owing to a more efficient relaxation. Consequently, the more dissipative compartment is necessarily the colder.

c. Exchange balance between compartments The exchange entropy production can be decomposed by the exchange of each compound as:

$$\sigma_{d1} = \frac{\lambda^2 \kappa^2}{1 + \lambda^2 \kappa^2} \sigma_d \quad (21)$$

$$\sigma_{d2} = \frac{1}{1 + \lambda^2 \kappa^2} \sigma_d \quad (22)$$

It is symmetrically distributed between the two compounds when $\lambda \kappa = 1$. The asymmetrization of this exchange is quantified by $\lambda \kappa$, with a $\sigma_d \approx \sigma_{d1}$ for $\lambda \kappa \gg 1$ (the exchange entropy production is then governed by U_1), and with a $\sigma_d \approx \sigma_{d2}$ for $\lambda \kappa \ll 1$ (the exchange entropy production is then governed by U_2).

5. Optimal conditions

Considering that the temperature gradient is fixed and cannot be optimized, several criteria can be used to evaluate the efficiency of the system to generate a steady nonequilibrium reaction-diffusion process. The chemical force α reflects how far the system is pushed away from the equilibrium state ($\alpha = 0$ corresponding to the equilibrium state). The chemical flux φ quantifies the system response as the intensity of the resulting reaction-diffusion flux from the chemical force, as the quantity of matter that is converted at each moment in each compartment, and the quantity of matter that is transferred at each moment from one compartment to another ($\varphi = 0$ corresponding to a static, kinetically locked

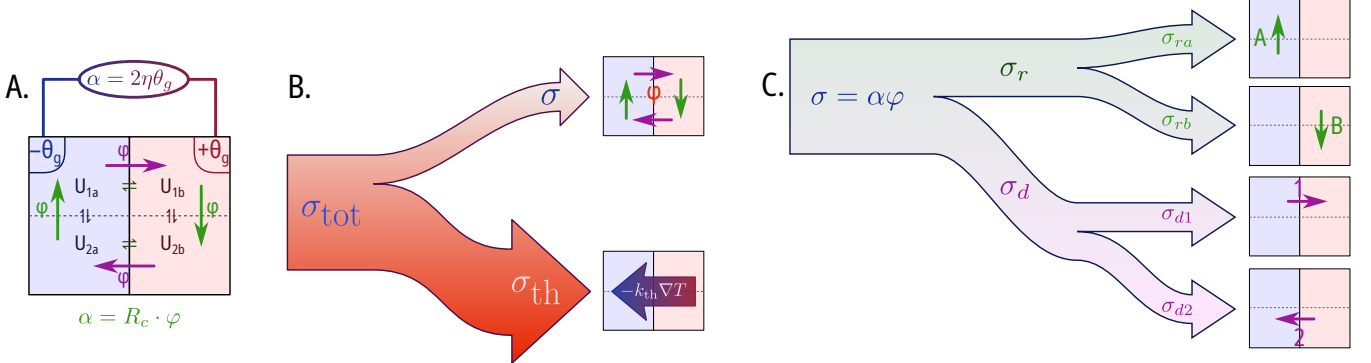


FIG. 2. Establishment of a nonequilibrium steady reaction-diffusion cycle driven by a temperature gradient. Cyclic flux φ in response to nonzero chemical force α (**A**); full entropy production σ_{tot} as a sum of thermal (σ_{th} , see appendix B) and chemical (σ) contributions (**B**); distribution of the entropy production in each chemical reaction or exchange process (**C**).

system). The rate of entropy production σ combines both thermodynamic and kinetic aspects, and quantifies the nonequilibrium activity of the system.

At first, according to Eq. (11), the chemical force α is simply proportional to both θ_g and η ; this entails that the temperature gradient shall be applied to a high-enthalpy chemical reaction as a first requirement from driving the system in a non-equilibrium state.

Secondly, from Eqs. (12)-(13), maximizing the steady nonequilibrium flux $\varphi = \alpha/R_{\text{tot}}$ implies the minimization of its chemical resistance R_{tot} . This implies:

- to maximize parameter κ' ; its largest possible value is $\kappa' = 1$, corresponding to a chemical reaction perfectly balanced between the backward and forward reactions at T_0 (i.e. $K_0 = 1$),
- to maximize parameter λ' to 1, corresponding to symmetric matter exchange (see Eqs. (21)-(22)); this implies that an imbalance in the chemical equilibrium at T_0 (characterized by κ) can be compensated for by an imbalance in the chemical exchange of each compound (characterized by λ'),
- to maximize both the global chemical rate ρ and the chemical exchange rate δ , thus minimizing the chemical resistance of each process.

Overall, this implies that each process should be fast and symmetrical at mean temperature T_0 . The corresponding simultaneous optimization of α and ρ implies the maximization of the entropy production σ (Eq. (18)), which represents the part of entropy production generated by the targeted chemical reaction-diffusion process. In practice, this represents only a fraction of the thermal entropy production (see Appendix B).

Moreover, it is possible to focus on a specific process to be optimized, i.e. either the reaction or the transport process, via the σ_r or the σ_d values. The optimization of the reaction process via σ_r (see Eqs. (C22) and Fig. S1 in the SI) implies that:

- for a given value of $\lambda'\delta$, a maximal σ_r value is obtained for $\rho = \lambda'\delta$,

- for a given value of ρ , high values of $\lambda'\delta$ are required; however, increasing $\lambda'\delta$ to much higher values than ρ is useless, as σ_r reaches a plateau.

A similar reasoning can be used to optimize the transport process via σ_d (see Eqs. (C23)):

- for a given value of ρ , a maximal σ_d value is obtained for $\lambda'\delta = \rho$,
- for a given value of $\lambda'\delta$, high values of ρ are required; however, increasing ρ to much higher values than $\lambda'\delta$ is useless, as σ_d reaches a plateau.

Consequently, general optimization involves maximizing θ_g , η , λ' , and κ' . Furthermore, $\lambda'\delta$ should be of the same order of magnitude as ρ , with $\lambda'\delta > \rho$ to sustain chemical reactions, $\lambda'\delta < \rho$ for sustaining chemical transport, and $\lambda'\delta \simeq \rho$ for sustaining reaction-diffusion cycles.

C. Spatial localization of chemical processes

1. Model description

The spatial extension of the system was considered by introducing the chemical diffusion of all compounds. We limited our study to closed one-dimensional systems. A stationary temperature gradient $\theta(\bar{x})$ was imposed over the entire system. This corresponds to an unstirred system, with free internal diffusion of chemical compounds, without matter exchange with the surroundings. The system was described using a set of partial differential equations (see Eqs. (D1)), which was numerically solved for a wide range of parameters, with a focus on determining its steady state (see Appendix A). The characteristic parameter l_0 must be introduced to account for the spatial extension, describing a one dimensional system:

$$\bar{x} = \frac{x}{l_0} \in [0, 1] \quad (23)$$

Chemical diffusion is described based on the diffusion parameter d_i for each compound U_i , which is nondimensionalized by the characteristic parameter D_0 corresponding to the average diffusion constant of the

chemical reactants. Consistently with the description of the chemical exchange kinetics of the previous model, chemical diffusion is described as a function of the geometric mean of the diffusion constant d and the exchange ratio λ :

$$d_1 = \lambda d \quad (24a)$$

$$d_2 = \lambda^{-1} d \quad (24b)$$

In each point of the system, the reaction processes is still characterized as (see Eq. (D2a)):

$$\sigma_r = \varphi_r \cdot \alpha_r \quad (25)$$

where the chemical flux φ_r and force α_r are defined as in the two compartment system (Eqs. (C1a)-(C1b)), on each point of the system.

The transport process of compound i is now expressed as [36, 37] (see Eq. (D2a)):

$$\sigma_d = j_i \cdot \alpha_d \quad (26a)$$

$$\text{with } j_i = d_i \left(\frac{\partial u_i}{\partial \bar{x}} \right) \quad (26b)$$

$$\text{and } \alpha_{d,i} = \frac{1}{u_i} \left(\frac{\partial u_i}{\partial \bar{x}} \right) \quad (26c)$$

j_i is the transport flux of compound i , and $\alpha_{d,i}$ the corresponding transport force.

The characteristic time t_0 is additionally fixed by l_0 and D_0 (see Table. I). All parameters corresponding to chemical reactions are defined as in the stirred compartment model; however, they are now functions of position \bar{x} .

Taking into account both the reaction and diffusion parameters, each chemical system can be additionally characterized by its nondimensionalized reaction-diffusion length w defined as:

$$w = \sqrt{\frac{\lambda' d}{2\rho}} \quad (27)$$

w represents the scale at which both reaction and diffusion processes operate at similar rates.

For simplicity, and to clearly identify and quantify the specific role of a temperature gradient on the generation of reaction diffusion fluxes, we made the following assumptions:

- We neglected the influence of temperature on the diffusion coefficient. Several simulations were performed, indicating that considering the variability of d_i with θ did not qualitatively change the system behavior; this essentially led to an increase in the asymmetry between the cold and warm regions (see Fig. S2 in SI).
- The Soret effect was neglected, which is expected to be satisfactory for systems based on small molecular reactants [38]. However, emergent thermophoretic behaviors that originate from the coupling of chemical reactions and temperature gradients [34, 36] may occur within the framework of this model, and were specifically studied.

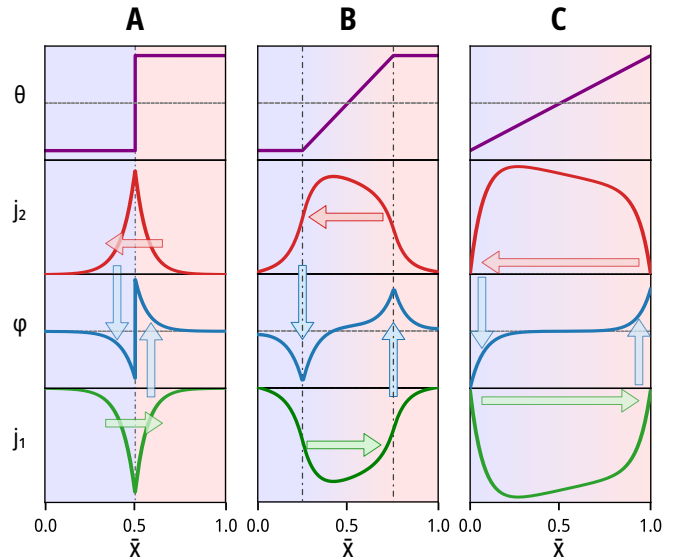


FIG. 3. Schematic representation of the steady reaction-diffusion cycle in unsteady systems driven by Heaviside (A), mixed (B) and linear (C) temperature profiles. The horizontal wide arrows represent the direction of U_1 and U_2 diffusion and the vertical wide arrows represent the global reaction fluxes $U_1 \rightarrow U_2$ (up arrows) and $U_2 \rightarrow U_1$ (down arrows). The diffusion and reaction processes are processed in the same area for the Heaviside profile, close to the cold/warm interface (A). In contrast, they are physically separated with the chemical reaction occurring at the linear gradient boundaries, and the chemical diffusion taking place between these two points (B,C). Model parameters: $\kappa = 1$, $\lambda = 1$, $\gamma = 0.2$, $d = 1$, $\beta = 1$, $\theta_g = 10^{-1}$, and $\rho = 10^2$.

- Convection was not considered in this study. This assumption is anticipated to be satisfactory for sufficiently small systems in the direction of gravity or sufficiently highly viscous systems, so that the major transport mode is processed by molecular diffusion. This condition is compatible with a large system in which the temperature gradient is applied on the horizontal x axis, as long as the vertical spatial extension is sufficiently small (e.g., for horizontal capillary systems).
- The endothermic or exothermic effects of the chemical reactions were neglected. This case is relevant to chemical systems connected to sufficiently efficient heat sources and sinks to reliably fix temperature profiles.

2. Steady state flux profiles

a. System with two homogeneously thermostated regions The first temperature gradient is defined as a Heaviside profile, defined by $\theta = -\theta_g$ for $\bar{x} \in [0, 0.5]$ and $\theta = +\theta_g$ for $\bar{x} \in [0.5, 1]$. This corresponds to a system in which two contiguous spatial regions are maintained by an external thermostat at two different homogeneous temperatures $-\theta_g$ and $+\theta_g$, while free chemical diffusion can occur throughout the chemical system.

In the spatial region that is sufficiently close to the $\bar{x} = 0.5$ cold / warm boundary—that is, at a scale smaller

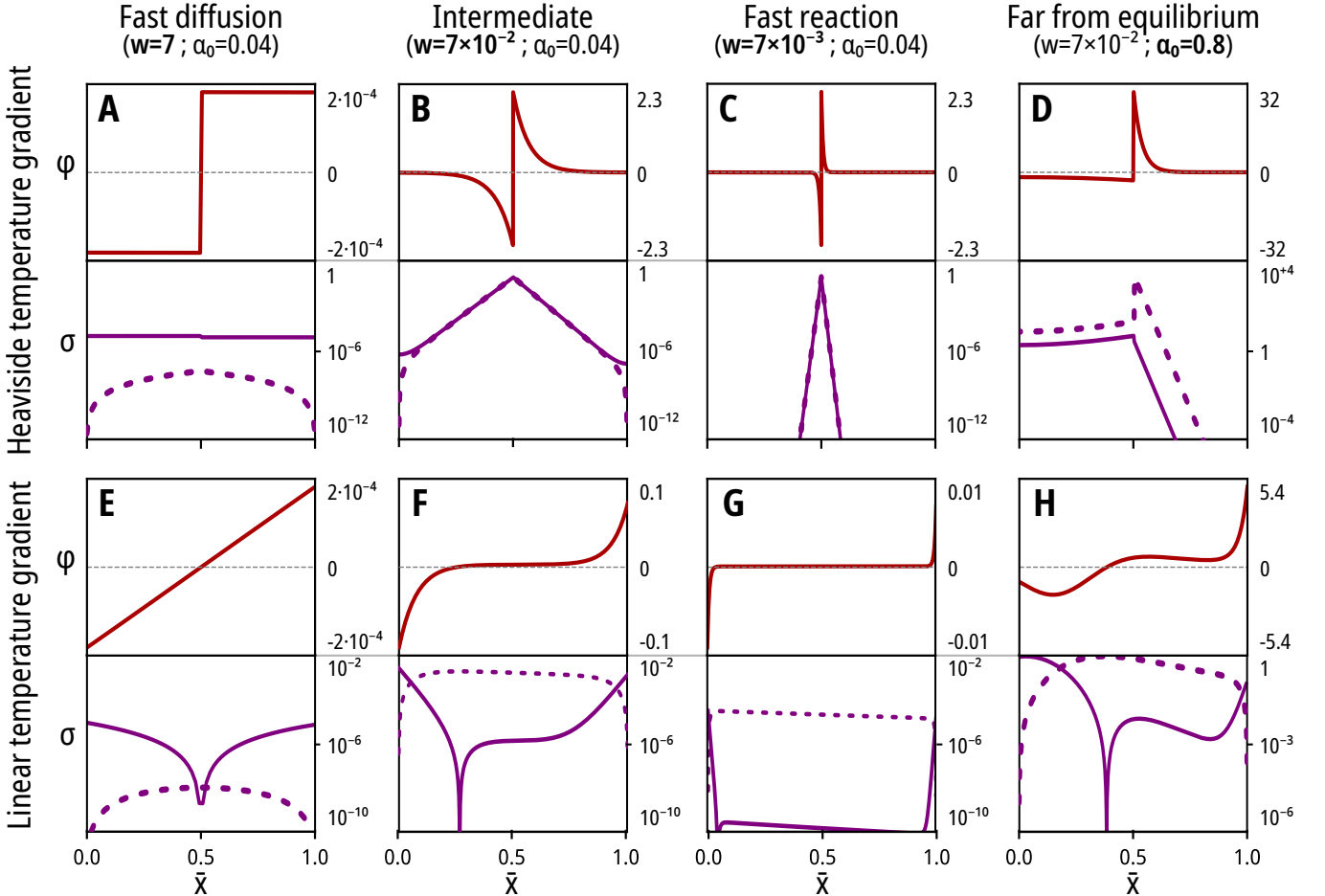


FIG. 4. Steady state spatial profiles of chemical flux of reaction φ (red) and entropy production (solid purple, σ_r and dotted purple, σ_d) as a function of the reaction-diffusion length w as defined in Eq. (27), and the characteristic chemical force α_0 as defined in Eq. (30a). Model parameters: $\kappa = 1$, $\lambda = 1$, and $\gamma = 0.2$; $d = 1$, $\rho = 10^{-2}$ ($w = 7$, fast diffusion: A, E), $d = 1$, $\rho = 10^2$ ($w = 0.07$, intermediate: B, D, F, H) and $d = 10^{-2}$, $\rho = 10^2$ ($w = 0.007$, fast reaction: C, G); $\beta = 1$, $\theta_g = 10^{-1}$ ($\alpha_0 = 0.04$, linear regime: A-C, E-G) and $\beta = 4$, $\theta_g = 0.5$ ($\alpha_0 = 0.8$, far from equilibrium: D, H).

than the reaction-diffusion length w —chemical diffusion is much faster than chemical reactions. The concentrations are consequently essentially constant on each side of the temperature boundary; the system is then equivalent to the “two compartments” model in the vicinity of the boundary. The values of the flux φ and force α determined for the two-compartment model correspond to the values observed at the boundaries $x = 0.5^+$ and $x = 0.5^-$.

When $w > 0.5$, the reaction-diffusion length is larger than the sizes of the cold and warm regions $\bar{x} \in [0, 0.5]$ and $\bar{x} \in [0.5, 1]$. Both are homogeneous; the full system is then equivalent to the stirred-compartment model. This system is characterized by fast diffusion throughout the system, whereas the chemical reaction flux and dissipation are evenly distributed throughout the entire system (see Fig. 4A).

When $w < 0.5$, an exponential decrease is observed in the values of φ and α , from their boundary values at $\bar{x} = 0.5$ to $x = 0$ or $x = 1$, with a half-length equal to w . If $w \ll 1$, the activity of the system is restricted to a short region close to the boundary, most of the system being in equilibrium and characterized by $\varphi \approx 0$, $\alpha \approx 0$, $\sigma \approx 0$ (see Fig. 4C).

In both cases, a reaction-diffusion cycle is established, with chemical reaction and diffusion occurring simultaneously in the same spatial region, at the system boundary (see Fig. 3A, more details are available in Fig. S4).

The spatial extension of chemical activity in each region becomes asymmetric when the intensity of the temperature gradient is sufficiently high. This can be described by considering the difference in the kinetic rate in each region based on Eq. (6a)-(6b), as:

$$\rho_{\text{cold}} = \rho e^{-\beta \frac{\theta_g}{1-\theta_g}} \quad \text{for } \bar{x} \in [0, 0.5] \quad (28)$$

$$\rho_{\text{warm}} = \rho e^{\beta \frac{\theta_g}{1+\theta_g}} \quad \text{for } \bar{x} \in [0.5, 1] \quad (29)$$

Thus, the half-length of each exponential relaxation is different in each region; it is equal to the corrected value $w_i = \sqrt{\lambda' d / 2\rho_i}$. Consequently, chemical fluxes spread to a greater extent in the cold zone than in the warm zone.

When $\beta\theta_g > 1$, the system becomes highly nonlinear, with a large behavioral asymmetry between each region. Typically, situations with $w_{\text{cold}} > 1$ and $w_{\text{warm}} \ll 1$ can be obtained, with a homogeneous system in the cold zone and restricted to a short region in the warm zone (see Fig. 4D).

b. System connected to two thermostats at its extremities An imposed linear temperature profile corresponds to a chemical system in contact with two external thermostats at its extremities, fixing the temperatures $-\theta_g$ and $+\theta_g$ at each boundary $\bar{x} = 0$ and $\bar{x} = 1$. Similarly as in the previous model, two limit regimes are observed, but with distinctive differences:

- Fast-diffusion systems (i.e. $w \gg 1$, see Fig. 4E) are characterized by a linear chemical flux profile. The system is more active at each extremity of the system, and cancels close to $\bar{x} = 1/2$, and the entropy production is dominated by the chemical reaction.
- In fast reaction systems (i.e. $w \ll 1$, see Fig. 4G), the central inactive region becomes much larger. The chemical reaction flux and entropy production by the chemical reaction is restricted at each extremity of the system, in a region of length w_{cold} at $\bar{x} \approx 0$ and w_{warm} at $\bar{x} \approx 1$. In turn, the entropy production is dominated by the diffusion, and the chemical transport spreads, linking these two extremities see Fig. 3C.

This general behavior implies a spatial separation *de facto* of the different chemical processes. Three regions can be identified: cold and warm regions at each extremity, of half-lengths equal to w_{cold} and w_{warm} , separated by a central region of length approximately equal to $1 - 2w$. The cold and warm regions are dominated by chemical reactions ($\sigma \approx \sigma_r$), and the central region is dominated by chemical transport ($\sigma \approx \sigma_d$). Thus, a spatially extended reaction-diffusion cycle is set in motion; the compounds are transported across the entire system between each chemically active region, the central transport region shrinking with w (see Fig. 4E-G, and Fig. S5 for more details). This is in sharp contrast with the Heaviside gradient, where both chemical reactions and transport are effective at the same spatial locations, close to the temperature boundary (see Fig. 4A-C).

Finally, the high asymmetrization of the profile induced by high $\beta\theta_g$ values leads to nontrivial and complex flux profiles (see Fig. 4H). The central region around $\bar{x} = 1/2$ is characterized by a non-negligible positive flux, corresponding to a low-activity extension of the warm region. Consequently, the spatial position of the zero flux is localized at $\bar{x} < 1/2$; the cold region of the negative flux shrinks and the warm region of the positive flux stretches.

c. System connected to two spatially extended thermostats A last temperature gradient was defined as a mix between a linear and a Heaviside gradient. This is defined as $\theta = -\theta_g$ for $\bar{x} < \bar{x}_1 = 1/4$, $\theta = +\theta_g$ for $\bar{x} > \bar{x}_2 = 3/4$, and a linear variation of θ from $-\theta_g$ to $+\theta_g$ for $\bar{x} \in [1/4, 3/4]$. This comes down to a system in contact with two spatially extended external thermostats.

The behaviors of both the linear and Heaviside profiles can be recognized (see Fig. 3B, and Fig. S6 for more details). The reaction-diffusion cycles are now in motion, with two chemical reaction zones located at \bar{x}_1 and \bar{x}_2 , connected by an active chemical transport region across $\bar{x} \in [\bar{x}_1, \bar{x}_2]$.

It appears that controlling the precise shape of an imposed temperature gradient enables precise control of

	Heaviside		Linear		Mixed	
	$w \ll 1$	$w \gg 1$	$w \ll 1$	$w \gg 1$	$w \ll 1$	$w \gg 1$
φ_{\max}/φ_0	1	1	$2w$	1	$3w/2$	1
$\varphi_{\text{int}}/\varphi_0$	w	$1/2$	$2w^2$	$1/4$	$4w^2$	$3/8$
α_{\max}/α_0	1	1	$2w$	1	$4w/3$	1
$\alpha_{\text{int}}/\alpha_0$	w	$1/2$	$2w^2$	$1/4$	$4w^2$	$3/8$
$\sigma_{r,\max}/\sigma_0$	1	1	$4w^2$	1	$4w^2$	1
$\sigma_{r,\text{int}}/\sigma_0$	w	1	$4w^3$	$1/3$	$8w^3$	$2/3$
$\sigma_{d,\max}/\sigma_0$	1	$1/2w^2$	$4w^2$	$1/15w^2$	$20w^2$	$2/15w^2$
$\sigma_{d,\text{int}}/\sigma_0$	w	$1/12w^2$	$4w^2$	$1/30w^2$	$8w^2$	$1/15w^2$
$\sigma_{t,\max}/\sigma_0$	2	1	$4w^2$	1	$20w^2$	1
$\sigma_{t,\text{int}}/\sigma_0$	$2w$	1	$4w^2$	$1/3$	$8w^2$	$2/3$
y_r	$1/2$	1	w	1	w	1
y_d	$1/2$	$1/12w^2$	1	$1/10w^2$	1	$1/10w^2$

TABLE II. First order values for φ , α and σ for low values of $\beta\theta$, as identified from numerical models (see Fig. S4-S6 in SI). The max index correspond to maximal values located at the cold/warm interface at $\bar{x} = 1/2$ for the Heaviside profile, at the system extremities $\bar{x} = 0$ and $\bar{x} = 1$ for the linear profile, and the inflection point of the temperature profile at $\bar{x} = 1/4$ and $\bar{x} = 3/4$. The integral values correspond to the integration of the corresponding variable on the full system $\bar{x} \in [0, 1]$ for the σ variables, or on the region restricted to the positive values of φ and α (i.e. $\bar{x} \in [\bar{x}_0, 1]$, where $\varphi > 0$ or $\alpha > 0$ for $x > \bar{x}_0$).

the shape of the induced reaction-diffusion cycle. Steady dissipative chemical reactions can be localized in regions characterized by temperature inflection points (i.e., high values of $\partial^2 T / \partial x^2$), whereas chemical transport can be sustained between these active regions along temperature gradients (i.e., following high values of $\partial T / \partial x$).

3. Steady state characteristics

The steady state can be described by a set of parameters α , φ , σ_r , σ_d and $\sigma_t = \sigma_r + \sigma_d$. Their maximal value assesses the optimal activity in a specific location, and their integral value assesses the optimal activity of the system as a whole (see the appendix D 2).

The values of the steady chemical flux φ , chemical force α and entropy production σ can be expressed as functions of the following characteristic values:

$$\alpha_0 = 2\beta\gamma\theta_g \quad (30a)$$

$$\varphi_0 = \kappa'\beta\gamma\theta_g\rho \quad (30b)$$

$$\sigma_0 = 2\kappa'\beta^2\gamma^2\theta_g^2\rho \quad (30c)$$

These characteristic values are related with each other as:

$$\alpha_0 = \frac{2}{\kappa'\rho}\varphi_0 \quad (31)$$

$$\sigma_0 = \alpha_0\varphi_0 \quad (32)$$

In the limit cases $w \ll 1$ and $w \gg 1$, and when the system is close to equilibrium (i.e. $\beta\theta_g < 1$), the ratio of each variable to its reference value is only dependent

on the reaction-diffusion length w as defined in Eq. (27). The corresponding values are summarized in Table II (see Fig. S7 in SI for a graphical representation).

The situation $w \gg 1$ (that is, small systems) is essentially independent of scale. This implies that, as long as the dimension of the system is smaller than the length of the reaction-diffusion, the steady-state behavior is essentially described by the characteristic values of Eqs. (30), modulated by a constant factor that depends on the shape of the temperature gradient profile. Diffusion entropy production is the only varying parameter; it is proportional to w^{-2} , and thus is essentially negligible for small systems. This situation is the optimal case for extracting energy from the temperature gradient (by maximizing σ_t , as well as driving nonequilibrium chemical reaction (by maximizing both σ_r and y_r).

When $w \ll 1$ (that is, large systems), the system is effective only on a small fraction of the full spatial extension, except for transport. This implies that all steady-state parameters are proportional to w^n , with $n \in [1, 3]$, except for σ_d , which remains constant. This is an optimal situation for transporting chemical compounds over large distances.

The intermediate case $w \sim 1$ is characterized by the maximal value of σ_r , that is, by optimal nonequilibrium transport. In this regime, the chemical reaction is also important, with a production of entropy equally shared in both processes for $w = 1$. This situation is thus optimal for observing nonequilibrium cycles of reaction-diffusion, as both diffusion and reaction can be simultaneously efficient.

This behavior is also influenced by the symmetry of the system defined by the parameters λ and κ . Optimal nonequilibrium reaction fluxes are obtained for symmetrical systems characterized by $\kappa = 1$ when $w > 1$ (Fig. 5A), and $\kappa = 1$ and $\lambda = 1$ when $w < 1$ (Fig. 5C and E). As observed by Liang *et al* [34], an asymmetry in the diffusion coefficient, characterized by $\lambda \neq 1$, can lead to so-called “emergent thermophoretic effect”, implying that the coupling of the chemical reaction to the temperature gradient can lead to concentrating the reactants in either the colder or the warmer region.

This effect is inefficient in small systems (Fig. 5B). Thus, a sufficiently large system is required (Fig. 5D and F) such that the dissipative processes are dominated by chemical transports. This process is especially efficient for values of $\lambda \neq 1$, and needs to be driven away from the equilibrium by high intensity gradients (Fig. 5F). Optimal κ values are also observed, with $\kappa > 1$ values associated with $\lambda < 1$ (and consequently $\kappa < 1$ values associated with $\lambda > 1$ values).

4. System scaling

a. Critical parameters From a general perspective, the efficiency of the system to be driven far from the equilibrium state is directly linked to the maximization of β , γ , θ_g and ρ . This trivially implies that the best chemical reaction candidates are characterized by high activation energies, high reaction enthalpies, and high reaction rates and should be placed in high-temperature

gradients.

More importantly, the results specifically emphasize the necessity of adapting the spatial scale of the chemical setup to the characteristic scale of the reaction-diffusion system. The temperature gradient should also be chosen carefully, so that the system is as symmetric as possible at the mean temperature, in terms of chemical diffusion (that is, $D_1(T_0) \approx D_2(T_0)$) and balance between the reactants (i.e. $K(T_0) \approx 1$).

The reaction-diffusion length w can be redimensionalized to the critical spatial dimension \mathcal{L}_0 as:

$$\mathcal{L}_0 = \sqrt{\frac{D_1 D_2}{k_{+,0} D_2 + k_{-,0} D_1}} \quad (33)$$

If $D_1 = D_2 = D_0$ and $k_{+,0} = k_{-,0} = k_0$ (i.e. $\lambda = \kappa = 1$), this expression comes down to:

$$\mathcal{L}_0 = \sqrt{\frac{D_0}{2k_0}} \quad (34)$$

The system spatial dimension l_0 should be adjusted accordingly. Nonequilibrium chemical reactions fluxes are obtained for $l_0 < \mathcal{L}_0$, nonequilibrium chemical transport over large distances for $l_0 > \mathcal{L}_0$, and nonequilibrium reaction-diffusion cycle for $l_0 \sim \mathcal{L}_0$,

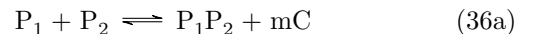
The second critical factor is the temperature gradient imposed on the system. T_0 indicates the critical temperature variation above which nonlinear far-from-equilibrium effects are observed:

$$T_0 = \frac{2RT_0^2}{E_{a,+} + E_{a,-}} \quad (35)$$

Symmetrical cold/warm behaviors will be obtained for $\Delta T \ll T_0$, and an asymmetry with increased activity in the cold region for $\Delta T > T_0$.

Finally, the shape of the temperature gradient can be tailored to control the localization of chemical activities. Typically, the chemical reaction will be concentrated in the spatial areas characterized by large local variation of the temperature gradient slope (i.e. large values of $\nabla^2 T$) on space scale smaller than \mathcal{L}_0 . In contrast, chemical transport is established across temperature gradients (i.e. following ∇T).

b. Example of peptide exchange reaction Reversible peptide exchange reaction mediated by N-methylcysteine is a good candidate for being driven by temperature gradients [39]. It possesses high activation energies, and its equilibrium constant is $K = 1$ close to the ambient temperature; its thermokinetic characteristics were experimentally obtained [40]:



$$E_a^+ = 55 \times 10^3 \text{ J.mol}^{-1} \quad (36b)$$

$$E_a^- = 43 \times 10^3 \text{ J.mol}^{-1} \quad (36c)$$

$$\Delta_r H_0 = 12 \times 10^3 \text{ J.mol}^{-1} \quad (36d)$$

$$k_0^+ = k_0^- = 1.4 \times 10^{-3} \text{ M}^{-1} \cdot \text{s}^{-1} \quad (36e)$$

$$\text{at } T_0 = 314 \text{ K} \quad (36f)$$

The setup conditions for efficiently sustaining nonequilibrium chemical reaction fluxes for this reaction—leading

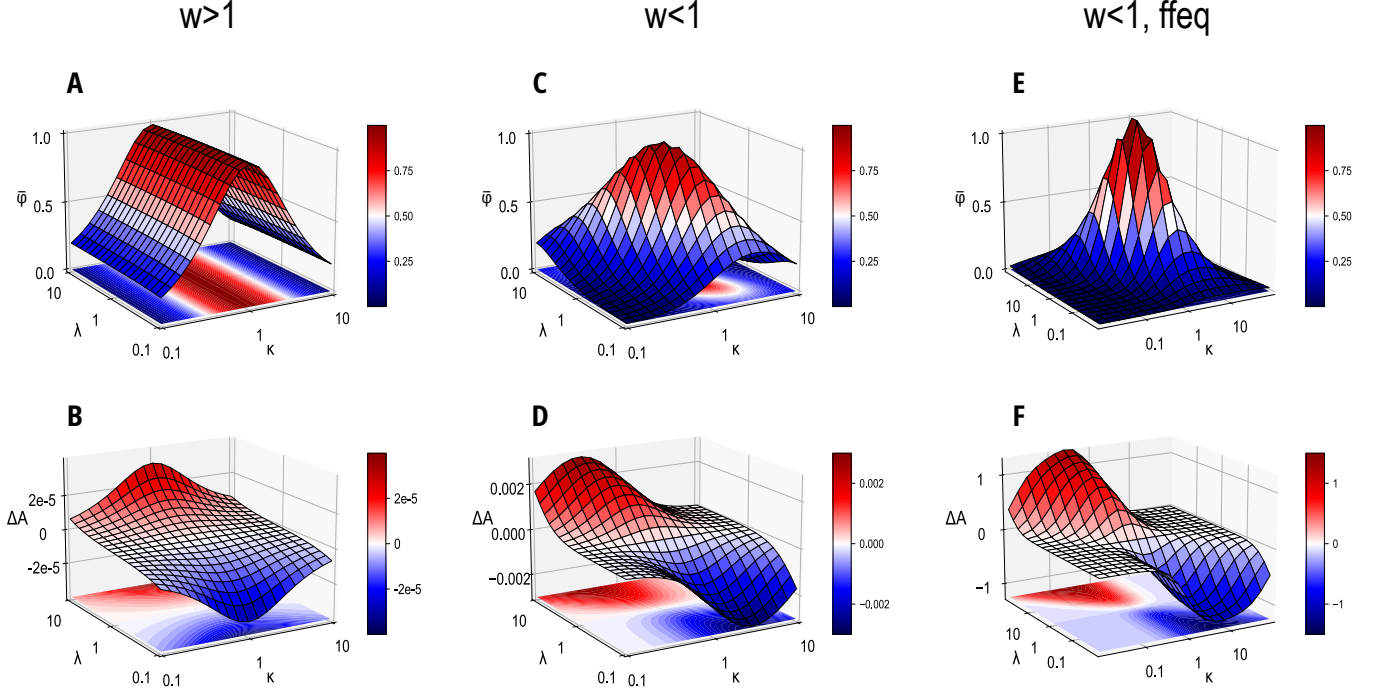


FIG. 5. Influence of the system asymmetry λ and κ on the steady normalized flux $\bar{\varphi} = \varphi_{\text{int}}/\varphi_{\text{int},0}$ (**A,C,E**) and the steady maximal difference of concentration across the system ΔA (**B,D,F**), with $\varphi_{\text{int},0}$ the integral flux value observed in the same conditions, except for $\kappa = \lambda = 1$. For all models, a linear temperature gradient was applied, with common model parameters $\gamma = 0.2$, $d = 1$, $\kappa \in [0.1; 10]$, $\lambda \in [0.1; 10]$. Additional parameters: $\theta_g = 0.01$, $\beta = 1$, $\rho = 0.01$ (**A-B**), $\theta_g = 0.01$, $\beta = 1$, $\rho = 100$ (**C-D**), and $\theta_g = 0.04$, $\beta = 4$, $\rho = 100$ (**E-F**).

to steady fluxes of polymerization-depolymerization—can be directly determined from these characteristics.

This is a second-order reaction. An apparent first-order constant (that depends on the global reactant concentrations) can be evaluated from k_0^+ to $k_{0,\text{app}} = 1.4 \times 10^{-6} \text{ s}^{-1}$ assuming a concentration $c_0 = 10^{-3} \text{ M}$. The diffusion coefficients of short oligopeptides [41, 42] are approximately equal to $D_0 = 5 \times 10^{-10} \text{ m}^2 \cdot \text{s}^{-1}$, and will be assumed that they are identical (that is, $\lambda = 1$). Under such conditions, the critical parameters of this reaction-diffusion system are $\mathcal{L}_0 = 1.3 \text{ cm}$ and $T_0 = 17^\circ\text{C}$.

We consider three systems of characteristic lengths $l_0 = 10^{-2} \text{ m}$, $l_1 = 3 \times 10^{-2} \text{ m}$ (i.e. $\sim 2\mathcal{L}_0$) and $l_2 = 10^{-1} \text{ m}$, each of which is subject to a Heaviside temperature gradient $T \in [9^\circ\text{C}, 71^\circ\text{C}]$. This scaling corresponds to a nondimensionalized system with $\beta = 18.8$, $\gamma = 0.122$, $\theta_g = 0.1$, $d = 1$, $\kappa = 1$, $\lambda = 1$, and respectively $\rho = 0.28$, $\rho = 2.5$, and $\rho = 28$ for l_0 , l_1 and l_2 . These systems are characterized by the following characteristic lengths:

- $l_0 = 1 \text{ cm}$: $w_{\text{cold}} = 3.8$, $w_{\text{warm}} = 0.57$. Both lengths are larger than the length of each cold/warm region; this corresponds to a small system in which the activity is fully extended to the entire system, dominated by dissipative reactions and small concentration gradients. Setups below this scale thus correspond to regimes for performing simultaneously a steady polymerization process in the warmer region, and a steady depolymerization process in the colder region.
- $l_2 = 10 \text{ cm}$: $w_{\text{cold}} = 0.38$, $w_{\text{warm}} = 0.057$. Both lengths are smaller than the length of each

cold/warm region; this corresponds to a large system where the activity is restricted in the region close to the $\bar{x} = 0.5$ boundary, dominated by dissipative transport and large concentration gradients. Setups above this scale thus correspond to regimes for transporting peptides across the system, the chemical reaction being locally at equilibrium.

- $l_1 = 3 \text{ cm}$: $w_{\text{cold}} = 1.27$, $w_{\text{warm}} = 0.19$. This corresponds to an intermediate system in which the activity is fully extended in the cold region and restricted in the region close to the warm boundary, dominated by a dissipative reaction-diffusion cycle across both regions.

The numerical models of these three systems confirm this scaling analysis (see Fig. S8 in SI).

From this analysis, the optimal setup conditions for sustaining steady polymerization/depolymerization process can thus be identified from the thermodynamic and kinetic characteristics of the system. The chemical system must be subjected to a temperature gradient centered on $T_0 = 314 \text{ K}$ (temperature for which $K = 1$). Setting this gradient from 297 K to 331 K will drive the system in a nonlinear far-non-equilibrium state (as $T = T_0 \pm \mathcal{T}_0$). Enforcing this gradient over a system length of $l_0 = 1 \text{ cm}$ (as $l_0 < \mathcal{L}_0$) will then ensure to sustain continuous depolymerization-polymerization cycles.

D. Coupling to a secondary reaction

Thus, energy can be directly extracted from a temperature gradient using these reaction-diffusion systems. We

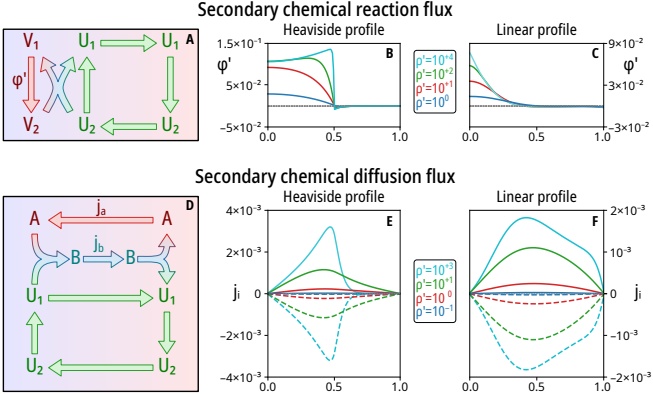


FIG. 6. Coupling to secondary processes. Model parameters: $\kappa = 1$, $\lambda = 1$, $\gamma = 0.2$, $d = 1$, $\beta = 4$, $\theta_g = 0.5$, $\rho = 10^2$, $u' = 0.1$, and **B,C**: $\rho' \in [10^0, 10^4]$, $\rho_0 = 10^{-3}$; **E, F**: $\rho' \in [10^{-1}, 10^3]$

further extended the minimalist network in Eq. (1) by adding additional chemical reactions. The purpose is to investigate the ability of the resulting chemical reaction network to efficiently perform free energy transduction [3, 14, 15, 43] from the temperature gradient to athermal reactions, mediated by the previously studied U₁/U₂-based reaction-diffusion cycle.

1. Maintaining a secondary chemical reaction flux

The U₁/U₂ reaction-diffusion cycle can be used to drive an athermal reaction in a steady reaction flux. In that purpose, an additional set of reactions involving a V₁/V₂ interconversion was introduced:



A direct uncoupled reaction (37a) is first introduced; it is assumed to be slow compared to the driving reaction (1), with a nondimensionalized reaction rate constant fixed at 10⁻³. It can be driven by a coupled reaction (37b), whose reaction rate constant is equal to the kinetic rates of the driving reaction (1), multiplied by a factor ρ'. Moreover, it is supposed to be athermal so that any steady nonequilibrium state would result from a transfer from the U₁/U₂ couple.

Numerical models (see Fig. 6A-C) show that the V₁/V₂ couple can be efficiently driven to an active nonequilibrium state with respect to reaction (37a), which is characterized by a sustained chemical flux ϕ'. A necessary condition is $\rho' \gg 1$, implying that the secondary driven reaction in Eq. (37b) must be faster than the primary driving reaction in Eq. (1). Furthermore, the total concentration of the compounds V_i must be lower than that of U₁, to avoid perturbation of the primary reaction.

2. Maintaining a secondary chemical diffusion flux

The U₁/U₂ reaction-diffusion cycle can also be used to drive the active transport of an additional compound A

throughout the system. This was performed by adding the following reaction for the initial system:



This reaction is assumed to be athermal, with a nondimensionalized kinetic rate ρ' in both directions, which does not depend on temperature. This implies that the compound A can be bound to U₁ as a complex B, then diffuses from the cold to the warm region, where it is released back as A; then it can diffuse back to the cold region.

Once again (see Fig. 6D-F), large gradients can be obtained as long as the coupling reaction (38) is faster than the driving reaction (1). Transport is also essentially efficient for lower concentrations of A compounds than for U₁/U₂ compounds.

III. CONCLUSIONS

A general model was established to describe how an nonequilibrium steady reaction-diffusion process can be sustained by a temperature gradient. A difference in temperature across the system induces spatial differences in the chemical equilibrium states. This results in a frustrated state because it is impossible to simultaneously sustain the chemical equilibrium (which would induce a concentration gradient) and the global transport equilibrium (which would imply homogeneous concentrations). Consequently, reaction-diffusion cycles are necessarily established, with chemical reactions counterbalancing chemical transports, as long as a temperature gradient is coupled to an endothermic or exothermic chemical process. We determined the parameters that enable the system to be dominated at will by either transport or reaction. Moreover, we demonstrated that the temperature gradient shape can be tuned so that both the reaction and transport processes can be spatially disconnected from each other or concentrated in the same spatial area.

We showed that this nonequilibrium steady state can be characterized in terms of:

- chemical force, describing the local distance from equilibrium. This essentially originates from the reaction enthalpy and the intensity of the temperature gradient.
- chemical flux, describing the resulting steady reaction rate. It is proportional to the chemical force, but additionally depends on the reaction rate constants and diffusion constants, as well as the system symmetry at the mean temperature.
- entropy production rate, which describes the dissipative efficiency. This results from the combination of chemical force and flux.

These characteristics can be understood as analogous to the electromotive force, current intensity, and dissipated power in an electric circuit, respectively. This yields a fruitful quantitative description of the nonequilibrium state. The expression of these characteristics was established analytically in the simple case of two homogeneous

compartments that exchange matter. This result was then extended to interpret the complete reaction-diffusion systems that were solved numerically.

From the model established in this work, it is possible to identify the best experimental conditions (i.e in terms of the values of the minimal, mean and maximal temperatures, the shape of the temperature gradient, and the system dimension) for sustaining efficiently a given a chemical system in a nonequilibrium steady state (characterized by a maximal values of entropy production by the targeted chemical process). Moreover, the entropy produced by the reaction-diffusion system is distributed unequally among each process. A net difference can be observed between the diffusion-dominated and reaction-dominated systems. The desired regime can be tailored by scaling the system to a critical system length \mathcal{L}_0 . It should be noted that the traditional “local equilibrium” approximation reduces to the limit case of fast reactions, that is, to large systems whose physical length is well above \mathcal{L}_0 . This regime is suboptimal for generating nonequilibrium reaction fluxes; it is the worst case for extracting chemical energy from the temperature gradient, as it leads to minimization of the chemical flux.

This framework also demonstrates the possibility of concentrating the chemical reactants in either the cold or warm region under the effect of the temperature gradient. This global effect is only effective in large systems compared to the critical length \mathcal{L}_0 , when the reactants possess sufficiently different diffusion coefficients, with large temperature gradients centered on an optimal temperature.

This study is based on an imposed steady temperature gradient. However, steady chemical reaction fluxes can act as secondary heat sources that can influence back the temperature gradient from which they originate. Having a steady temperature gradient comes down to the assumption of the presence of infinitely efficient external heat sources that can seamlessly absorb this chemical heat. Further work should describe the full coupling between the external and internal heat sources in these reaction-diffusion systems, to evaluate their impact. In addition, we should be able to explain how optimal reaction-mediated heat transport [24], leading to an increase in thermal conductivity [30], can be obtained.

ACKNOWLEDGMENTS

This work was supported by the ANR grant ”Sacerdotal” (ANR-19-CE6-0010-02). The authors thank Alois Würger for the fruitful discussions on thermophoresis. The authors thank Nicolas Giuseppone, Nicolas Capit, and Émilie Moulin for discussions on peptide exchange reactions.

DATA AVAILABILITY STATEMENT

Additional information, as referred to in the main text, is available in a supplementary PDF file. Simulation files (XMDS files, raw simulation data, and processed data results) are available upon request.

Appendix A: Numerical tools

Four geometries of increasing complexity were used:

1. Two homogeneous stirred compartments, each thermostated at a different temperature, were connected to each other, allowing chemical exchange between them.
2. A single unstirred system was connected to two thermostats, each of which maintained a homogeneous temperature in two contiguous regions, with free chemical diffusion throughout the compartment.
3. A single unstirred system was connected to two thermostats, each of which maintained a fixed temperature at each extremity of the system, leading to a steady linear gradient throughout the system, with free chemical diffusion throughout the compartment.
4. A single unstirred system was connected to two spatially extended thermostats, each of which maintained a fixed temperature at each extremity over a length $1/4$, leading to a steady linear gradient over the central part of the system $\bar{x} \in [1/4, 3/4]$, with free chemical diffusion throughout the compartment.

The first model was solved by calculating the steady state of the resulting ordinary differential equation (ODE) system. An analytical solution was obtained for a low gradient intensity. The full derivation of the steady state behavior was performed using the Python symbolic computation package `Sympy` [44, 45]. It is available as a `Jupyter` notebook [46] in the SI, and the major results are detailed in Section C.

The other models were solved numerically by integrating the resulting partial differential equation (PDE) system (see Section D 1). The steady states of the reaction-diffusion systems were numerically calculated for a wide set of values of $\beta \in [0.5, 5]$, $\theta_g \in [0.01, 0.5]$, $\rho \in [10^{-3}, 10^{+3}]$, $d \in [10^{-3}, 10^{+3}]$, $\gamma \in [0.2, 1]$, $\kappa \in [0.1, 10]$, and $\lambda \in [0.1, 10]$. The steady state was considered to be reached when the relative residual flux was sufficiently small, following:

$$\frac{\int_0^1 \varphi d\bar{x}}{|\int_0^{\bar{x}_0} \varphi d\bar{x}| + |\int_{\bar{x}_0}^1 \varphi d\bar{x}|} < \omega \quad (\text{A1})$$

where \bar{x}_0 is the position at which $\varphi = 0$ (see D 2). In all simulations, $\omega = 10^{-6}$ was used. When necessary, the total simulation time was increased until the condition of Eq. (A1) was met.

The calculations were performed using XMDS2, an open source software for solving PDEs using spectral methods for computing spatial derivatives [47]. In each simulation, a steady temperature gradient was imposed with either a Heaviside, linear, or mixed profile. In all models, the influence of temperature on the chemical reaction was introduced via the Arrhenius relationship for the reaction rate constants. Integration was performed using the 8th (embedded 9th) order adaptive Runge-Kutta method. Spatial derivation was performed on the basis of a discrete cosine transform for the implementation of zero Neumann boundaries, thus describing a closed system.

Appendix B: Entropy production due to thermal diffusion

The system is submitted to a temperature gradient. It is thus subjected to a steady heat flux, generating a production of entropy \dot{S}_{th} , nondimensionalized as σ_{th} . Assuming a linear gradient from $T_0(1 - \theta_g)$ to $T_0(1 + \theta_g)$ over a length l_g , inside a system of length l_0 , this term can be expressed at each position x as [36]:

$$T = T_0 \cdot \left(1 + \left(\frac{2\theta_g}{l_g} x - \theta_g \right) \right) \quad (\text{B1a})$$

$$\dot{S}_{\text{th}}(x) = k_{\text{th}} \left(\frac{1}{T} \cdot \frac{\partial T}{\partial x} \right)^2 \quad (\text{B1b})$$

$$= k_{\text{th}} \frac{4\theta_g^2}{(l_g(1 - \theta_g) + 2\theta_g x)^2} \quad (\text{B1c})$$

k_{th} being the thermal conductivity of the medium (in $\text{J.s}^{-1} \cdot \text{m}^{-1} \cdot \text{K}^{-1}$).

On average, the entropy production in the full system is thus:

$$\dot{S}_{\text{th}} = \frac{1}{l_0} \int_0^{l_g} \dot{S}_{\text{th}}(x) \, dx \quad (\text{B2a})$$

$$= \frac{4k_{\text{th}}}{l_0 l_g} \cdot \frac{\theta_g^2}{1 - \theta_g^2} \quad (\text{B2b})$$

This can be nondimensionalized as:

$$\sigma_{\text{th}} = \dot{S}_{\text{th}} \cdot \frac{l_0^2}{R c_0 D_0} \quad (\text{B3a})$$

$$= \frac{4\bar{k}_{\text{th}}}{\bar{l}_g} \cdot \frac{\theta_g^2}{1 - \theta_g^2} \quad (\text{B3b})$$

$$\approx \frac{4\bar{k}_{\text{th}}}{\bar{l}_g} \theta_g^2 \quad \text{for } \theta_g \ll 1 \quad (\text{B3c})$$

$$\text{with } \bar{k}_{\text{th}} = \frac{k_{\text{th}}}{R c_0 D_0} \quad (\text{B3d})$$

\bar{k}_{th} is the nondimensionalized thermal conductivity. For example, in the case of water as the system solvent, $k_{\text{th}} = 0.61 \text{ J.s}^{-1} \cdot \text{K}^{-1}$ at 300 K [48]; with a characteristic reactant concentration $c_0 = 10^3 \text{ mol.m}^{-3}$ and chemical diffusion $D_0 = 10^{-9} \text{ m}^2 \cdot \text{s}^{-1}$, $\bar{k}_{\text{th}} = 7.3 \times 10^4$. This value can be compared with η^2 , in order to compare the intensity of the thermal entropy production with the chemical entropy production (Eq. (C21)). An example system, with $\eta^2 = 1600$ for a reaction enthalpy $\Delta_r H = 100 \text{ kJ.mol}^{-1}$ at 300 K, would imply a chemical entropy production that represents at most 1% of the thermal entropy production.

\bar{l}_g represents the fraction on the system where the gradient is established (1 for the linear gradient, $1/2$ for the mixed gradient, and 0 for the Heaviside gradient and a two-compartment system). It shall be noted that the entropy production thus tends to infinity in the case of the Heaviside gradient; this is due to the non-physicality of sustaining an infinitely sharp temperature gradient.

Appendix C: Mathematical derivation in the stirred compartments model

1. Steady state

The steady state u_{ij}^∞ (with $i \in [1, 2]$ and $j \in [a, b]$) can be obtained directly from the resolution of the set of equations (8), for $\frac{du_{ij}}{dt} = 0$. Each chemical force and flux of any reaction or exchange process k can be expressed as:

$$\varphi_k = r_k^+ - r_k^- \quad (\text{C1a})$$

$$\alpha_k = \ln \frac{r_k^+}{r_k^-} \quad (\text{C1b})$$

where r_k^+ and r_k^- are the process rates of direct and indirect reactions, respectively.

It is then possible to express the on-equilibrium steady state of each reaction and compound exchange in terms of $[\alpha, \varphi]$ as:

$$\varphi_{ra} = \bar{k}_{+,a} u_{1a}^\infty - \bar{k}_{-,a} u_{2a}^\infty \quad (\text{C2a})$$

$$\alpha_{ra} = \ln \left(K_a \frac{u_{1a}^\infty}{u_{2a}^\infty} \right) \quad (\text{C2b})$$

for the reaction in compartment A ,

$$\varphi_{rb} = \bar{k}_{+,b} u_{1b}^\infty - \bar{k}_{-,b} u_{2b}^\infty \quad (\text{C2c})$$

$$\alpha_{rb} = \ln \left(K_b \frac{u_{1b}^\infty}{u_{2b}^\infty} \right) \quad (\text{C2d})$$

for the reaction in compartment B ,

$$\varphi_{d1} = \lambda^{-1} \delta(u_{1a}^\infty - u_{1b}^\infty) \quad (\text{C2e})$$

$$\alpha_{d1} = \ln \left(\frac{u_{1a}^\infty}{u_{1b}^\infty} \right) \quad (\text{C2f})$$

for the diffusion of U_1 , and

$$\varphi_{d2} = \lambda \delta(u_{2a}^\infty - u_{2b}^\infty) \quad (\text{C2g})$$

$$\alpha_{d2} = \ln \left(\frac{u_{2a}^\infty}{u_{2b}^\infty} \right) \quad (\text{C2h})$$

for the diffusion of U_2 .

At the steady state, all the chemical fluxes compensate for each other, following Eqs. (8) such that:

$$\varphi = -\varphi_{ra} = \varphi_{rb} = \varphi_{d1} = -\varphi_{d2} \quad (\text{C3})$$

This implies that each process k is characterized by α_k and $\varphi_k = \pm \varphi$. Thus, each process is characterized by its chemical resistance R_k :

$$R_k = \frac{\alpha_k}{\varphi_k} \quad (\text{C4})$$

Each process produces entropy as:

$$\sigma_k = \alpha_k \varphi_k \quad (\text{C5a})$$

$$= R_k \varphi_k^2 = R_k \varphi^2 \quad (\text{C5b})$$

Each term σ_k is positive, so $R_k \geq 0$; α_k and φ_k are thus necessarily of the same sign.

The full entropy production is then:

$$\sigma = \sum_k \sigma_k \quad (\text{C6a})$$

$$= \sum_k R_k \varphi^2 \quad (\text{C6b})$$

This yields the total production of entropy in the system as:

$$\sigma_{ra} = \alpha_{ra} \varphi_{ra} = -\alpha_{ra} \varphi \quad (\text{C7a})$$

$$= R_{ra} \varphi^2 \quad (\text{C7b})$$

$$\sigma_{rb} = \alpha_{rb} \varphi_{rb} = +\alpha_{rb} \varphi \quad (\text{C7c})$$

$$= R_{rb} \varphi^b \quad (\text{C7d})$$

$$\sigma_{d1} = \alpha_{d1} \varphi_{d1} = +\alpha_{d1} \varphi \quad (\text{C7e})$$

$$= R_{d1} \varphi^2 \quad (\text{C7f})$$

$$\sigma_{d2} = \alpha_{d2} \varphi_{d2} = -\alpha_{d2} \varphi \quad (\text{C7g})$$

$$= R_{d2} \varphi^2 \quad (\text{C7h})$$

$$\sigma_r = \sigma_{ra} + \sigma_{rb} = (\alpha_{rb} - \alpha_{ra}) \varphi \quad (\text{C7i})$$

$$= R_r \varphi^2 \quad (\text{C7j})$$

$$\sigma_d = \sigma_{d1} + \sigma_{d2} = (\alpha_{d1} - \alpha_{d2}) \varphi \quad (\text{C7k})$$

$$= R_d \varphi^2 \quad (\text{C7l})$$

$$\sigma = \sigma_r + \sigma_d = (\alpha_{r2} - \alpha_{r1} + \alpha_{d1} - \alpha_{d2}) \varphi \quad (\text{C7m})$$

$$= \alpha \varphi = R_{\text{tot}} \varphi^2 \quad (\text{C7n})$$

with

$$R_{\text{tot}} = R_r + R_d \quad (\text{C7o})$$

$$R_r = R_{ra} + R_{rb} \quad (\text{C7p})$$

$$R_d = R_{d1} + R_{d2} \quad (\text{C7q})$$

According to Eqs. (C2), (C3) and (6c), the total chemical force α can be expressed as:

$$\alpha = -\alpha_{ra} + \alpha_{rb} + \alpha_{d1} - \alpha_{d2} \quad (\text{C8a})$$

$$= \ln \left(K_a^{-1} \frac{u_{2a}^\infty}{u_{1a}^\infty} \cdot K_b \frac{u_{1b}^\infty}{u_{2b}^\infty} \cdot \frac{u_{1a}^\infty}{u_{1b}^\infty} \cdot \frac{u_{2b}^\infty}{u_{2a}^\infty} \right) \quad (\text{C8b})$$

$$= \ln \left(\frac{K_b}{K_a} \right) \quad (\text{C8c})$$

$$= \left(\frac{\theta_g}{\theta_g + 1} - \frac{\theta_g}{\theta_g - 1} \right) \eta \quad (\text{C8d})$$

$$= \frac{2\eta\theta_g}{1 - \theta_g^2} \quad (\text{C8e})$$

Solving the corresponding set of equations exactly leads to complex expressions of α_i , φ_i , and σ_i parameters. Thus, we simplified the system by assuming relatively small variations in temperature, using a second order Taylor expansion; α is further simplified to:

$$\alpha = 2\eta\theta_g + O(\theta_g^3) \approx 2\eta\theta_g \quad (\text{C9})$$

2. Expression of the steady chemical flux

The expression of the steady chemical flux can also be evaluated with a second order Taylor expansion as a function of θ_g , leading to:

$$\varphi = \frac{\rho\lambda'\delta}{\lambda'\delta + \rho} \frac{\kappa'\eta\theta_g}{2} \quad (\text{C10a})$$

with

$$\kappa' = \frac{2\kappa}{1 + \kappa^2} \quad (\text{C10b})$$

and:

$$\lambda' = \frac{2\kappa\lambda}{1 + \kappa^2\lambda^2} \quad (\text{C10c})$$

κ' and λ' are parameters that characterize the asymmetry of the chemical reaction and chemical exchange, respectively. The chemical flux in Eq. (C10a) indicates that the behavior of the system depends on the relative values of ρ and $\lambda'\delta$, with the intensity proportional to the reaction asymmetry κ' .

a. *Distribution between chemical reaction and exchange* The total entropy production is distributed between the chemical reactions and exchanges:

$$\alpha_r = \frac{\lambda'\delta}{\lambda'\delta + \rho} \alpha \quad (\text{C11a})$$

$$\alpha_d = \frac{\rho}{\lambda'\delta + \rho} \alpha \quad (\text{C11b})$$

This implies the following distribution of entropy distribution:

$$\sigma_r = \frac{\lambda'\delta}{\lambda'\delta + \rho} \sigma \quad (\text{C12a})$$

$$\sigma_d = \frac{\rho}{\lambda'\delta + \rho} \sigma \quad (\text{C12b})$$

b. *Distribution of the reaction entropy production in each compartment* The chemical forces for each chemical reaction can be evaluated as:

$$\alpha_{ra} = -\frac{1 + \varepsilon}{2} \alpha_r \quad (\text{C13a})$$

$$\alpha_{rb} = +\frac{1 - \varepsilon}{2} \alpha_r \quad (\text{C13b})$$

with

$$\varepsilon = \beta + \frac{\eta\rho}{2(\lambda'\delta + \rho)} \frac{1 - \kappa^2\lambda^2}{1 + \kappa^2\lambda^2} \quad (\text{C13c})$$

implying the following distribution of entropy production:

$$\sigma_{ra} = \frac{1 + \varepsilon\theta_g}{2} \sigma_r \quad (\text{C14a})$$

$$\sigma_{rb} = \frac{1 - \varepsilon\theta_g}{2} \sigma_r \quad (\text{C14b})$$

The parameter ε tends to β when $\kappa \approx \lambda^{-1}$, to $\beta(1 - \gamma) = \varepsilon_+$ when κ or λ tends to large values and to $\beta(1 + \gamma) = \varepsilon_-$ when κ or λ tends to zero. ε can be interpreted as the global activation energy for the whole system, varying from ε_+ to ε_- through the average value of β , depending on the global symmetry of the system.

c. Distribution of the exchange entropy production for each compound The chemical forces for each chemical reaction can be evaluated as:

$$\alpha_{d1} = + \frac{\lambda^2 \kappa^2}{1 + \lambda^2 \kappa^2} \alpha_d \quad (\text{C15a})$$

$$\alpha_{d2} = - \frac{1}{1 + \lambda^2 \kappa^2} \alpha_d \quad (\text{C15b})$$

implying the following distribution of entropy production:

$$\sigma_{d1} = \frac{\lambda^2 \kappa^2}{1 + \lambda^2 \kappa^2} \sigma_d \quad (\text{C16a})$$

$$\sigma_{d2} = \frac{1}{1 + \lambda^2 \kappa^2} \sigma_d \quad (\text{C16b})$$

The dissipation due to the exchange is equally shared by the exchange of each compound U_1 and U_2 when the system is symmetrical ($\kappa = \lambda^{-1}$), but is diverted towards U_1 for large values of $\kappa\lambda$, and towards U_2 for small values of $\kappa\lambda$.

3. Chemical resistance

By analogy with electric circuits, the relationship between the chemical fluxes φ_i and the chemical forces α_i leads to the chemical resistance of process R_i as:

$$R_i = \frac{\alpha_i}{\varphi_i} \quad (\text{C17a})$$

$$R_{ra} = \frac{2(1 + \varepsilon\theta_g)}{\kappa'\rho} \quad (\text{C17b})$$

$$R_{rb} = \frac{2(1 - \varepsilon\theta_g)}{\kappa'\rho} \quad (\text{C17c})$$

$$R_{d1} = \frac{2\kappa\lambda}{\kappa'\delta} \quad (\text{C17d})$$

$$R_{d2} = \frac{2}{\kappa'\delta\kappa\lambda} \quad (\text{C17e})$$

$$R_r = \frac{4}{\kappa'\rho} \quad (\text{C17f})$$

$$R_d = \frac{4}{\kappa'\lambda'\delta} \quad (\text{C17g})$$

$$R_{\text{tot}} = \frac{4}{\kappa'} \left(\frac{1}{\rho} + \frac{1}{\lambda'\delta} \right) \quad (\text{C17h})$$

4. Entropy yield

The ratio $y_k = \sigma_k/\sigma$ provides the fraction of entropy produced by the process k . This can be linked to the energy yield, which is the fraction of the energy produced by a specific process of interest. This can be calculated as:

$$y_k = \frac{\sigma_k}{\sigma} \quad (\text{C18a})$$

$$= \frac{R_k \varphi^2}{R_{\text{tot}} \varphi^2} = \frac{R_k}{R_{\text{tot}}} \quad (\text{C18b})$$

The efficiency of a given system to be used for chemical reactions is y_r , and that for chemical transport is y_d :

$$y_r = \frac{\lambda'\delta}{\lambda'\delta + \rho} \quad (\text{C19a})$$

$$y_d = \frac{\rho}{\lambda'\delta + \rho} \quad (\text{C19b})$$

5. System characteristics

All φ , α_k and σ_k values can be directly derived from the expression of R_k in Eqs. (C17) and α from Eq. (C9):

$$\varphi = \frac{\alpha}{R_{\text{tot}}} \quad (\text{C20a})$$

$$\alpha_k = \frac{R_k}{R_{\text{tot}}} \alpha \quad (\text{C20b})$$

$$\sigma_k = \frac{R_k}{R_{\text{tot}}^2} \alpha^2 \quad (\text{C20c})$$

In all situations, the steady state can thus be described as:

$$\varphi = \frac{\lambda'\delta\rho}{\lambda'\delta + \rho} \varphi_0 \quad (\text{C21a})$$

with

$$\varphi_0 = \frac{1}{2} \kappa' \eta \theta_g \quad (\text{C21b})$$

for the chemical flux,

$$\alpha_r = \frac{\lambda'\delta}{\lambda'\delta + \rho} \alpha_0 \quad (\text{C21c})$$

$$\alpha_d = \frac{\rho}{\lambda'\delta + \rho} \alpha_0 \quad (\text{C21d})$$

with

$$\alpha_0 = 2\eta\theta_g \quad (\text{C21e})$$

for the chemical force, and

$$\sigma_r = \frac{(\lambda'\delta)^2 \rho}{(\lambda'\delta + \rho)^2} \sigma_0 \quad (\text{C21f})$$

$$\sigma_d = \frac{\lambda'\delta\rho^2}{(\lambda'\delta + \rho)^2} \sigma_0 \quad (\text{C21g})$$

$$(C21h)$$

$$\sigma = \sigma_r + \sigma_d = \frac{\lambda'\delta\rho}{\lambda'\delta + \rho} \kappa' \cdot \eta^2 \theta_g^2 \quad (\text{C21i})$$

with

$$\sigma_0 = \kappa'(\eta\theta_g)^2 \quad (\text{C21j})$$

for the entropy production.

This results in a reference steady state $([\alpha_0, \varphi_0, \sigma_0])$, which depends on the thermokinetic characteristics of the chemical reaction. The state of a given system can be retrieved from this reference state based on Eqs. (C21).

6. Entropy production variations

The variation of σ_r can be expressed as:

$$\left(\frac{\partial \sigma_r}{\partial \rho} \right)_{\delta, \sigma_0} = \frac{(\lambda' \delta)^2}{(\delta \lambda' + \rho)^3} \sigma_0 (\lambda' \delta - \rho) \quad (\text{C22a})$$

$$\left(\frac{\partial \sigma_r}{\partial \delta} \right)_{\rho, \sigma_0} = \frac{2 \lambda' \delta \rho^2}{(\delta \lambda' + \rho)^3} \sigma_0 \quad (\text{C22b})$$

For a given value of $\lambda' \delta$, σ_r is thus maximal for $\rho = \lambda' \delta$; it varies proportionally to ρ for $\rho \ll \lambda' \delta$ and to ρ^{-1} for $\rho \gg \lambda' \delta$. For a given value of ρ , σ_r increases monotonically with $\lambda' \delta$; it varies proportionally to $(\lambda' \delta)^2$ for $\lambda' \delta \ll \rho$, and reaches a plateau for $\lambda' \delta \gg \rho$.

Similarly, the variation of σ_d can be expressed as:

$$\left(\frac{\partial \sigma_d}{\partial \rho} \right)_{\delta, \sigma_0} = \frac{2(\lambda' \delta)^2 \rho}{(\delta \lambda' + \rho)^3} \sigma_0 \quad (\text{C23a})$$

$$\left(\frac{\partial \sigma_d}{\partial \delta} \right)_{\rho, \sigma_0} = \frac{\rho^2}{(\delta \lambda' + \rho)^3} \sigma_0 (\rho - \lambda' \delta) \quad (\text{C23b})$$

For a given value of ρ , σ_d is thus maximal for $\lambda' \delta = \rho$; it varies proportionally to $\lambda' \delta$ for $\lambda' \delta \ll \rho$ and to $(\lambda' \delta)^{-1}$ for $\lambda' \delta \gg \rho$. For a given value of $\lambda' \delta$, σ_d increases monotonically with ρ , varying proportionally to ρ^2 for $\rho \ll \lambda' \delta$, but reaches a plateau for $\rho \gg \lambda' \delta$ (see fig. S1 in SI.).

Appendix D: PDE system

1. Expression of the PDE model

Chemical reaction-diffusion is described based on the following set of partial differential equations (PDEs):

$$\frac{\partial u_1}{\partial \bar{t}} = d_1 \frac{\partial^2 u_1}{\partial \bar{x}^2} - \varphi_r(\bar{x}), \quad (\text{D1a})$$

$$\frac{\partial u_2}{\partial \bar{t}} = d_2 \frac{\partial^2 u_2}{\partial \bar{x}^2} + \varphi_r(\bar{x}), \quad (\text{D1b})$$

with

$$\varphi_r(\bar{x}) = \bar{k}_+(\bar{x}) u_1(\bar{x}) - \bar{k}_-(\bar{x}) u_2(\bar{x}) \quad (\text{D1c})$$

In contrast to the two-compartment model, the variables are expressed as a function of the nondimensionalized spatial position \bar{x} , following an imposed temperature gradient $\theta(\bar{x})$, with $\theta(\bar{x}) \in [-\theta_g, +\theta_g]$.

The general properties of the system are described based on its characteristic concentration c_0 and temperature T_0 . However, the introduction of the spatial dimension introduces two new characteristics: length

l_0 (corresponding to the system dimension), and diffusion constant D_0 (corresponding to the average diffusion constant of the reactants). The characteristic time is then directly obtained as $t_0 = l_0^2/D_0$. The system is thus described in terms of the nondimensionalized concentrations u_i , position \bar{x} , temperature deviation θ , diffusion constants d_i , and time \bar{t} .

Chemical transport is now defined as molecular diffusion; it cannot be treated anymore as a chemical reaction. The rates of entropy production of the chemical reaction (σ_r) and chemical diffusion of compound U_i ($\sigma_{d,i}$) are expressed as [36, 37]:

$$\sigma_r = \varphi_r \cdot \alpha_r = (\bar{k}_+ u_1 - \bar{k}_- u_2) \cdot \ln \frac{\bar{k}_+ u_1}{\bar{k}_- u_2} \quad (\text{D2a})$$

$$\sigma_{d,i} = \varphi_d \cdot \alpha_d = j_i \cdot \frac{1}{u_i} \left(\frac{\partial u_i}{\partial \bar{x}} \right) \quad (\text{D2b})$$

$$= \frac{d_i}{u_i} \left(\frac{\partial u_i}{\partial \bar{x}} \right)^2 \quad (\text{D2c})$$

2. Steady state characteristics

The steady-state conditions must consider the spatial extension of the system. In steady state, the total concentrations of each compound U_1 and U_2 are constant. This implies that the global reaction flux is zero, i.e.:

$$\int_0^1 \varphi \, d\bar{x} = 0 \quad (\text{D3})$$

In all situations, $\varphi < 0$ in the cold region (for $\bar{x} \in [0, \bar{x}_0[$), and $\varphi > 0$ in the warm region (for $\bar{x} \in]\bar{x}_0, 1]$), where \bar{x}_0 is the position at which $\varphi = 0$. This implies that:

$$\int_0^{\bar{x}_0} \varphi \, d\bar{x} = - \int_{\bar{x}_0}^1 \varphi \, d\bar{x} \quad (\text{D4})$$

For quantities whose sign changes across the system, this integral value is thus calculated as:

$$\varphi_{\text{int}} = \left| \int_0^{\bar{x}_0} \varphi \, d\bar{x} \right| \quad (\text{D5a})$$

$$\alpha_{\text{int}} = \left| \int_0^{\bar{x}_0} \alpha \, d\bar{x} \right| \quad (\text{D5b})$$

A positive rate of entropy production σ is present at each system location. The full entropy production comes down to the integral value is calculated over the full system extension:

$$\sigma_{\text{int}} = \int_0^1 \sigma \, d\bar{x} \quad (\text{D6})$$

[1] D. A. Beard and H. Qian, *Chemical biophysics: quantitative analysis of cellular systems*, Vol. 126 (Cambridge University Press Cambridge, 2008).

[2] N. Lane, J. F. Allen, and W. Martin, *BioEssays* **32**, 271

- (2010).
- [3] T. Hill, *Free energy transduction in biology: the steady-state kinetic and thermodynamic formalism* (Elsevier, 2012).
- [4] H. Morowitz and E. Smith, *Complexity* **13**, 51 (2007).
- [5] R. Pascal and L. Boiteau, *Phil. Trans. Roy. Soc. B: Biol. Sci.* **366**, 2949 (2011).
- [6] G. Nicolis and I. Prigogine, *Self-Organization in Nonequilibrium Systems: From Dissipative Structures to Order through Fluctuations* (Wiley, 1977).
- [7] C. Vidal and H. Lemarchand, *La réaction créatrice: dynamique des systèmes chimiques* (Hermann, 1988).
- [8] I. R. Epstein and J. A. Pojman, *An introduction to nonlinear chemical dynamics: oscillations, waves, patterns, and chaos* (Oxford university press, 1998).
- [9] B. A. Grzybowski and W. T. S. Huck, *Nature Nanotechnology* **11**, 585–592 (2016).
- [10] L. Jullien, A. Lemarchand, S. Charier, O. Ruel, and J.-B. Baudin, *The Journal of Physical Chemistry B* **107**, 9905 (2003).
- [11] A. Lemarchand and L. Jullien, *Physical Chemistry Chemical Physics* **6**, 398 (2004).
- [12] G. Ragazzon and L. J. Prins, *Nature nanotechnology* **13**, 882 (2018).
- [13] R. D. Astumian, *Annual review of biophysics* **40**, 289 (2011).
- [14] M. Emond, T. Le Saux, J.-F. Allemand, P. Pelupessy, R. Plasson, and L. Jullien, *Chem Eur J* **18**, 14375 (2012).
- [15] T. L. Saux, R. Plasson, and L. Jullien, *Chem. Commun.* **50**, 6189 (2014).
- [16] B. N. Kholodenko, *Nat. Rev. Mol. Cell. Biol.* **7**, 165 (2006).
- [17] S. Soh, M. Byrska, K. Kandere-Grzybowska, and B. A. Grzybowski, *Angew. Chem. Int. Ed.* **49**, 4170 (2010).
- [18] W. Nernst, Johann Ambrosium Barth, Leipzig, Germany , 904 (1904).
- [19] P. A. Dirac, in *Mathematical Proceedings of the Cambridge Philosophical Society*, Vol. 2 (Cambridge University Press, 1924) pp. 132–137.
- [20] I. Prigogine and R. Buess, *Acad. roy. Belg., Bull. Cl. Sc.* , 711 (1952).
- [21] I. Prigogine and R. Buess, *Acad. roy. Belg., Bull. Cl. Sc.* , 851 (1952).
- [22] J. Meixner, *Zeitschrift für Naturforschung A* **7**, 553 (1952).
- [23] R. Haase, *Zeitschrift für Naturforschung A* **8**, 729 (1953).
- [24] J. N. Butler and R. S. Brokaw, *The Journal of Chemical Physics* **26**, 1636 (1957).
- [25] W. B. Brown, *Transactions of the Faraday Society* **54**, 772 (1958).
- [26] H. Kehlen, M. T. Rätzsch, and T. Drzisga, *Journal of Non-Equilibrium Thermodynamics* **6**, 10.1515/jnet.1981.6.2.93 (1981).
- [27] J. Xu, S. Kjelstrup, and D. Bedeaux, *Physical Chemistry Chemical Physics* **8**, 2017 (2006).
- [28] J. Xu, S. Kjelstrup, D. Bedeaux, and J.-M. Simon, *Physical Chemistry Chemical Physics* **9**, 969 (2007).
- [29] J. M. O. de Zárate, D. Bedeaux, I. Pagonabarraga, J. V. Sengers, and S. Kjelstrup, *Comptes Rendus Mécanique* **339**, 287 (2011).
- [30] R. Skorpa, T. J. H. Vlugt, D. Bedeaux, and S. Kjelstrup, *The Journal of Physical Chemistry C* **119**, 12838 (2015).
- [31] L. M. Keil, F. M. Möller, M. Kieß, P. W. Kudella, and C. B. Mast, *Nature communications* **8**, 1897 (2017).
- [32] T. Matreux, B. Altaner, J. Raith, D. Braun, C. B. Mast, and U. Gerland, *Communications Physics* **6**, 14 (2023).
- [33] D. M. Busiello, S. Liang, F. Piazza, and P. De Los Rios, *Communications Chemistry* **4**, 16 (2021).
- [34] S. Liang, D. M. Busiello, and P. De Los Rios, *New Journal of Physics* **24**, 123006 (2022).
- [35] R. Plasson and H. Bersini, *The Journal of Physical Chemistry B* **113**, 3477 (2009), 0804.4834.
- [36] S. R. de Groot and P. Mazur, *Non-equilibrium thermodynamics* (North-Holland Publishing Co., Amsterdam, 1969) p. 510.
- [37] H. Mahara and T. Yamaguchi, *Physica D: Nonlinear Phenomena Emergent Phenomena in Spatially Distributed Systems*, **239**, 729–734 (2010).
- [38] A. Würger, *Reports on Progress in Physics* **73**, 126601 (2010).
- [39] Y. Ruff, V. Garavini, and N. Giuseppone, *Journal of the American Chemical Society* **136**, 6333–6339 (2014).
- [40] N. Capit, *Designing a reversible peptide system for out of equilibrium chemistry exploration*, Phd thesis, Université de Strasbourg (2021).
- [41] R. Plasson, *Molecular Origin of Life: Study of the Polymerization of α-amino acid N-carboxyanhydrides under prebiotic conditions by capillary electrophoresis*, Phd thesis, Université Montpellier II, Montpellier, France (2003).
- [42] R. Plasson and H. Cottet, *Analytical Chemistry* **77**, 6047–6054 (2005).
- [43] A. Wachtel, R. Rao, and M. Esposito, *The Journal of Chemical Physics* **157**, 024109 (2022).
- [44] A. Meurer, C. P. Smith, M. Paprocki, O. Čertík, S. B. Kirpichev, M. Rocklin, A. Kumar, S. Ivanov, J. K. Moore, S. Singh, T. Rathnayake, S. Vig, B. E. Granger, R. P. Muller, F. Bonazzi, H. Gupta, S. Vats, F. Johansson, F. Pedregosa, M. J. Curry, A. R. Terrel, S. Roučka, A. Saboo, I. Fernando, S. Kulal, R. Cimrman, and A. Scopatz, *PeerJ Computer Science* **3**, e103 (2017).
- [45] K. J. Millman and M. Aivazis, *Computing in Science & Engineering* **13**, 9 (2011).
- [46] B. E. Granger and F. Pérez, *Computing in Science & Engineering* **23**, 7 (2021).
- [47] G. R. Dennis, J. J. Hope, and M. T. Johnsson, *Computer Physics Communications* **184**, 201 (2013).
- [48] D. R. Lide, *CRC handbook of chemistry and physics*, 73rd ed. (CRC Press, Boca Raton, Florida, 1992).

Optimizing reaction and transport fluxes in temperature gradient-driven chemical reaction-diffusion systems: Supplementary Information

Mohammed Loukili,¹ Ludovic Jullien,² Guillaume Baffou,³ and Raphaël Plasson⁴

¹⁾*Institut de Recherche de l'École Navale, EA 3634, IRENav, Brest, France*

²⁾*CPCV, Département de chimie, École normale supérieure, PSL University, Sorbonne Université, CNRS, 24, rue Lhomond, 75005 Paris, France*

³⁾*Institut Fresnel, CNRS, Aix Marseille University, Centrale Med, 13013 Marseille, France*

⁴⁾*Avignon University, INRAE, UMR408 SQPOV, 84000 Avignon, France*

(*Electronic mail: raphael.plasson@univ-avignon.fr)

CONTENTS

Notebook: Analytical development of the compartment model	2
A. Solving the steady state from the equation system	2
1. Solution	2
2. Check equations	3
B. Data derivation	4
1. Fluxes	4
2. α and σ	5
C. Switch to $\beta/\gamma/\rho$ description	6
D. Taylor expansion for low values of θ	7
1. Thermokinetic constant	7
2. x Simplification	8
3. φ	10
4. α	10
5. Chemical resistance $R = \alpha/\varphi$	19
6. σ	20
7. $\tilde{\mathcal{A}}$	22
List of Figures	25
Reaction diffusion profiles	31

NOTEBOOK: ANALYTICAL DEVELOPMENT OF THE COMPARTMENT MODEL

```
[1]: import sympy as sp
```

A. Solving the steady state from the equation system

Chemical reactions:

- Compartment A: $U_{1a} \rightleftharpoons U_{2a}$, kinetic rates \bar{k}_{+a} and \bar{k}_{-a}
- Compartment B: $U_{1b} \rightleftharpoons U_{2b}$, kinetic rates \bar{k}_{+b} and \bar{k}_{-b}
- Exchange of U_1 : $U_{1a} \rightleftharpoons U_{1b}$, kinetic rate $\lambda^{-1}\delta$
- Exchange of U_2 : $U_{2a} \rightleftharpoons U_{2b}$, kinetic rate $\lambda\delta$

All following calculations are performed from nondimensionalized parameters.

```
[2]: u1a, u1b, u2a, u2b, delta, kpa, kma, kpb, kmb, theta, lamb = sp.symbols("u1a, u1b, u2a, u2b, delta, \u0331{u1a}, \u0331{u1b}, \u0331{u2a}, \u0331{u2b}, kpa, kma, kpb, kmb, theta, lamb", real=True)
```

1. Solution

$$\frac{dU_{1a}}{dt} :$$

```
[3]: eq1 = delta / lamb * (u1b - u1a) - kpa * u1a + kma * u2a
```

$$\frac{dU_{1b}}{dt} :$$

```
[4]: eq2 = delta / lamb * (u1a - u1b) - kpb * u1b + kmb * u2b
```

$$\frac{dU_{2a}}{dt} :$$

```
[5]: eq3 = lamb * delta * (u2b - u2a) + kpa * u1a - kma * u2a
```

$$\frac{dU_{2b}}{dt} :$$

```
[6]: eq4 = lamb * delta * (u2a - u2b) + kpb * u1b - kmb * u2b
```

Matter conservation: total initial concentration is 1 in each compartment

```
[7]: eq5 = u1a + u1b + u2a + u2b - 2
```

The steady state comes thus down to solve {eq1=0; eq2=0; eq3=0; eq4=0; eq5=0}

```
[8]: res = sp.solve([eq1, eq2, eq3, eq4, eq5], [u1a, u1b, u2a, u2b])
u1as = res[u1a].simplify().factor(delta)
u1bs = res[u1b].simplify().factor(delta)
u2as = res[u2a].simplify().factor(delta)
u2bs = res[u2b].simplify().factor(delta)
```

2. Check equations

Checking that everything is correct:

```
[9]: def replace(x):
    res = x.replace(u1a, u1as).simplify()
    res = res.replace(u1b, u1bs).simplify()
    res = res.replace(u2a, u2as).simplify()
    res = res.replace(u2b, u2bs).simplify()
    return res
```

```
[10]: replace(eq5)
```

```
[10]:
```

0

```
[11]: replace(eq4)
```

```
[11]:
```

0

```
[12]: replace(eq3)
```

```
[12]:
```

0

```
[13]: replace(eq2)
```

```
[13]:
```

0

```
[14]: replace(eq1)
```

```
[14]:
```

0

Total concentration in both compartments shall be 2 (matter conservation):

```
[15]: (u1as+u2as+u1bs+u2bs).simplify()
```

```
[15]:
```

2

$u_{1a} + u_{2a}$ should not be 1 (differences due to λ)

```
[16]: (u1as+u2as).simplify()
```

```
[16]:
```

$$\frac{2 \left(\bar{k}_{+a} \bar{k}_{+b} \lambda^2 + \bar{k}_{+a} \bar{k}_{-b} + \bar{k}_{+b} \bar{k}_{-a} \lambda^2 + \bar{k}_{-a} \bar{k}_{-b} + \delta \lambda (\bar{k}_{+a} + \bar{k}_{+b}) + \delta \lambda (\bar{k}_{-a} + \bar{k}_{-b}) \right)}{2 \bar{k}_{+a} \bar{k}_{+b} \lambda^2 + \bar{k}_{+a} \bar{k}_{-b} \lambda^2 + \bar{k}_{+a} \bar{k}_{-b} + \bar{k}_{+b} \bar{k}_{-a} \lambda^2 + \bar{k}_{+b} \bar{k}_{-a} + 2 \bar{k}_{-a} \bar{k}_{-b} + 2 \delta \lambda (\bar{k}_{+a} + \bar{k}_{+b} + \bar{k}_{-a} + \bar{k}_{-b})}$$

$u_{1b} + u_{2b}$ should not be 1 (differences due to λ)

[17]: `(u1bs+u2bs).simplify()`

[17]:

$$\frac{2 \left(\bar{k}_{+a} \bar{k}_{+b} \lambda^2 + \bar{k}_{+a} \bar{k}_{-b} \lambda^2 + \bar{k}_{+b} \bar{k}_{-a} + \bar{k}_{-a} \bar{k}_{-b} + \delta \lambda (\bar{k}_{+a} + \bar{k}_{+b}) + \delta \lambda (\bar{k}_{-a} + \bar{k}_{-b})\right)}{2 \bar{k}_{+a} \bar{k}_{+b} \lambda^2 + \bar{k}_{+a} \bar{k}_{-b} \lambda^2 + \bar{k}_{+a} \bar{k}_{-b} + \bar{k}_{+b} \bar{k}_{-a} \lambda^2 + \bar{k}_{+b} \bar{k}_{-a} + 2 \bar{k}_{-a} \bar{k}_{-b} + 2 \delta \lambda (\bar{k}_{+a} + \bar{k}_{+b} + \bar{k}_{-a} + \bar{k}_{-b})}$$

B. Data derivation

1. Fluxes

φ_a (Signs chosen according to the directions indicated in Fig. 1 of the main text)

[18]: `phia = (kpa* u1as - kma * u2as).simplify().factor(delta)`

[19]: `phib = (kpb* u1bs - kmb * u2bs).simplify().factor(delta)`

[20]: `phidiff1 = (delta/lamb * (u1as-u1bs)).simplify().factor(delta)`

[21]: `phidiff2 = (lamb*delta * (u2as-u2bs)).simplify().factor(delta)`

Check that $\varphi_a = -\varphi_b$

[22]: `(phia+phib).simplify()`

[22]:

0

Check that $\varphi_{d,1} = -\varphi_{d,2}$

[23]: `(phidiff1+phidiff2).simplify()`

[23]:

0

Check that $\varphi_a = -\varphi_{d,1}$

[24]: `(phidiff1+phia).simplify()`

[24]:

0

Define φ as the reaction-diffusion flux, defined as $\varphi = -\varphi_a = \varphi_b = \varphi_{d,1} = -\varphi_{d,2}$

[25]: `phi = -phia
phi`

[25]:

$$-\frac{2 \delta \lambda (\bar{k}_{+a} \bar{k}_{-b} - \bar{k}_{+b} \bar{k}_{-a})}{2 \bar{k}_{+a} \bar{k}_{+b} \lambda^2 + \bar{k}_{+a} \bar{k}_{-b} \lambda^2 + \bar{k}_{+a} \bar{k}_{-b} + \bar{k}_{+b} \bar{k}_{-a} \lambda^2 + \bar{k}_{+b} \bar{k}_{-a} + 2 \bar{k}_{-a} \bar{k}_{-b} + \delta (2 \bar{k}_{+a} \lambda + 2 \bar{k}_{+b} \lambda + 2 \bar{k}_{-a} \lambda + 2 \bar{k}_{-b} \lambda)}$$

2. α and σ

a. Chemical reaction

```
[26]: Ka = kpa/kma
      Kb = kpb/kmb
```

```
[27]: Qa = u2as/u1as
      Qb = u2bs/u1bs
```

```
[28]: KQa=(Ka/Qa).simplify()
```

```
[29]: KQb=(Kb/Qb).simplify()
```

```
[30]: alpha_a = sp.log(KQa).simplify()
```

```
[31]: alpha_b = sp.log(KQb).simplify()
```

```
[32]: sigma_a = (phia*alpha_a).simplify()
```

```
[33]: sigma_b = (phib*alpha_b).simplify()
```

```
[34]: sigmar=(sigma_a+sigma_b).simplify()
      sigmar
```

[34] :

$$\frac{2\delta\lambda (\bar{k}_{+a}\bar{k}_{-b} - \bar{k}_{+b}\bar{k}_{-a})}{2\bar{k}_{+a}\bar{k}_{+b}\lambda^2 + \bar{k}_{+a}\bar{k}_{-b}\lambda^2 + \bar{k}_{+a}\bar{k}_{-b} + \bar{k}_{+b}\bar{k}_{-a}\lambda^2 + \bar{k}_{+b}\bar{k}_{-a} + 2\bar{k}_{-a}\bar{k}_{-b} + 2\delta\lambda (\bar{k}_{+a} + \bar{k}_{+b} + \bar{k}_{-a} + \bar{k}_{-b})} \cdot \left(\log \left(\frac{\bar{k}_{+a}(\bar{k}_{+b}\bar{k}_{-a}\lambda^2 + \bar{k}_{-a}\bar{k}_{-b} + \delta\lambda (\bar{k}_{-a} + \bar{k}_{-b}))}{\bar{k}_{-a}(\bar{k}_{+a}\bar{k}_{+b}\lambda^2 + \bar{k}_{+a}\bar{k}_{-b} + \delta\lambda (\bar{k}_{+a} + \bar{k}_{+b}))} \right) - \log \left(\frac{\bar{k}_{+b}(\bar{k}_{+a}\bar{k}_{-b}\lambda^2 + \bar{k}_{-a}\bar{k}_{-b} + \delta\lambda (\bar{k}_{-a} + \bar{k}_{-b}))}{\bar{k}_{-b}(\bar{k}_{+a}\bar{k}_{+b}\lambda^2 + \bar{k}_{+b}\bar{k}_{-a} + \delta\lambda (\bar{k}_{+a} + \bar{k}_{+b}))} \right) \right)$$

b. Chemical diffusion

```
[35]: KQ_diff1 = (u1as/u1bs).simplify()
```

```
[36]: KQ_diff2 = (u2as/u2bs).simplify()
```

```
[37]: alpha_diff1 = sp.log(KQ_diff1)
```

```
[38]: alpha_diff2 = sp.log(KQ_diff2)
```

```
[39]: sigma_diff1 = (phidiff1 * alpha_diff1).simplify()
```

```
[40]: sigma_diff2 = (phidiff2 * alpha_diff2).simplify()
```

```
[41]: sigma_diff = (sigma_diff1+sigma_diff2).simplify()
```

```
[42]: alphar = alpha_b-alpha_a
```

```
[43]: alpha_diff=alpha_diff1-alpha_diff2
```

```
[44]: alpha_tot = (alphar+alpha_diff).simplify()
alpha_tot.simplify()
```

[44] :

$$\begin{aligned} & -\log \left(\frac{\bar{k}_{+a}\bar{k}_{+b}\lambda^2 + \bar{k}_{+a}\bar{k}_{-b} + \delta\lambda(\bar{k}_{+a} + \bar{k}_{+b})}{\bar{k}_{+a}\bar{k}_{+b}\lambda^2 + \bar{k}_{+b}\bar{k}_{-a} + \delta\lambda(\bar{k}_{+a} + \bar{k}_{+b})} \right) \\ & + \log \left(\frac{\bar{k}_{+b}\bar{k}_{-a}\lambda^2 + \bar{k}_{-a}\bar{k}_{-b} + \delta\lambda(\bar{k}_{-a} + \bar{k}_{-b})}{\bar{k}_{+a}\bar{k}_{-b}\lambda^2 + \bar{k}_{-a}\bar{k}_{-b} + \delta\lambda(\bar{k}_{-a} + \bar{k}_{-b})} \right) \\ & - \log \left(\frac{\bar{k}_{+a}(\bar{k}_{+b}\bar{k}_{-a}\lambda^2 + \bar{k}_{-a}\bar{k}_{-b} + \delta\lambda(\bar{k}_{-a} + \bar{k}_{-b}))}{\bar{k}_{-a}(\bar{k}_{+a}\bar{k}_{+b}\lambda^2 + \bar{k}_{+a}\bar{k}_{-b} + \delta\lambda(\bar{k}_{+a} + \bar{k}_{+b}))} \right) \\ & + \log \left(\frac{\bar{k}_{+b}(\bar{k}_{+a}\bar{k}_{-b}\lambda^2 + \bar{k}_{-a}\bar{k}_{-b} + \delta\lambda(\bar{k}_{-a} + \bar{k}_{-b}))}{\bar{k}_{-b}(\bar{k}_{+a}\bar{k}_{+b}\lambda^2 + \bar{k}_{+b}\bar{k}_{-a} + \delta\lambda(\bar{k}_{+a} + \bar{k}_{+b}))} \right) \end{aligned}$$

C. Switch to $\beta/\gamma/\rho$ description

Previous description misses information. Switch to better parameters $\kappa, \beta, \gamma, \rho, \theta$. New parameters suffixed by ‘x’. Suppose from here $\kappa = 1$

```
[45]: kappa, rho, gamma, beta, epsilon = sp.symbols("kappa, rho, gamma, beta, \varepsilon",  
    real=True)  
epsilon
```

[45] :

$$\varepsilon$$

```
[46]: kpax = kappa * rho*sp.exp(-theta/(1-theta)*(1+gamma)*beta)
```

```
[47]: kpbx = kappa * rho*sp.exp(theta/(1+theta)*(1+gamma)*beta)
```

```
[48]: kmax = kappa**-1 * rho*sp.exp(-theta/(1-theta)*(1-gamma)*beta)
```

```
[49]: kmbx = kappa**-1 * rho*sp.exp(theta/(1+theta)*(1-gamma)*beta)
```

```
[50]: def replacek(x):  
    """ Substitute old k parameters with the new kx parameters"""  
    res = x.replace(kpa,kpax).simplify()  
    res = res.replace(kpb,kpbx).simplify()  
    res = res.replace(kma,kmax).simplify()  
    res = res.replace(kmb,kmbx).simplify()  
    return res
```

```
[51]: alphax = replacek(sp.log(Kb/Ka)).expand(force=True).simplify()  
alphax
```

[51] :

$$-\frac{4\beta\gamma\theta}{\theta^2 - 1}$$

```
[52]: phix = replacek(phi).expand(force=True).simplify()
phix
```

[52]:

$$\begin{aligned} & \frac{2\delta\kappa^2\lambda\rho \left(e^{\frac{2\beta\theta(\gamma(\theta-1)+2\theta)}{(\theta-1)(\theta+1)}} - e^{\frac{2\beta\theta(\gamma(\theta+1)+2\theta)}{(\theta-1)(\theta+1)}} \right) \cdot e^{-\beta\theta\left(\frac{1}{\theta+1} + \frac{1}{\theta-1}\right)}}{2\delta\kappa\lambda \left(\kappa^2 e^{\frac{2\beta\gamma\theta}{\theta-1}} + 1 \right) e^{\beta\theta\left(\frac{\gamma}{\theta+1} + \frac{1}{\theta-1}\right)} + 2\delta\kappa\lambda \left(\kappa^2 e^{\frac{2\beta\gamma\theta}{\theta+1}} + 1 \right) e^{\beta\theta\left(\frac{\gamma}{\theta-1} + \frac{1}{\theta+1}\right)} + 2\kappa^4\lambda^2\rho e^{\beta\theta\left(\frac{2\gamma\theta}{\theta^2-1} + \frac{\gamma}{\theta+1} + \frac{\gamma}{\theta-1} + \frac{2\theta}{\theta^2-1}\right)}} \\ & + \rho \left(\kappa^2\lambda^2 e^{\frac{2\beta\gamma\theta}{\theta-1}} + \kappa^2\lambda^2 e^{\frac{2\beta\gamma\theta}{\theta+1}} + \kappa^2 e^{\frac{2\beta\gamma\theta}{\theta-1}} + \kappa^2 e^{\frac{2\beta\gamma\theta}{\theta+1}} + 2 \right) e^{\beta\theta\left(\frac{1}{\theta+1} + \frac{1}{\theta-1}\right)} \end{aligned}$$

D. Taylor expansion for low values of θ

This still remains complex... and needs simplification. Taylor expansion with θ (order 3 is sufficient). Corresponding parameters are suffixed by ‘d’, and with ‘d2’ with +O(...) removed

```
[53]: def develop(x, order=3):
    """Shortcut for Taylor expansion for theta"""
    return sp.series(x, theta, n=order)

def full_remove0(x, order=3):
    """Sympy sometimes need to be tricked for removing the O(...)"""
    Sometimes useful for better simplification after simplify() steps"""
    return develop(x, order).remove0().simplify().factor()
```

1. Thermokinetic constant

```
[54]: kpad = develop(kpax).simplify()
```

```
[55]: kpad2 = full_remove0(kpad).factor([theta, beta])
kpad2
```

[55]:

$$\frac{\kappa\rho \left(\beta^2\theta^2 (\gamma^2 + 2\gamma + 1) + \beta\theta^2 (-2\gamma - 2) + \beta\theta (-2\gamma - 2) + 2 \right)}{2}$$

```
[56]: kpbd = develop(kpbx).simplify()
```

```
[57]: kpbd2 = full_remove0(kpbd).factor([theta, beta])
kpbd2
```

[57]:

$$\frac{\kappa\rho \left(\beta^2\theta^2 (\gamma^2 + 2\gamma + 1) + \beta\theta^2 (-2\gamma - 2) + \beta\theta (2\gamma + 2) + 2 \right)}{2}$$

```
[58]: kmad = develop(kmax).simplify()
```

```
[59]: kmad2 = full_remove0(kmad).factor(theta)
      kmad2
```

[59]:

$$\frac{\rho \left(\theta^2 (\beta^2 \gamma^2 - 2\beta^2 \gamma + \beta^2 + 2\beta \gamma - 2\beta) + \theta (2\beta \gamma - 2\beta) + 2 \right)}{2\kappa}$$

```
[60]: kmbd = develop(kmbx).simplify()
```

```
[61]: kmbd2 = full_remove0(kmbd).factor(theta)
      kmbd2
```

[61]:

$$\frac{\rho \left(\theta^2 (\beta^2 \gamma^2 - 2\beta^2 \gamma + \beta^2 + 2\beta \gamma - 2\beta) + \theta (-2\beta \gamma + 2\beta) + 2 \right)}{2\kappa}$$

```
[62]: def replaced(x, order=3):
    """Replace old parameters k with new DL'd kd parameters
    and computes corresponding DL"""
    res = x.replace(kpa,kpad)
    res = res.replace(kpb,kpb0)
    res = res.replace(kma,kmad)
    res = res.replace(kmb,kmbd)
    if order == -1:
        return res.simplify().factor()
    return develop(res, order).simplify().factor()
```

2. κ Simplification

Further, we will need identification of $\lambda' = \frac{2\lambda\kappa}{1+\lambda^2\kappa^2}$ and $\kappa' = \frac{2\kappa}{1+\kappa^2}$

```
[63]: lp, kp, x, y, h = sp.symbols(["\lambda", "\kappa", "x", "y", "\eta"], real=True)
      lp
```

[63]:

$$\lambda'$$

```
[64]: def to_h_kp(res, debug=False):
    """ simplify the expression by attempting to identify
    \lambda', \kappa' and \eta parameters
    """
    if debug:
        sp.pprint(res)
    res = res.subs(kappa**2*lamb**2+1, x)
    if debug:
        sp.pprint(res)
    res = res.subs(2*lamb*kappa, y)
```

```

if debug:
    sp.pprint(res)
res = res.factor(x/y)
if debug:
    sp.pprint(res)
res = res.subs(y,lp*x)
if debug:
    sp.pprint(res)
res = res.subs(beta*gamma, h/2)
if debug:
    sp.pprint(res)
res = res.simplify()
res = res.subs(x,kappa**2*lamb**2+1)
res = res.subs(y, 2*lamb*kappa)
if debug:
    sp.pprint(res)
res = res.subs(kappa**2+1, x)
if debug:
    sp.pprint(res)
res = res.subs(2*kappa, y)
if debug:
    sp.pprint(res)
res = res.factor(x/y)
if debug:
    sp.pprint(res)
res = res.subs(y,kp*x)
if debug:
    sp.pprint(res)
res = res.simplify()
if debug:
    sp.pprint(res)
res = res.subs(x,kappa**2+1)
res = res.subs(y, 2*kappa)
return res.simplify()

```

[65]: Kad = replaced(Ka)

[66]: Kad2 = full_remove0(Kad).factor(theta)

[67]: Ka_ok = to_h_kp(Kad2).factor(theta)
Ka_ok

[67]:

$$\frac{\kappa^2 \left(-2\eta\theta + \theta^2 (\eta^2 - 2\eta) + 2\right)}{2}$$

[68]: Kbd = replaced(Kb)

[69]: Kbd2 = full_remove0(Kbd).factor(theta)

[70]: Kb_ok = to_h_kp(Kbd2).factor(theta)
Kb_ok

[70]:

$$\frac{\kappa^2 \cdot \left(2\eta\theta + \theta^2 (\eta^2 - 2\eta) + 2 \right)}{2}$$

3. φ

[71]: phid=replaced(phi)
phid

[71]:

$$\frac{4\beta\delta\gamma\kappa^2\lambda\rho\theta + O(\theta^3)}{(\kappa^2 + 1)(2\delta\kappa\lambda + \kappa^2\lambda^2\rho + \rho)}$$

[72]: phid2 = full_remove0(phid)
phid2.factor(rho)

[72]:

$$\frac{4\beta\delta\gamma\kappa^2\lambda\rho\theta}{(\kappa^2 + 1)(2\delta\kappa\lambda + \rho(\kappa^2\lambda^2 + 1))}$$

[73]: phi_ok = to_h_kp(phid2*2).factor(rho)/2
phi_ok

[73]:

$$\frac{\eta\kappa'\lambda'\delta\rho\theta}{2(\lambda'\delta + \rho)}$$

4. α

a. Reaction in compartment A

[74]: KQad = replaced(KQa)
KQad

[74]:

$$\frac{\rho^2 + 2\kappa^2\lambda^2\rho^2 + \kappa^4\lambda^4\rho^2 + 4\delta\kappa\lambda\rho + 4\delta\kappa^3\lambda^3\rho + 4\delta^2\kappa^2\lambda^2 - 4\beta\delta\gamma\kappa\lambda\rho\theta - 4\beta\delta\gamma\kappa^3\lambda^3\rho\theta - 8\beta\delta^2\gamma\kappa^2\lambda^2\theta - 4\beta^2\delta\gamma\kappa\lambda\rho\theta^2 - 4\beta^2\delta\gamma\kappa^3\lambda^3\rho\theta^2 - 4\beta^2\delta\gamma^2\kappa\lambda\rho\theta^2 + 4\beta^2\delta\gamma^2\kappa^3\lambda^3\rho\theta^2 - 8\beta^2\delta^2\gamma\kappa^2\lambda^2\theta^2 + 8\beta^2\delta^2\gamma^2\kappa^2\lambda^2\theta^2 + O(\theta^3)}{(2\delta\kappa\lambda + \kappa^2\lambda^2\rho + \rho)^2}$$

[75]: alpha_ad = develop(sp.log(KQad)).simplify()
alpha_ad

[75]:

$$\begin{aligned}
& -4\beta\delta\gamma\kappa\lambda\theta \left(2\delta\kappa\lambda + \kappa^2\lambda^2\rho + \rho \right) \left(4\delta^2\kappa^2\lambda^2 + 4\delta\kappa^3\lambda^3\rho + 4\delta\kappa\lambda\rho + \kappa^4\lambda^4\rho^2 + 2\kappa^2\lambda^2\rho^2 + \rho^2 \right)^3 \\
& -4\beta^2\delta\gamma\kappa\lambda\theta^2 \left(4\delta^2\kappa^2\lambda^2 + 4\delta\kappa^3\lambda^3\rho + 4\delta\kappa\lambda\rho + \kappa^4\lambda^4\rho^2 + 2\kappa^2\lambda^2\rho^2 + \rho^2 \right)^2 \\
& \cdot \left(2\delta\gamma\kappa\lambda \left(2\delta\kappa\lambda + \kappa^2\lambda^2\rho + \rho \right)^2 \right. \\
& \quad \left. + \left(4\delta^2\kappa^2\lambda^2 + 4\delta\kappa^3\lambda^3\rho + 4\delta\kappa\lambda\rho + \kappa^4\lambda^4\rho^2 + 2\kappa^2\lambda^2\rho^2 + \rho^2 \right) \right. \\
& \quad \left. \cdot \left(-2\delta\gamma\kappa\lambda + 2\delta\kappa\lambda - \gamma\kappa^2\lambda^2\rho + \gamma\rho + \kappa^2\lambda^2\rho + \rho \right) \right) \\
& + O(\theta^3)
\end{aligned}$$

$$(4\delta^2\kappa^2\lambda^2 + 4\delta\kappa^3\lambda^3\rho + 4\delta\kappa\lambda\rho + \kappa^4\lambda^4\rho^2 + 2\kappa^2\lambda^2\rho^2 + \rho^2)^4$$

[76]: `alpha_ad2=full_remove0(alpha_ad)`
`alpha_ad2`

[76]:

$$-\frac{4\beta\delta\gamma\kappa\lambda\theta \left(2\beta\delta\kappa\lambda\theta - \beta\gamma\kappa^2\lambda^2\rho\theta + \beta\gamma\rho\theta + \beta\kappa^2\lambda^2\rho\theta + \beta\rho\theta + 2\delta\kappa\lambda + \kappa^2\lambda^2\rho + \rho \right)}{(2\delta\kappa\lambda + \kappa^2\lambda^2\rho + \rho)^2}$$

[77]: `alpha_a_ok = to_h_kp(alpha_ad2)`
`alpha_a_ok`

[77]:

$$\begin{aligned}
& \eta\lambda'\delta\theta \left(\kappa^2\lambda^2 + 1 \right) \\
& \cdot \left(-\eta\kappa^2\lambda^2\rho\theta + \eta\rho\theta + \kappa'\beta\kappa\lambda^2\rho\theta \left(\kappa^2 + 1 \right) + \kappa'\kappa\lambda^2\rho \left(\kappa^2 + 1 \right) \right. \\
& \quad \left. + 2\lambda'\beta\delta\kappa^2\lambda^2\theta + 2\lambda'\beta\delta\theta + 2\lambda'\delta\kappa^2\lambda^2 + 2\lambda'\delta + 2\beta\rho\theta + 2\rho \right) \\
& - \frac{2 \left(\lambda'\delta\kappa^2\lambda^2 + \lambda'\delta + \kappa^2\lambda^2\rho + \rho \right)^2}{2 \left(\lambda'\delta\kappa^2\lambda^2 + \lambda'\delta + \kappa^2\lambda^2\rho + \rho \right)^2}
\end{aligned}$$

b. Reaction in compartment B

[78]: `KQbd = replaced(KQb)`
`KQbd`

[78]:

$$\begin{aligned}
& \rho^2 + 2\kappa^2\lambda^2\rho^2 + \kappa^4\lambda^4\rho^2 + 4\delta\kappa\lambda\rho + 4\delta\kappa^3\lambda^3\rho + 4\delta^2\kappa^2\lambda^2 + 4\beta\delta\gamma\kappa\lambda\rho\theta + 4\beta\delta\gamma\kappa^3\lambda^3\rho\theta + 8\beta\delta^2\gamma\kappa^2\lambda^2\theta \\
& - 4\beta^2\delta\gamma\kappa\lambda\rho\theta^2 - 4\beta^2\delta\gamma\kappa^3\lambda^3\rho\theta^2 - 4\beta^2\delta\gamma^2\kappa\lambda\rho\theta^2 + 4\beta^2\delta\gamma^2\kappa^3\lambda^3\rho\theta^2 - 8\beta^2\delta^2\gamma\kappa^2\lambda^2\theta^2 + 8\beta^2\delta^2\gamma^2\kappa^2\lambda^2\theta^2 + O(\theta^3)
\end{aligned}$$

$$(2\delta\kappa\lambda + \kappa^2\lambda^2\rho + \rho)^2$$

[79]: `alpha_bd = develop(sp.log(KQbd)).simplify()`
`alpha_bd`

[79]:

$$\begin{aligned}
& \frac{4\beta\delta\gamma\kappa\lambda\theta(2\delta\kappa\lambda + \kappa^2\lambda^2\rho + \rho)(4\delta^2\kappa^2\lambda^2 + 4\delta\kappa^3\lambda^3\rho + 4\delta\kappa\lambda\rho + \kappa^4\lambda^4\rho^2 + 2\kappa^2\lambda^2\rho^2 + \rho^2)^3}{(4\delta^2\kappa^2\lambda^2 + 4\delta\kappa^3\lambda^3\rho + 4\delta\kappa\lambda\rho + \kappa^4\lambda^4\rho^2 + 2\kappa^2\lambda^2\rho^2 + \rho^2)^4} \\
& - \frac{4\beta^2\delta\gamma\kappa\lambda\theta^2(4\delta^2\kappa^2\lambda^2 + 4\delta\kappa^3\lambda^3\rho + 4\delta\kappa\lambda\rho + \kappa^4\lambda^4\rho^2 + 2\kappa^2\lambda^2\rho^2 + \rho^2)^2}{(4\delta^2\kappa^2\lambda^2 + 4\delta\kappa^3\lambda^3\rho + 4\delta\kappa\lambda\rho + \kappa^4\lambda^4\rho^2 + 2\kappa^2\lambda^2\rho^2 + \rho^2)^4} \\
& \cdot \left(2\delta\gamma\kappa\lambda(2\delta\kappa\lambda + \kappa^2\lambda^2\rho + \rho)^2 \right. \\
& + \left(4\delta^2\kappa^2\lambda^2 + 4\delta\kappa^3\lambda^3\rho + 4\delta\kappa\lambda\rho + \kappa^4\lambda^4\rho^2 + 2\kappa^2\lambda^2\rho^2 + \rho^2 \right) \\
& \cdot \left(-2\delta\gamma\kappa\lambda + 2\delta\kappa\lambda - \gamma\kappa^2\lambda^2\rho + \gamma\rho + \kappa^2\lambda^2\rho + \rho \right) \\
& \left. + O(\theta^3) \right)
\end{aligned}$$

[80]: alpha_bd2=full_remove0(alpha_bd)
alpha_bd2

[80]:

$$-\frac{4\beta\delta\gamma\kappa\lambda\theta(2\beta\delta\kappa\lambda\theta - \beta\gamma\kappa^2\lambda^2\rho\theta + \beta\gamma\rho\theta + \beta\kappa^2\lambda^2\rho\theta + \beta\rho\theta - 2\delta\kappa\lambda - \kappa^2\lambda^2\rho - \rho)}{(2\delta\kappa\lambda + \kappa^2\lambda^2\rho + \rho)^2}$$

c. Total reaction

[81]: alpha_rd = (alpha_bd-alpha_ad).simplify()
alpha_rd

[81]:

$$\frac{8\beta\delta\gamma\kappa\lambda\theta(2\delta\kappa\lambda + \kappa^2\lambda^2\rho + \rho)(4\delta^2\kappa^2\lambda^2 + 4\delta\kappa^3\lambda^3\rho + 4\delta\kappa\lambda\rho + \kappa^4\lambda^4\rho^2 + 2\kappa^2\lambda^2\rho^2 + \rho^2)^3 + O(\theta^3)}{(4\delta^2\kappa^2\lambda^2 + 4\delta\kappa^3\lambda^3\rho + 4\delta\kappa\lambda\rho + \kappa^4\lambda^4\rho^2 + 2\kappa^2\lambda^2\rho^2 + \rho^2)^4}$$

[82]: alpha_rd2 = (alpha_bd2-alpha_ad2).simplify()
alpha_rd2

[82]:

$$\frac{8\beta\delta\gamma\kappa\lambda\theta}{2\delta\kappa\lambda + \kappa^2\lambda^2\rho + \rho}$$

[83]: alpha_r_ok = to_h_kp(alpha_rd2)
alpha_r_ok

[83]:

$$\frac{2\eta\lambda'\delta\theta}{\lambda'\delta + \rho}$$

d. Further simplification of independent reactions:

e. identification of ϵ

```
[84]: f_d2 = (((-alpha_ad2-alpha_bd2).simplify()/alpha_rd2/theta)-beta).simplify()
f_d2
```

[84] :

$$\frac{\beta \gamma \rho (-\kappa^2 \lambda^2 + 1)}{2 \delta \kappa \lambda + \kappa^2 \lambda^2 \rho + \rho}$$

```
[85]: epsilon_d2 = (beta+f_d2)
epsilon_d2
```

[85] :

$$\frac{\beta \gamma \rho (-\kappa^2 \lambda^2 + 1)}{2 \delta \kappa \lambda + \kappa^2 \lambda^2 \rho + \rho} + \beta$$

```
[86]: epsilon_ok = to_h_kp(f_d2.factor(rho))+beta
epsilon_ok
```

[86] :

$$-\frac{\eta \rho (\kappa^2 \lambda^2 - 1)}{2(\lambda' \delta + \rho)(\kappa^2 \lambda^2 + 1)} + \beta$$

f. ϵ properties

```
[87]: epsilon_d2.replace(kappa,0).simplify()
```

[87] :

$$\beta(\gamma+1)$$

```
[88]: epsilon_d2.replace(lamb,0).simplify()
```

[88] :

$$\beta(\gamma+1)$$

```
[89]: epsilon_d2.replace(kappa,1/lamb).replace(lp,1).simplify()
```

[89] :

$$\beta$$

```
[90]: sp.limit(epsilon_d2, kappa,sp.oo).simplify()
```

[90] :

$$\beta(1-\gamma)$$

```
[91]: sp.limit(epsilon_d2, lamb,sp.oo).simplify()
```

[91] :

$$\beta(1-\gamma)$$

```
[92]: sp.limit(epsilon_ok-beta, rho,sp.oo)+beta
```

[92] :

$$-\frac{\eta (\kappa^2 \lambda^2 - 1)}{2 (\kappa^2 \lambda^2 + 1)} + \beta$$

```
[93]: sp.limit(epsilon_d2, rho,0).simplify()
```

[93] :

$$\beta$$

g. Simplified expressions

```
[94]: (alpha_ad2 + alpha_rd2/2*(epsilon_d2*theta+1)).simplify()
```

[94] :

$$0$$

```
[95]: alpha_a_s = -alpha_rd2/2*(epsilon*theta+1)
alpha_a_s
```

[95] :

$$-\frac{4\beta\delta\gamma\kappa\lambda\theta(\varepsilon\theta+1)}{2\delta\kappa\lambda+\kappa^2\lambda^2\rho+\rho}$$

```
[96]: alpha_a_ok = to_h_kp(alpha_a_s)
alpha_a_ok
```

[96] :

$$-\frac{\eta\lambda'\delta\theta(\varepsilon\theta+1)}{\lambda'\delta+\rho}$$

```
[97]: alpha_a_ok/alpha_r_ok
```

[97] :

$$-\frac{\varepsilon\theta}{2} - \frac{1}{2}$$

```
[98]: (alpha_bd2 - alpha_rd2/2*(1-epsilon_d2*theta)).simplify()
```

[98] :

$$0$$

```
[99]: alpha_b_s = alpha_rd2/2*(1-epsilon*theta)
alpha_b_s
```

[99] :

$$\frac{4\beta\delta\gamma\kappa\lambda\theta(-\varepsilon\theta+1)}{2\delta\kappa\lambda+\kappa^2\lambda^2\rho+\rho}$$

```
[100]: alpha_b_ok = to_h_kp(alpha_b_s)
alpha_b_ok
```

[100]:

$$\frac{\eta \lambda' \delta \theta (-\varepsilon \theta + 1)}{\lambda' \delta + \rho}$$

```
[101]: alpha_b_ok/alpha_r_ok
```

[101]:

$$-\frac{\varepsilon \theta}{2} + \frac{1}{2}$$

h. Diffusion of U_1

```
[102]: KQ_diff1d = replaced(KQ_diff1)
KQ_diff1d
```

[102]:

$$\frac{\rho^2 + 2\kappa^2\lambda^2\rho^2 + \kappa^4\lambda^4\rho^2 + 4\delta\kappa\lambda\rho + 4\delta\kappa^3\lambda^3\rho + 4\delta^2\kappa^2\lambda^2 + 4\beta\gamma\kappa^2\lambda^2\rho^2\theta + 4\beta\gamma\kappa^4\lambda^4\rho^2\theta + 8\beta\delta\gamma\kappa^3\lambda^3\rho\theta + 8\beta^2\gamma^2\kappa^4\lambda^4\rho^2\theta^2 + O(\theta^3)}{(2\delta\kappa\lambda + \kappa^2\lambda^2\rho + \rho)^2}$$

```
[103]: alpha_diff1d = develop(sp.log(KQ_diff1d)).simplify()
alpha_diff1d
```

[103]:

$$\frac{4\beta\gamma\kappa^2\lambda^2\rho\theta(2\delta\kappa\lambda + \kappa^2\lambda^2\rho + \rho)(4\delta^2\kappa^2\lambda^2 + 4\delta\kappa^3\lambda^3\rho + 4\delta\kappa\lambda\rho + \kappa^4\lambda^4\rho^2 + 2\kappa^2\lambda^2\rho^2 + \rho^2)^3 + 8\beta^2\gamma^2\kappa^4\lambda^4\rho^2\theta^2(4\delta^2\kappa^2\lambda^2 + 4\delta\kappa^3\lambda^3\rho + 4\delta\kappa\lambda\rho + \kappa^4\lambda^4\rho^2 + 2\kappa^2\lambda^2\rho^2 + \rho^2)^2 \cdot (4\delta^2\kappa^2\lambda^2 + 4\delta\kappa^3\lambda^3\rho + 4\delta\kappa\lambda\rho + \kappa^4\lambda^4\rho^2 + 2\kappa^2\lambda^2\rho^2 + \rho^2 - (2\delta\kappa\lambda + \kappa^2\lambda^2\rho + \rho)^2) + O(\theta^3)}{(4\delta^2\kappa^2\lambda^2 + 4\delta\kappa^3\lambda^3\rho + 4\delta\kappa\lambda\rho + \kappa^4\lambda^4\rho^2 + 2\kappa^2\lambda^2\rho^2 + \rho^2)^4}$$

```
[104]: alpha_diff1d2=full_remove0(alpha_diff1d)
alpha_diff1d2
```

[104]:

$$\frac{4\beta\gamma\kappa^2\lambda^2\rho\theta}{2\delta\kappa\lambda + \kappa^2\lambda^2\rho + \rho}$$

```
[105]: alpha_diff1_ok = to_h_kp(alpha_diff1d2/kappa)*kappa
alpha_diff1_ok
```

[105]:

$$\frac{\eta \lambda' \kappa \lambda \rho \theta}{\lambda' \delta + \rho}$$

i. Diffusion of U_2

```
[106]: KQ_diff2d = replaced(KQ_diff2)
KQ_diff2d
```

[106]:

$$\frac{\rho^2 + 2\kappa^2\lambda^2\rho^2 + \kappa^4\lambda^4\rho^2 + 4\delta\kappa\lambda\rho + 4\delta\kappa^3\lambda^3\rho + 4\delta^2\kappa^2\lambda^2 - 4\beta\gamma\rho^2\theta - 4\beta\gamma\kappa^2\lambda^2\rho^2\theta - 8\beta\delta\gamma\kappa\lambda\rho\theta + 8\beta^2\gamma^2\rho^2\theta^2 + O(\theta^3)}{(2\delta\kappa\lambda + \kappa^2\lambda^2\rho + \rho)^2}$$

```
[107]: alpha_diff2d = develop(sp.log(KQ_diff2d)).simplify()
alpha_diff2d
```

[107]:

$$\frac{-4\beta\gamma\rho\theta(2\delta\kappa\lambda + \kappa^2\lambda^2\rho + \rho)(4\delta^2\kappa^2\lambda^2 + 4\delta\kappa^3\lambda^3\rho + 4\delta\kappa\lambda\rho + \kappa^4\lambda^4\rho^2 + 2\kappa^2\lambda^2\rho^2 + \rho^2)^3 + 8\beta^2\gamma^2\rho^2\theta^2(4\delta^2\kappa^2\lambda^2 + 4\delta\kappa^3\lambda^3\rho + 4\delta\kappa\lambda\rho + \kappa^4\lambda^4\rho^2 + 2\kappa^2\lambda^2\rho^2 + \rho^2)^2 \cdot (4\delta^2\kappa^2\lambda^2 + 4\delta\kappa^3\lambda^3\rho + 4\delta\kappa\lambda\rho + \kappa^4\lambda^4\rho^2 + 2\kappa^2\lambda^2\rho^2 + \rho^2) - (2\delta\kappa\lambda + \kappa^2\lambda^2\rho + \rho)^2 + O(\theta^3)}{(4\delta^2\kappa^2\lambda^2 + 4\delta\kappa^3\lambda^3\rho + 4\delta\kappa\lambda\rho + \kappa^4\lambda^4\rho^2 + 2\kappa^2\lambda^2\rho^2 + \rho^2)^4}$$

```
[108]: alpha_diff2d2=full_remove0(alpha_diff2d)
alpha_diff2d2
```

[108]:

$$-\frac{4\beta\gamma\rho\theta}{2\delta\kappa\lambda + \kappa^2\lambda^2\rho + \rho}$$

```
[109]: alpha_diff2_ok = to_h_kp(alpha_diff2d2*kappa*lamb*4)/kappa/lamb/4
alpha_diff2_ok
```

[109]:

$$-\frac{\eta\lambda'\rho\theta}{\kappa\lambda(\lambda'\delta + \rho)}$$

j. Total diffusion

```
[110]: alpha_diffd = (alpha_diff1d-alpha_diff2d).simplify()
alpha_diffd
```

[110]:

$$\frac{4\beta\gamma\rho\theta(2\delta\kappa\lambda + \kappa^2\lambda^2\rho + \rho)(4\delta^2\kappa^2\lambda^2 + 4\delta\kappa^3\lambda^3\rho + 4\delta\kappa\lambda\rho + \kappa^4\lambda^4\rho^2 + 2\kappa^2\lambda^2\rho^2 + \rho^2)^3 + 4\beta\gamma\kappa^2\lambda^2\rho\theta(2\delta\kappa\lambda + \kappa^2\lambda^2\rho + \rho)(4\delta^2\kappa^2\lambda^2 + 4\delta\kappa^3\lambda^3\rho + 4\delta\kappa\lambda\rho + \kappa^4\lambda^4\rho^2 + 2\kappa^2\lambda^2\rho^2 + \rho^2)^3 + 8\beta^2\gamma^2\rho^2\theta^2(4\delta^2\kappa^2\lambda^2 + 4\delta\kappa^3\lambda^3\rho + 4\delta\kappa\lambda\rho + \kappa^4\lambda^4\rho^2 + 2\kappa^2\lambda^2\rho^2 + \rho^2)^2 \cdot (-4\delta^2\kappa^2\lambda^2 - 4\delta\kappa^3\lambda^3\rho - 4\delta\kappa\lambda\rho - \kappa^4\lambda^4\rho^2 - 2\kappa^2\lambda^2\rho^2 - \rho^2 + (2\delta\kappa\lambda + \kappa^2\lambda^2\rho + \rho)^2) + 8\beta^2\gamma^2\kappa^4\lambda^4\rho^2\theta^2(4\delta^2\kappa^2\lambda^2 + 4\delta\kappa^3\lambda^3\rho + 4\delta\kappa\lambda\rho + \kappa^4\lambda^4\rho^2 + 2\kappa^2\lambda^2\rho^2 + \rho^2)^2 \cdot (4\delta^2\kappa^2\lambda^2 + 4\delta\kappa^3\lambda^3\rho + 4\delta\kappa\lambda\rho + \kappa^4\lambda^4\rho^2 + 2\kappa^2\lambda^2\rho^2 + \rho^2 - (2\delta\kappa\lambda + \kappa^2\lambda^2\rho + \rho)^2) + O(\theta^3)}{(4\delta^2\kappa^2\lambda^2 + 4\delta\kappa^3\lambda^3\rho + 4\delta\kappa\lambda\rho + \kappa^4\lambda^4\rho^2 + 2\kappa^2\lambda^2\rho^2 + \rho^2)^4}$$

```
[111]: alpha_diffd2 = (alpha_diff1d2-alpha_diff2d2).simplify()
alpha_diffd2
```

[111]:

$$\frac{4\beta\gamma\rho\theta(\kappa^2\lambda^2+1)}{2\delta\kappa\lambda+\kappa^2\lambda^2\rho+\rho}$$

```
[112]: alpha_diff_ok = to_h_kp(alpha_diffd2)
alpha_diff_ok
```

[112]:

$$\frac{2\eta\rho\theta}{\lambda'\delta+\rho}$$

```
[113]: alpha_diff1_ok/alpha_diff_ok
```

[113]:

$$\frac{\lambda'\kappa\lambda}{2}$$

```
[114]: alpha_diff2_ok/alpha_diff_ok
```

[114]:

$$-\frac{\lambda'}{2\kappa\lambda}$$

k. Total α

```
[115]: alpha_d = (alpha_rd+alpha_diffd).simplify()
alpha_d
```

[115]:

$$\begin{aligned} & \frac{4\beta\gamma\rho\theta(2\delta\kappa\lambda+\kappa^2\lambda^2\rho+\rho)(4\delta^2\kappa^2\lambda^2+4\delta\kappa^3\lambda^3\rho+4\delta\kappa\lambda\rho+\kappa^4\lambda^4\rho^2+2\kappa^2\lambda^2\rho^2+\rho^2)^3}{(4\delta^2\kappa^2\lambda^2+4\delta\kappa^3\lambda^3\rho+4\delta\kappa\lambda\rho+\kappa^4\lambda^4\rho^2+2\kappa^2\lambda^2\rho^2+\rho^2)^4} \\ & + 4\beta\gamma\kappa^2\lambda^2\rho\theta(2\delta\kappa\lambda+\kappa^2\lambda^2\rho+\rho)(4\delta^2\kappa^2\lambda^2+4\delta\kappa^3\lambda^3\rho+4\delta\kappa\lambda\rho+\kappa^4\lambda^4\rho^2+2\kappa^2\lambda^2\rho^2+\rho^2)^3 \\ & + 8\beta\delta\gamma\kappa\lambda\theta(2\delta\kappa\lambda+\kappa^2\lambda^2\rho+\rho)(4\delta^2\kappa^2\lambda^2+4\delta\kappa^3\lambda^3\rho+4\delta\kappa\lambda\rho+\kappa^4\lambda^4\rho^2+2\kappa^2\lambda^2\rho^2+\rho^2)^3 \\ & + 8\beta^2\gamma^2\rho^2\theta^2(4\delta^2\kappa^2\lambda^2+4\delta\kappa^3\lambda^3\rho+4\delta\kappa\lambda\rho+\kappa^4\lambda^4\rho^2+2\kappa^2\lambda^2\rho^2+\rho^2)^2 \\ & \cdot \left(-4\delta^2\kappa^2\lambda^2-4\delta\kappa^3\lambda^3\rho-4\delta\kappa\lambda\rho-\kappa^4\lambda^4\rho^2-2\kappa^2\lambda^2\rho^2-\rho^2 + (2\delta\kappa\lambda+\kappa^2\lambda^2\rho+\rho)^2 \right) \\ & + 8\beta^2\gamma^2\kappa^4\lambda^4\rho^2\theta^2(4\delta^2\kappa^2\lambda^2+4\delta\kappa^3\lambda^3\rho+4\delta\kappa\lambda\rho+\kappa^4\lambda^4\rho^2+2\kappa^2\lambda^2\rho^2+\rho^2)^2 \\ & \cdot \left(4\delta^2\kappa^2\lambda^2+4\delta\kappa^3\lambda^3\rho+4\delta\kappa\lambda\rho+\kappa^4\lambda^4\rho^2+2\kappa^2\lambda^2\rho^2+\rho^2 - (2\delta\kappa\lambda+\kappa^2\lambda^2\rho+\rho)^2 \right) \\ & + O(\theta^3) \end{aligned}$$

```
[116]: alpha_d2 = (alpha_rd2+alpha_diffd2).simplify()
alpha_d2
```

[116]:

$$4\beta\gamma\theta$$

```
[117]: alpha_ok = to_h_kp(alpha_d2)
alpha_ok
```

[117]:

$$2\eta\theta$$

l. Ratios

```
[118]: alpha_diff_ok/alpha_ok
```

[118]:

$$\frac{\rho}{\lambda'\delta + \rho}$$

```
[119]: alpha_r_ok/alpha_ok
```

[119]:

$$\frac{\lambda'\delta}{\lambda'\delta + \rho}$$

```
[120]: (alpha_a_ok/alpha_r_ok).factor()
```

[120]:

$$-\frac{\varepsilon\theta + 1}{2}$$

```
[121]: (alpha_b_ok/alpha_r_ok).factor()
```

[121]:

$$-\frac{\varepsilon\theta - 1}{2}$$

```
[122]: (alpha_diff1_ok/alpha_diff_ok).simplify()
```

[122]:

$$\frac{\lambda'\kappa\lambda}{2}$$

```
[123]: (-alpha_diff2_ok/alpha_diff_ok).simplify()
```

[123]:

$$\frac{\lambda'}{2\kappa\lambda}$$

[124]: `alpha_r_ok/alpha_diff_ok`

[124]:

$$\frac{\lambda' \delta}{\rho}$$

5. *Chemical resistance* $R = \alpha/\varphi$

[125]: `r_tot = alpha_ok/phi_ok`
`r_tot`

[125]:

$$\frac{4(\lambda' \delta + \rho)}{\kappa' \lambda' \delta \rho}$$

[126]: `r_r = alpha_r_ok/phi_ok`
`r_r`

[126]:

$$\frac{4}{\kappa' \rho}$$

[127]: `r_diff = alpha_diff_ok/phi_ok`
`r_diff`

[127]:

$$\frac{4}{\kappa' \lambda' \delta}$$

[128]: `r_a = -alpha_a_ok/phi_ok`
`r_a`

[128]:

$$\frac{2(\varepsilon \theta + 1)}{\kappa' \rho}$$

[129]: `r_b = alpha_b_ok/phi_ok`
`r_b`

[129]:

$$\frac{2(-\varepsilon \theta + 1)}{\kappa' \rho}$$

[130]: `r_diff1 = alpha_diff1_ok/phi_ok`
`r_diff1`

[130]:

$$\frac{2\kappa\lambda}{\kappa' \delta}$$

```
[131]: r_diff2 = -alpha_diff2_ok/phi_ok
r_diff2
```

[131]:

$$\frac{2}{\kappa' \delta \kappa \lambda}$$

6. σ

```
[132]: sigmad = (alpha_d*phid).simplify()
sigmad
```

[132]:

$$\begin{aligned} & \left(4\beta\delta\gamma\kappa^2\lambda\rho\theta + O(\theta^3) \right) \\ & \cdot \left(4\beta\gamma\rho\theta (2\delta\kappa\lambda + \kappa^2\lambda^2\rho + \rho) \left(4\delta^2\kappa^2\lambda^2 + 4\delta\kappa^3\lambda^3\rho + 4\delta\kappa\lambda\rho + \kappa^4\lambda^4\rho^2 + 2\kappa^2\lambda^2\rho^2 + \rho^2 \right)^3 \right. \\ & \quad \left. + 4\beta\gamma\kappa^2\lambda^2\rho\theta (2\delta\kappa\lambda + \kappa^2\lambda^2\rho + \rho) \left(4\delta^2\kappa^2\lambda^2 + 4\delta\kappa^3\lambda^3\rho + 4\delta\kappa\lambda\rho + \kappa^4\lambda^4\rho^2 + 2\kappa^2\lambda^2\rho^2 + \rho^2 \right)^3 \right. \\ & \quad \left. + 8\beta\delta\gamma\kappa\lambda\theta (2\delta\kappa\lambda + \kappa^2\lambda^2\rho + \rho) \left(4\delta^2\kappa^2\lambda^2 + 4\delta\kappa^3\lambda^3\rho + 4\delta\kappa\lambda\rho + \kappa^4\lambda^4\rho^2 + 2\kappa^2\lambda^2\rho^2 + \rho^2 \right)^3 \right. \\ & \quad \left. + 8\beta^2\gamma^2\rho^2\theta^2 (4\delta^2\kappa^2\lambda^2 + 4\delta\kappa^3\lambda^3\rho + 4\delta\kappa\lambda\rho + \kappa^4\lambda^4\rho^2 + 2\kappa^2\lambda^2\rho^2 + \rho^2)^2 \right. \\ & \quad \left. \cdot \left(-4\delta^2\kappa^2\lambda^2 - 4\delta\kappa^3\lambda^3\rho - 4\delta\kappa\lambda\rho - \kappa^4\lambda^4\rho^2 - 2\kappa^2\lambda^2\rho^2 - \rho^2 + (2\delta\kappa\lambda + \kappa^2\lambda^2\rho + \rho)^2 \right) \right. \\ & \quad \left. + 8\beta^2\gamma^2\kappa^4\lambda^4\rho^2\theta^2 (4\delta^2\kappa^2\lambda^2 + 4\delta\kappa^3\lambda^3\rho + 4\delta\kappa\lambda\rho + \kappa^4\lambda^4\rho^2 + 2\kappa^2\lambda^2\rho^2 + \rho^2)^2 \right. \\ & \quad \left. \cdot \left(4\delta^2\kappa^2\lambda^2 + 4\delta\kappa^3\lambda^3\rho + 4\delta\kappa\lambda\rho + \kappa^4\lambda^4\rho^2 + 2\kappa^2\lambda^2\rho^2 + \rho^2 - (2\delta\kappa\lambda + \kappa^2\lambda^2\rho + \rho)^2 \right) \right. \\ & \quad \left. + O(\theta^3) \right) \\ & \hline (\kappa^2 + 1) (2\delta\kappa\lambda + \kappa^2\lambda^2\rho + \rho) (4\delta^2\kappa^2\lambda^2 + 4\delta\kappa^3\lambda^3\rho + 4\delta\kappa\lambda\rho + \kappa^4\lambda^4\rho^2 + 2\kappa^2\lambda^2\rho^2 + \rho^2)^4 \end{aligned}$$

```
[133]: sigmad2 = full_remove0(alpha_d2*phid2).simplify()
sigmad2
```

[133]:

$$\frac{16\beta^2\delta\gamma^2\kappa^2\lambda\rho\theta^2}{(\kappa^2 + 1) (2\delta\kappa\lambda + \kappa^2\lambda^2\rho + \rho)}$$

```
[134]: sigma_ok = to_h_kp(sigmad2)
sigma_ok
```

[134]:

$$\frac{\eta^2\kappa'\lambda'\delta\rho\theta^2}{\lambda'\delta + \rho}$$

```
[135]: sigma_diffd = (alpha_diffd*phid).simplify()
sigma_diffd
```

[135]:

$$\begin{aligned} & \left(4\beta\delta\gamma\kappa^2\lambda\rho\theta + O(\theta^3)\right) \\ & \cdot \left(4\beta\gamma\rho\theta(2\delta\kappa\lambda + \kappa^2\lambda^2\rho + \rho)(4\delta^2\kappa^2\lambda^2 + 4\delta\kappa^3\lambda^3\rho + 4\delta\kappa\lambda\rho + \kappa^4\lambda^4\rho^2 + 2\kappa^2\lambda^2\rho^2 + \rho^2)^3\right. \\ & \quad \left.+ 4\beta\gamma\kappa^2\lambda^2\rho\theta(2\delta\kappa\lambda + \kappa^2\lambda^2\rho + \rho)(4\delta^2\kappa^2\lambda^2 + 4\delta\kappa^3\lambda^3\rho + 4\delta\kappa\lambda\rho + \kappa^4\lambda^4\rho^2 + 2\kappa^2\lambda^2\rho^2 + \rho^2)^3\right. \\ & \quad \left.+ 8\beta^2\gamma^2\rho^2\theta^2(4\delta^2\kappa^2\lambda^2 + 4\delta\kappa^3\lambda^3\rho + 4\delta\kappa\lambda\rho + \kappa^4\lambda^4\rho^2 + 2\kappa^2\lambda^2\rho^2 + \rho^2)^2\right. \\ & \quad \left.\cdot \left(-4\delta^2\kappa^2\lambda^2 - 4\delta\kappa^3\lambda^3\rho - 4\delta\kappa\lambda\rho - \kappa^4\lambda^4\rho^2 - 2\kappa^2\lambda^2\rho^2 - \rho^2 + (2\delta\kappa\lambda + \kappa^2\lambda^2\rho + \rho)^2\right)\right. \\ & \quad \left.+ 8\beta^2\gamma^2\kappa^4\lambda^4\rho^2\theta^2(4\delta^2\kappa^2\lambda^2 + 4\delta\kappa^3\lambda^3\rho + 4\delta\kappa\lambda\rho + \kappa^4\lambda^4\rho^2 + 2\kappa^2\lambda^2\rho^2 + \rho^2)^2\right. \\ & \quad \left.\cdot \left(4\delta^2\kappa^2\lambda^2 + 4\delta\kappa^3\lambda^3\rho + 4\delta\kappa\lambda\rho + \kappa^4\lambda^4\rho^2 + 2\kappa^2\lambda^2\rho^2 + \rho^2 - (2\delta\kappa\lambda + \kappa^2\lambda^2\rho + \rho)^2\right) + O(\theta^3)\right) \\ & \hline (\kappa^2 + 1)(2\delta\kappa\lambda + \kappa^2\lambda^2\rho + \rho)(4\delta^2\kappa^2\lambda^2 + 4\delta\kappa^3\lambda^3\rho + 4\delta\kappa\lambda\rho + \kappa^4\lambda^4\rho^2 + 2\kappa^2\lambda^2\rho^2 + \rho^2)^4 \end{aligned}$$

```
[136]: sigma_diffd2 = full_remove0(sigma_diffd)
sigma_diffd2
```

[136]:

$$\frac{16\beta^2\delta\gamma^2\kappa^2\lambda\rho^2\theta^2(\kappa^2\lambda^2 + 1)}{(\kappa^2 + 1)(2\delta\kappa\lambda + \kappa^2\lambda^2\rho + \rho)^2}$$

```
[137]: sigma_diff_ok = to_h_kp(sigma_diffd2).factor()
sigma_diff_ok
```

[137]:

$$\frac{\eta^2\kappa'\lambda'\delta\rho^2\theta^2}{(\lambda'\delta + \rho)^2}$$

```
[138]: sigma_rd = (alpha_rd*phid).simplify()
sigma_rd
```

[138]:

$$\begin{aligned} & \left(4\beta\delta\gamma\kappa^2\lambda\rho\theta + O(\theta^3)\right) \\ & \cdot \left(8\beta\delta\gamma\kappa\lambda\theta(2\delta\kappa\lambda + \kappa^2\lambda^2\rho + \rho)(4\delta^2\kappa^2\lambda^2 + 4\delta\kappa^3\lambda^3\rho + 4\delta\kappa\lambda\rho + \kappa^4\lambda^4\rho^2 + 2\kappa^2\lambda^2\rho^2 + \rho^2)^3 + O(\theta^3)\right) \\ & \hline (\kappa^2 + 1)(2\delta\kappa\lambda + \kappa^2\lambda^2\rho + \rho)(4\delta^2\kappa^2\lambda^2 + 4\delta\kappa^3\lambda^3\rho + 4\delta\kappa\lambda\rho + \kappa^4\lambda^4\rho^2 + 2\kappa^2\lambda^2\rho^2 + \rho^2)^4 \end{aligned}$$

```
[139]: sigma_rd2 = full_remove0(sigma_rd)
sigma_rd2
```

[139]:

$$\frac{32\beta^2\delta^2\gamma^2\kappa^3\lambda^2\rho\theta^2}{(\kappa^2+1)(2\delta\kappa\lambda+\kappa^2\lambda^2\rho+\rho)^2}$$

[140]: `sigma_r_ok = to_h_kp(sigma_rd2).factor()`

[140]:

$$\frac{\eta^2\kappa'\lambda'^2\delta^2\rho\theta^2}{(\lambda'\delta+\rho)^2}$$

[141]: `(sigma_diff_ok+sigma_r_ok).simplify()`

[141]:

$$\frac{\eta^2\kappa'\lambda'\delta\rho\theta^2}{\lambda'\delta+\rho}$$

a. Ratios

[142]: `sigma_r_ok/sigma_diff_ok`

[142]:

$$\frac{\lambda'\delta}{\rho}$$

[143]: `sigma_diff_ok/sigma_ok`

[143]:

$$\frac{\rho}{\lambda'\delta+\rho}$$

7. \mathcal{A}

[144]: `a_a_d = develop((1-theta)*alpha_ad)`
`a_a_d`

[144]:

$$\begin{aligned}
& \theta \left(-\frac{8\beta\delta^2\gamma\kappa^2\lambda^2}{4\delta^2\kappa^2\lambda^2 + 4\delta\kappa^3\lambda^3\rho + 4\delta\kappa\lambda\rho + \kappa^4\lambda^4\rho^2 + 2\kappa^2\lambda^2\rho^2 + \rho^2} \right. \\
& \quad - \frac{4\beta\delta\gamma\kappa^3\lambda^3\rho}{4\delta^2\kappa^2\lambda^2 + 4\delta\kappa^3\lambda^3\rho + 4\delta\kappa\lambda\rho + \kappa^4\lambda^4\rho^2 + 2\kappa^2\lambda^2\rho^2 + \rho^2} \\
& \quad \left. - \frac{4\beta\delta\gamma\kappa\lambda\rho}{4\delta^2\kappa^2\lambda^2 + 4\delta\kappa^3\lambda^3\rho + 4\delta\kappa\lambda\rho + \kappa^4\lambda^4\rho^2 + 2\kappa^2\lambda^2\rho^2 + \rho^2} \right) \\
& + \theta^2 \left(-\frac{8\beta^2\delta^2\gamma^2\kappa^2\lambda^2(2\delta\kappa\lambda + \kappa^2\lambda^2\rho + \rho)^2}{(4\delta^2\kappa^2\lambda^2 + 4\delta\kappa^3\lambda^3\rho + 4\delta\kappa\lambda\rho + \kappa^4\lambda^4\rho^2 + 2\kappa^2\lambda^2\rho^2 + \rho^2)^2} \right. \\
& \quad - \frac{4\beta^2\delta\gamma\kappa\lambda(-2\delta\gamma\kappa\lambda + 2\delta\kappa\lambda - \gamma\kappa^2\lambda^2\rho + \gamma\rho + \kappa^2\lambda^2\rho + \rho)}{4\delta^2\kappa^2\lambda^2 + 4\delta\kappa^3\lambda^3\rho + 4\delta\kappa\lambda\rho + \kappa^4\lambda^4\rho^2 + 2\kappa^2\lambda^2\rho^2 + \rho^2} \\
& \quad + \frac{8\beta\delta^2\gamma\kappa^2\lambda^2}{4\delta^2\kappa^2\lambda^2 + 4\delta\kappa^3\lambda^3\rho + 4\delta\kappa\lambda\rho + \kappa^4\lambda^4\rho^2 + 2\kappa^2\lambda^2\rho^2 + \rho^2} \\
& \quad + \frac{4\beta\delta\gamma\kappa^3\lambda^3\rho}{4\delta^2\kappa^2\lambda^2 + 4\delta\kappa^3\lambda^3\rho + 4\delta\kappa\lambda\rho + \kappa^4\lambda^4\rho^2 + 2\kappa^2\lambda^2\rho^2 + \rho^2} \\
& \quad \left. + \frac{4\beta\delta\gamma\kappa\lambda\rho}{4\delta^2\kappa^2\lambda^2 + 4\delta\kappa^3\lambda^3\rho + 4\delta\kappa\lambda\rho + \kappa^4\lambda^4\rho^2 + 2\kappa^2\lambda^2\rho^2 + \rho^2} \right) \\
& + O(\theta^3)
\end{aligned}$$

[145]: a_a_d2 = full_remove0(a_a_d)
a_a_d2

[145]:

$$-\frac{4\beta\delta\gamma\kappa\lambda\theta(2\beta\delta\kappa\lambda\theta - \beta\gamma\kappa^2\lambda^2\rho\theta + \beta\gamma\rho\theta + \beta\kappa^2\lambda^2\rho\theta + \beta\rho\theta - 2\delta\kappa\lambda\theta + 2\delta\kappa\lambda - \kappa^2\lambda^2\rho\theta + \kappa^2\lambda^2\rho - \rho\theta + \rho)}{(2\delta\kappa\lambda + \kappa^2\lambda^2\rho + \rho)^2}$$

[146]: a_a_s = (alpha_a_s+a_a_d2-alpha_ad2).simplify()
a_a_s

[146]:

$$\frac{4\beta\delta\gamma\kappa\lambda\theta(-\varepsilon\theta + \theta - 1)}{2\delta\kappa\lambda + \kappa^2\lambda^2\rho + \rho}$$

[147]: a_a_ok = to_h_kp(a_a_s)
a_a_ok

[147]:

$$\frac{\eta\lambda'\delta\theta(-\varepsilon\theta + \theta - 1)}{\lambda'\delta + \rho}$$

```
[148]: a_b_d = develop((1+theta)*alpha_bd)
a_b_d2 = full_remove0(a_b_d)
a_b_d2
```

[148] :

$$-\frac{4\beta\delta\gamma\kappa\lambda\theta(2\beta\delta\kappa\lambda\theta - \beta\gamma\kappa^2\lambda^2\rho\theta + \beta\gamma\rho\theta + \beta\kappa^2\lambda^2\rho\theta + \beta\rho\theta - 2\delta\kappa\lambda\theta - 2\delta\kappa\lambda - \kappa^2\lambda^2\rho\theta - \kappa^2\lambda^2\rho - \rho\theta - \rho)}{(2\delta\kappa\lambda + \kappa^2\lambda^2\rho + \rho)^2}$$

```
[149]: a_b_s = (alpha_b_s+a_b_d2-alpha_bd2).simplify()
a_b_s
```

[149] :

$$\frac{4\beta\delta\gamma\kappa\lambda\theta(-\varepsilon\theta + \theta + 1)}{2\delta\kappa\lambda + \kappa^2\lambda^2\rho + \rho}$$

```
[150]: a_b_ok = to_h_kp(a_b_s)
a_b_ok
```

[150] :

$$\frac{\eta\lambda'\delta\theta(-\varepsilon\theta + \theta + 1)}{\lambda'\delta + \rho}$$

```
[151]: E = (a_b_s - a_a_s).simplify()
E
```

[151] :

$$\frac{8\beta\delta\gamma\kappa\lambda\theta}{2\delta\kappa\lambda + \kappa^2\lambda^2\rho + \rho}$$

Same values are thus obtained for α and \mathcal{A} considering the Taylor expansion.

```
[152]: E_ok = to_h_kp(E)
E_ok
```

[152] :

$$\frac{2\eta\lambda'\delta\theta}{\lambda'\delta + \rho}$$

```
[153]: alpha_r_ok
```

[153] :

$$\frac{2\eta\lambda'\delta\theta}{\lambda'\delta + \rho}$$

LIST OF FIGURES

S1	Normalized entropy production σ/σ_0 in a two-compartment system, as a function of $\rho \in [10^{-10}, 10^{10}]$ and $\lambda'\delta \in [10^{-10}, 10^{10}]$ (defined in Eq. (C24) in MT). A, total entropy production σ ; B, entropy production by chemical reaction σ_r ; C, entropy production by chemical diffusion σ_d	26
S2	Effect of the dependence on temperature on the diffusion coefficient. A first order correction on the diffusion coefficient was introduced as $d = d_0(1 + \delta d \cdot \theta)$. $\beta = 1$, $\gamma = 0.2$, $\theta_g=0.1$, $\rho = 1000$, $\kappa = 1$, $\lambda = 1$, $d_0 = 1$, $\delta d = 0$ (red) or $\delta d = 5$ (green). A: Heaviside temperature profile; B: Linear temperature profile.	26
S3	Energetic profiles. A: activation energies ε_+ and ε_- , and reaction enthalpy η . B: Evolution of energetic profiles as a function of γ for a constant β value.	26
S4	Steady state spatial profiles of key parameters in unstirred systems driven by Heaviside temperature profiles. Solid blue, steady u_2 concentration profile; dotted green, local equilibrium u_2 concentration profile; solid light blue, j_2 concentration gradient; dotted light blue, j_1 concentration gradient; red: steady chemical flux of reaction φ ; dark green, steady chemical force α , purple: steady dissipation of entropy σ_r (plain line) and σ_d (dotted line). The horizontal wide arrows represent the direction of U_1 and U_2 diffusion; vertical wide arrows represent the global reaction fluxes $U_1 \rightarrow U_2$ (up arrows) and $U_2 \rightarrow U_1$ (down arrows). Model parameters: $\kappa = 1$, $\lambda = 1$, $\gamma = 0.2$, and Fast diffusion : $d = 1$, $\rho = 10^{-2}$, $\beta = 1$, $\theta_g = 10^{-1}$, Intermediate : $d = 1$, $\rho = 10^2$, $\beta = 1$, $\theta_g = 10^{-1}$, Fast reaction : $d = 10^{-2}$, $\rho = 10^2$, $\beta = 1$, $\theta_g = 10^{-1}$, Far from equilibrium : $d = 1$, $\rho = 10^2$, $\beta = 4$, $\theta_g = 0.4$	27
S5	Steady state spatial profiles of key parameters in unstirred systems driven by linear temperature profiles. Solid blue, steady u_2 concentration profile; dotted green, local equilibrium u_2 concentration profile; solid light blue, j_2 concentration gradient; dotted light blue, j_1 concentration gradient; red: steady chemical flux of reaction φ ; dark green, steady chemical force α , purple: steady dissipation of entropy σ_r (plain line) and σ_d (dotted line). The horizontal wide arrows represent the direction of U_1 and U_2 diffusion; vertical wide arrows represent the global reaction fluxes $U_1 \rightarrow U_2$ (up arrows) and $U_2 \rightarrow U_1$ (down arrows). Model parameters: $\kappa = 1$, $\lambda = 1$, $\gamma = 0.2$, and Fast diffusion : $d = 1$, $\rho = 10^{-2}$, $\beta = 1$, $\theta_g = 10^{-1}$, Intermediate : $d = 1$, $\rho = 10$, $\beta = 1$, $\theta_g = 10^{-1}$, Fast reaction : $d = 10^{-2}$, $\rho = 10$, $\beta = 1$, $\theta_g = 10^{-1}$, Far from equilibrium : $d = 1$, $\rho = 10^2$, $\beta = 4$, $\theta_g = 0.5$	28
S6	Mixed temperature profile. A precise localization of the reaction diffusion cycle is achieved by a tailored temperature gradient profile. Diffusion and reaction processes are physically separated. A: temperature, with constant temperature $-\theta_g$ until ①, linear variation of θ from ① to ②, and constant temperature $+\theta_g$ from ②; B, G, diffusion flux j_2 ; C, F, normalized reaction flux φ/φ_0 , with $\varphi_0 = 2\beta\gamma\theta_g\rho$; D, H, diffusion flux j_1 ; E, concentration u_2 . Model parameters: $\kappa = 1$, $\lambda = 1$, $\gamma = 0.2$, $d = 1$, $\beta = 1$, $\theta_g = 10^{-1}$, A-D: $\rho = 10^3$, E-H: $\rho \in [10^{-1}, 10^3]$	29
S7	Profile scaling of maximal and integral values on φ , σ and y (see Table 2 in Main Text). The dotted lines represent, for convenience of reading, slopes corresponding on scaling in w^n . Parameters: $\beta = 1$, $\kappa = 1$, $\gamma = 0.2$, $\theta_g = 0.1$. Heaviside and linear profiles: $d \in [10^{-3}, 10^3]$ and $\rho \in [10^{-3}, 10^3]$. Mixed profile: $d = 1$ and $\rho \in [10^{-3}, 10^3]$	30
S8	Peptide exchange reaction in Heaviside temperature gradient. A, entropy production (σ_r , solid lines; σ_d , dotted line); B, reaction flux φ , C concentrations (u_1 , dotted line; u_2 , solid line). $\beta = 18.8$, $\gamma = 0.122$, $\theta_g = 0.1$, $d = 1$, $\kappa = 1$ and $\lambda = 1$. Red lines , $\rho = 0.28$, $l_1 = 1$ cm; blue lines , $\rho = 2.5$, $l_0 = 3$ cm; green lines , $\rho = 28$, $l_2 = 10$ cm.	30

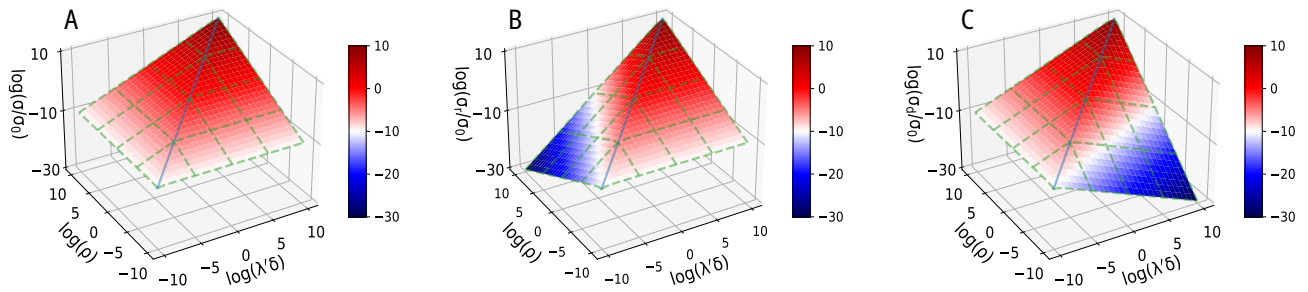


FIG. S1. Normalized entropy production σ/σ_0 in a two-compartment system, as a function of $\rho \in [10^{-10}, 10^{10}]$ and $\lambda'\delta \in [10^{-10}, 10^{10}]$ (defined in Eq. (C24) in MT). **A**, total entropy production σ ; **B**, entropy production by chemical reaction σ_r ; **C**, entropy production by chemical diffusion σ_d .

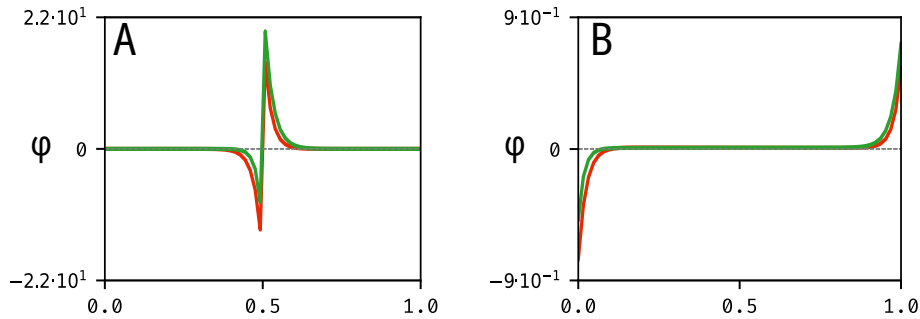


FIG. S2. Effect of the dependence on temperature on the diffusion coefficient. A first order correction on the diffusion coefficient was introduced as $d = d_0(1 + \delta d \cdot \theta)$. $\beta = 1$, $\gamma = 0.2$, $\theta_{g=0.1}$, $\rho = 1000$, $\kappa = 1$, $\lambda = 1$, $d_0 = 1$, $\delta d = 0$ (red) or $\delta d = 5$ (green). **A**: Heaviside temperature profile; **B**: Linear temperature profile.

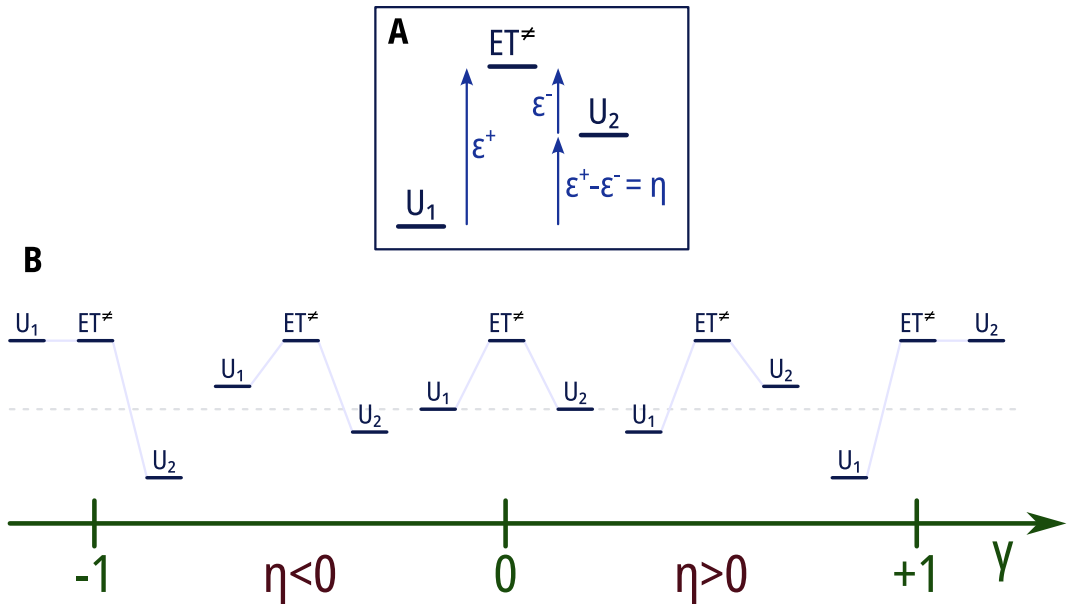


FIG. S3. Energetic profiles. **A**: activation energies ε_+ and ε_- , and reaction enthalpy η . **B**: Evolution of energetic profiles as a function of γ for a constant β value.

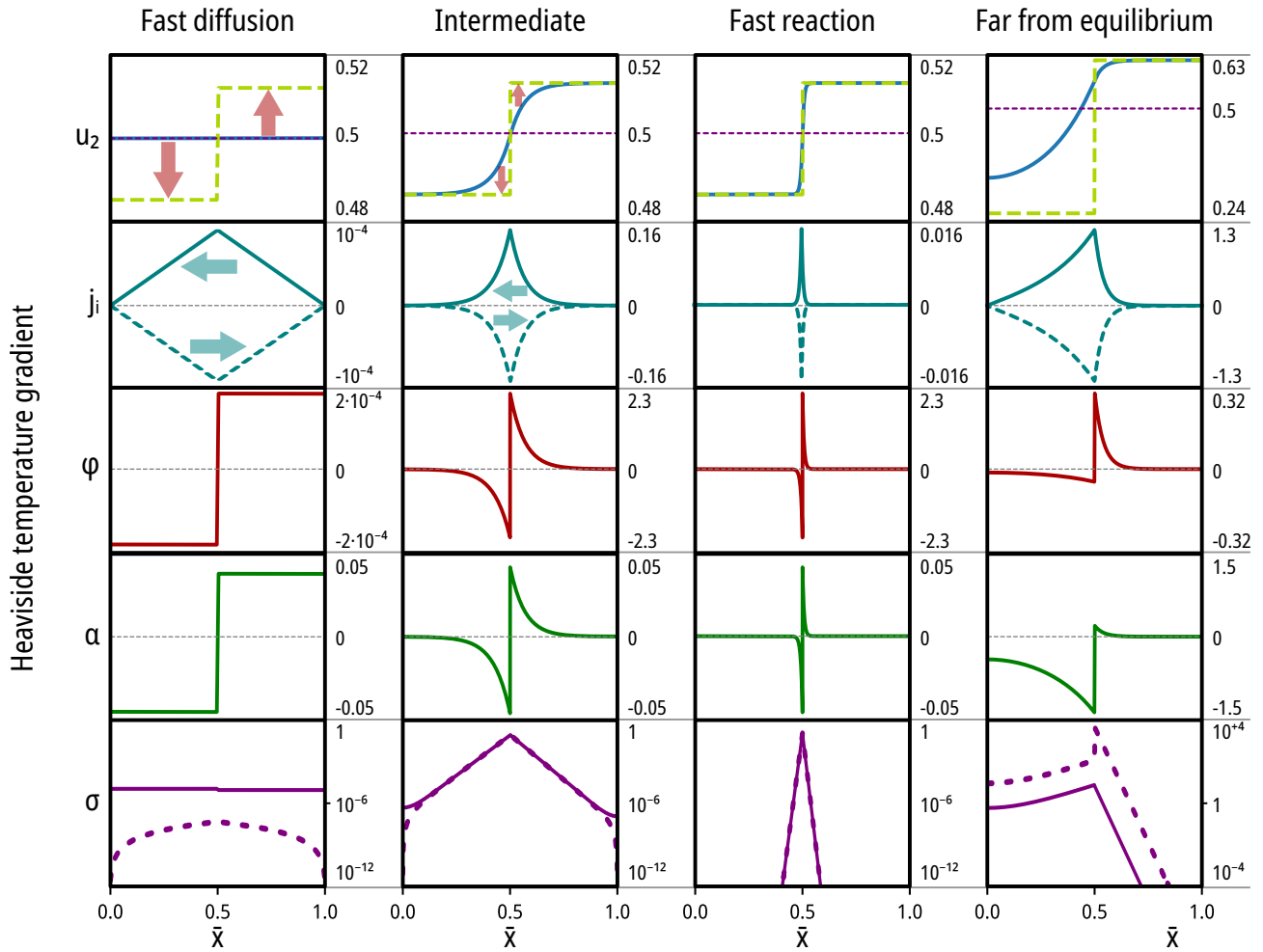


FIG. S4. Steady state spatial profiles of key parameters in unstirred systems driven by Heaviside temperature profiles. Solid blue, steady u_2 concentration profile; dotted green, local equilibrium u_2 concentration profile; solid light blue, j_2 concentration gradient; dotted light blue, j_1 concentration gradient; red: steady chemical flux of reaction φ ; dark green, steady chemical force α , purple: steady dissipation of entropy σ_r (plain line) and σ_d (dotted line). The horizontal wide arrows represent the direction of U_1 and U_2 diffusion; vertical wide arrows represent the global reaction fluxes $U_1 \rightarrow U_2$ (up arrows) and $U_2 \rightarrow U_1$ (down arrows). Model parameters: $\kappa = 1$, $\lambda = 1$, $\gamma = 0.2$, and **Fast diffusion:** $d = 1$, $\rho = 10^{-2}$, $\beta = 1$, $\theta_g = 10^{-1}$, **Intermediate:** $d = 1$, $\rho = 10^2$, $\beta = 1$, $\theta_g = 10^{-1}$, **Fast reaction:** $d = 10^{-2}$, $\rho = 10^2$, $\beta = 1$, $\theta_g = 10^{-1}$, **Far from equilibrium:** $d = 1$, $\rho = 10^2$, $\beta = 4$, $\theta_g = 0.4$.

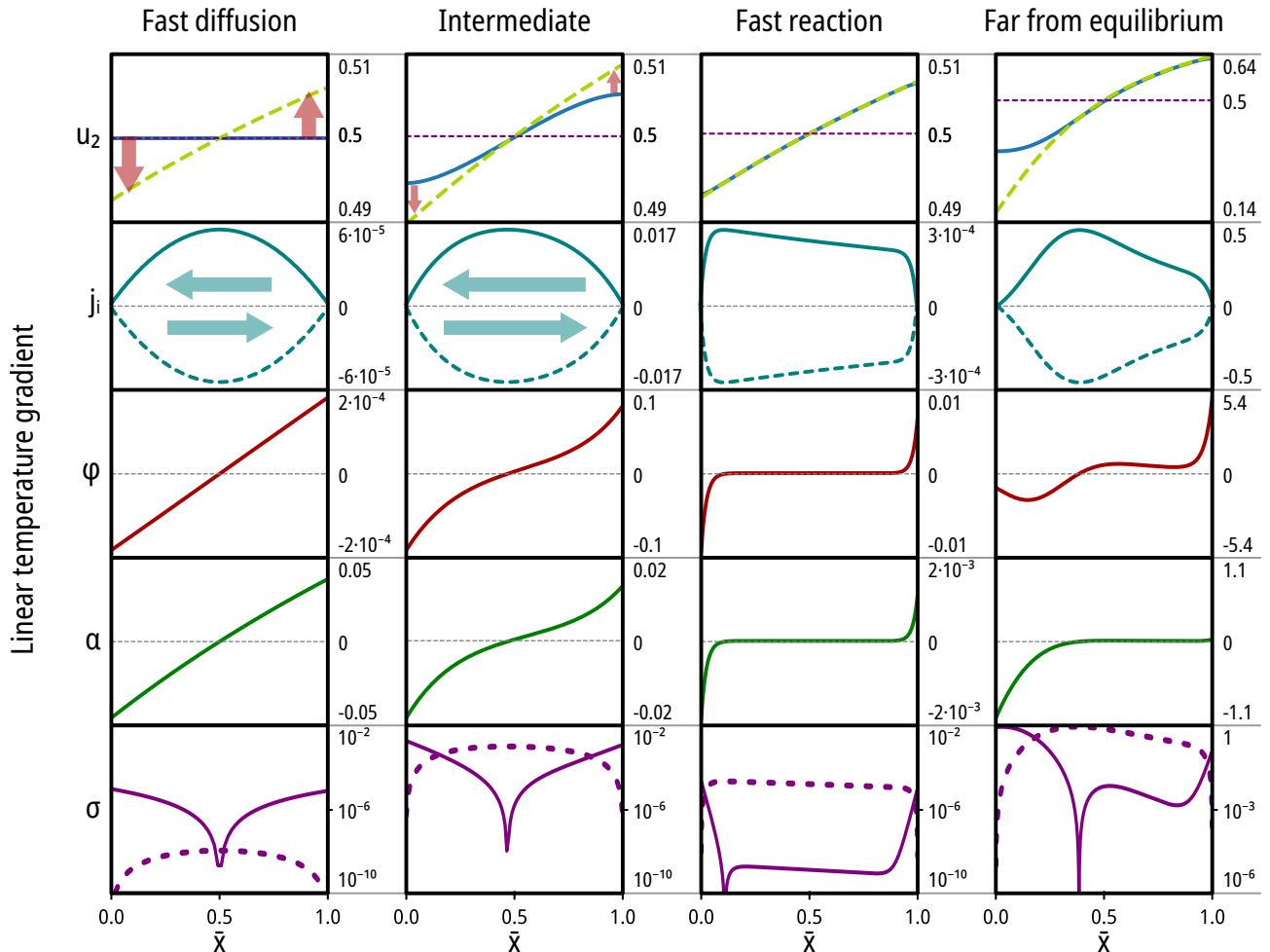


FIG. S5. Steady state spatial profiles of key parameters in unstirred systems driven by linear temperature profiles. Solid blue, steady u_2 concentration profile; dotted green, local equilibrium u_2 concentration profile; solid light blue, j_2 concentration gradient; dotted light blue, j_1 concentration gradient; red: steady chemical flux of reaction φ ; dark green, steady chemical force α , purple: steady dissipation of entropy σ_r (plain line) and σ_d (dotted line). The horizontal wide arrows represent the direction of U_1 and U_2 diffusion; vertical wide arrows represent the global reaction fluxes $U_1 \rightarrow U_2$ (up arrows) and $U_2 \rightarrow U_1$ (down arrows). Model parameters: $\kappa = 1$, $\lambda = 1$, $\gamma = 0.2$, and **Fast diffusion:** $d = 1$, $\rho = 10^{-2}$, $\beta = 1$, $\theta_g = 10^{-1}$, **Intermediate:** $d = 1$, $\rho = 10$, $\beta = 1$, $\theta_g = 10^{-1}$, **Fast reaction:** $d = 10^{-2}$, $\rho = 10$, $\beta = 1$, $\theta_g = 10^{-1}$, **Far from equilibrium:** $d = 1$, $\rho = 10^2$, $\beta = 4$, $\theta_g = 0.5$.

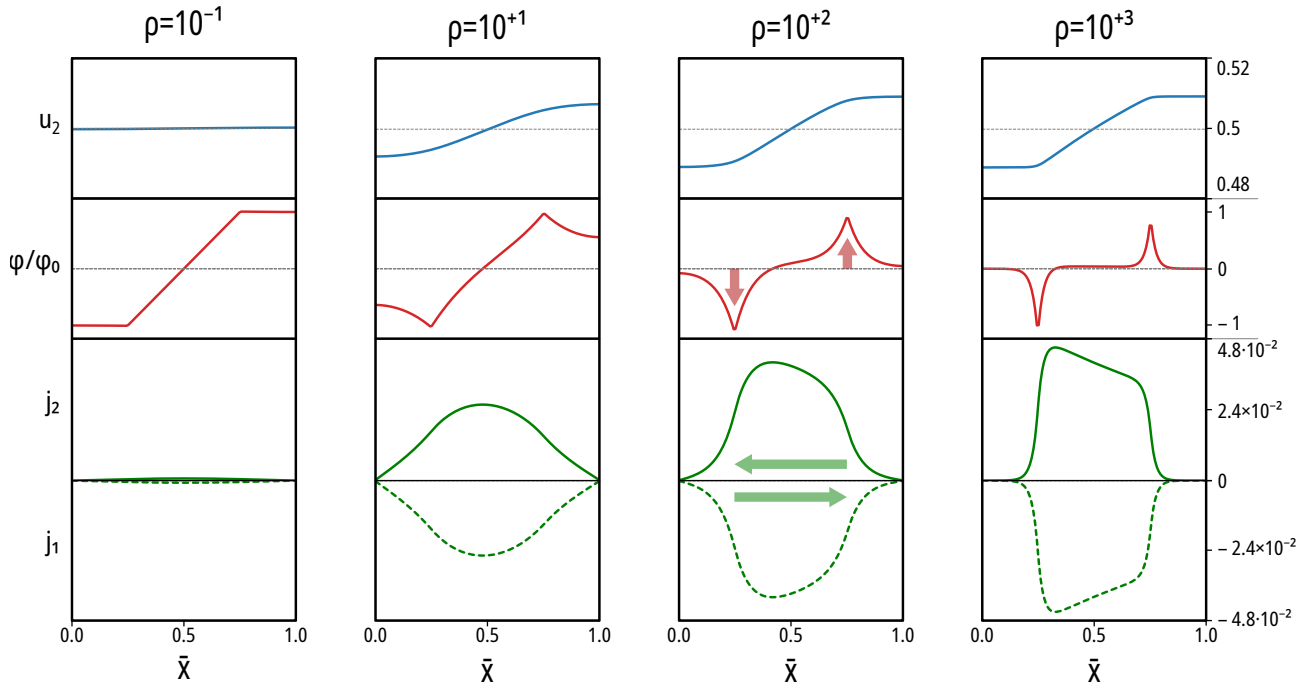


FIG. S6. Mixed temperature profile. A precise localization of the reaction diffusion cycle is achieved by a tailored temperature gradient profile. Diffusion and reaction processes are physically separated. **A**: temperature, with constant temperature $-\theta_g$ until ①, linear variation of θ from ① to ②, and constant temperature $+\theta_g$ from ②; **B, G**, diffusion flux j_2 ; **C, F**, normalized reaction flux φ/φ_0 , with $\varphi_0 = 2\beta\gamma\theta_g\rho$; **D, H**, diffusion flux j_1 ; **E**, concentration u_2 . Model parameters: $\kappa = 1$, $\lambda = 1$, $\gamma = 0.2$, $d = 1$, $\beta = 1$, $\theta_g = 10^{-1}$, **A-D**: $\rho = 10^3$, **E-H**: $\rho \in [10^{-1}, 10^3]$.

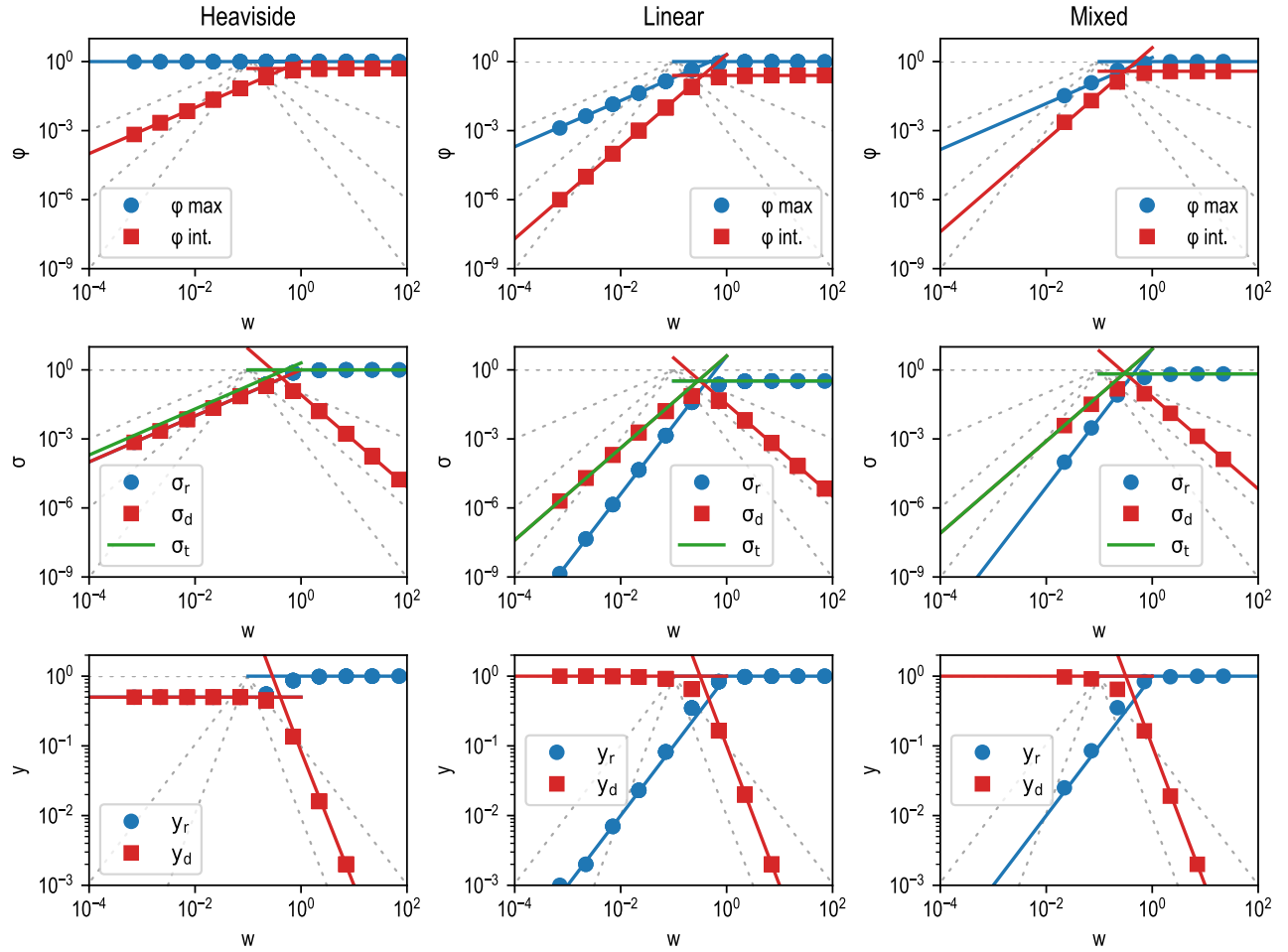


FIG. S7. Profile scaling of maximal and integral values on φ , σ and y (see Table 2 in Main Text). The dotted lines represent, for convenience of reading, slopes corresponding on scaling in w^n . Parameters: $\beta = 1$, $\kappa = 1$, $\gamma = 0.2$, $\theta_g = 0.1$. Heaviside and linear profiles: $d \in [10^{-3}, 10^3]$ and $\rho \in [10^{-3}, 10^3]$. Mixed profile: $d = 1$ and $\rho \in [10^{-3}, 10^3]$.

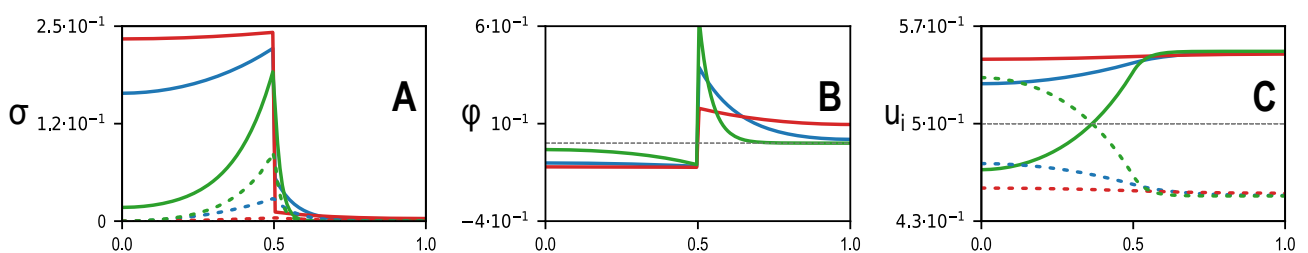


FIG. S8. Peptide exchange reaction in Heaviside temperature gradient. **A**, entropy production (σ_r , solid lines; σ_d , dotted line); **B**, reaction flux φ ; **C** concentrations (u_1 , dotted line; u_2 , solid line). $\beta = 18.8$, $\gamma = 0.122$, $\theta_g = 0.1$, $d = 1$, $\kappa = 1$ and $\lambda = 1$. **Red lines**, $\rho = 0.28$, $l_1 = 1$ cm; **blue lines**, $\rho = 2.5$, $l_0 = 3$ cm; **green lines**, $\rho = 28$, $l_2 = 10$ cm.

REACTION DIFFUSION PROFILES

In the next pages are available the automatically generated figures of the spatial profiles for all simulations reported in this work.

Optimizing reaction and transport fluxes in temperature gradient-driven chemical reaction-diffusion systems: Supplementary Information; reaction-diffusion profiles

Mohammed Loukili, Ludovic Jullien, Guillaume Baffou, Raphaël Plasson

The following figures give the profile of $\alpha, \varphi, R_{\text{tot}}, u_2, \sigma_r, \sigma_d, \sigma_{\text{tot}}$ as a function of $[d, \rho]$ values or $[\beta, \theta_g]$ values:

		α	φ	R_{tot}	u_2	σ_r	σ_d	σ_{tot}
Heaviside	$[d, \rho]$ (low θ_g)	Fig. 1	Fig. 2	Fig. 3	Fig. 4	Fig. 5	Fig. 6	Fig. 7
	$[d, \rho]$ (high θ_g)	Fig. 8	Fig. 9	Fig. 10	Fig. 11	Fig. 12	Fig. 13	Fig. 14
	$[\beta, \theta_g]$	Fig. 15	Fig. 16	Fig. 17	Fig. 18	Fig. 19	Fig. 20	Fig. 21
Linear	$[d, \rho]$ (low θ_g)	Fig. 22	Fig. 23	Fig. 24	Fig. 25	Fig. 26	Fig. 27	Fig. 28
	$[d, \rho]$ (high θ_g)	Fig. 29	Fig. 30	Fig. 31	Fig. 32	Fig. 33	Fig. 34	Fig. 35
	$[\beta/\theta_g]$	Fig. 36	Fig. 37	Fig. 38	Fig. 39	Fig. 40	Fig. 41	Fig. 42

Dotted line in R_{tot} figures represent the R value in the linear regime. Dotted line in u_2 figures represent the equilibrium value.

Common parameter values:

- $\kappa = 1$
- $\lambda = 1$
- $\gamma = 0.2$

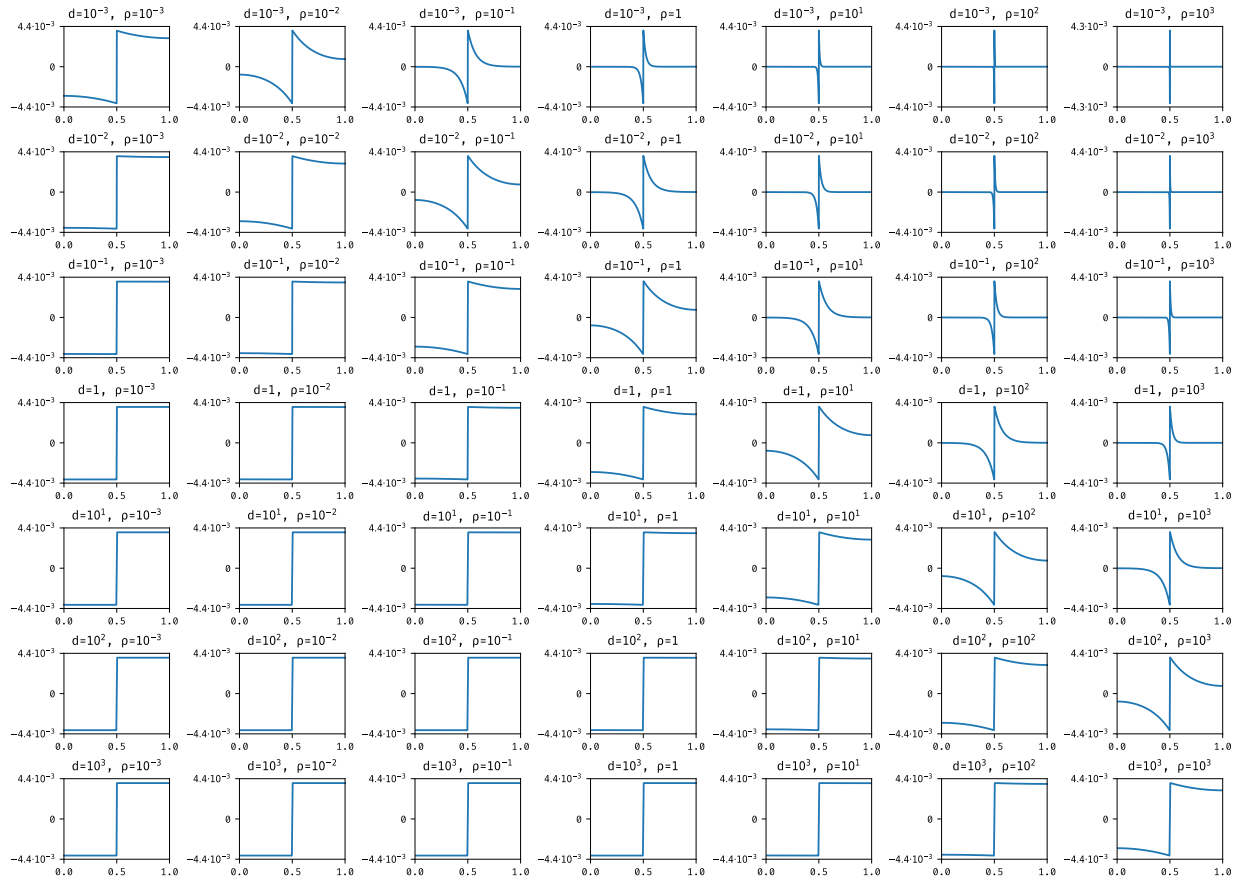


Figure 1: α for Heaviside profile, low θ_g value ($\beta = 1$, $\theta_g = 0.01$).

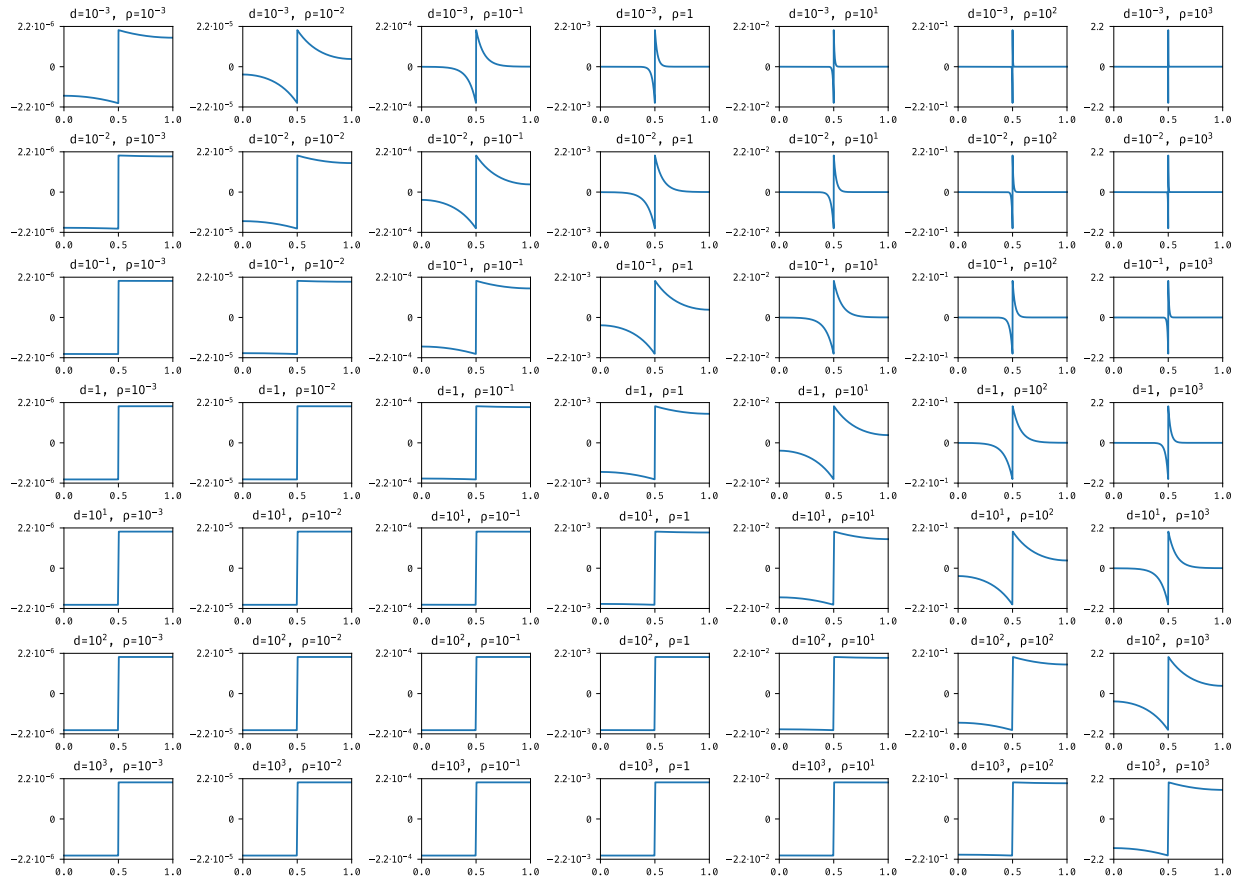


Figure 2: φ for Heaviside profile, low θ_g value ($\beta = 1$, $\theta_g = 0.01$).

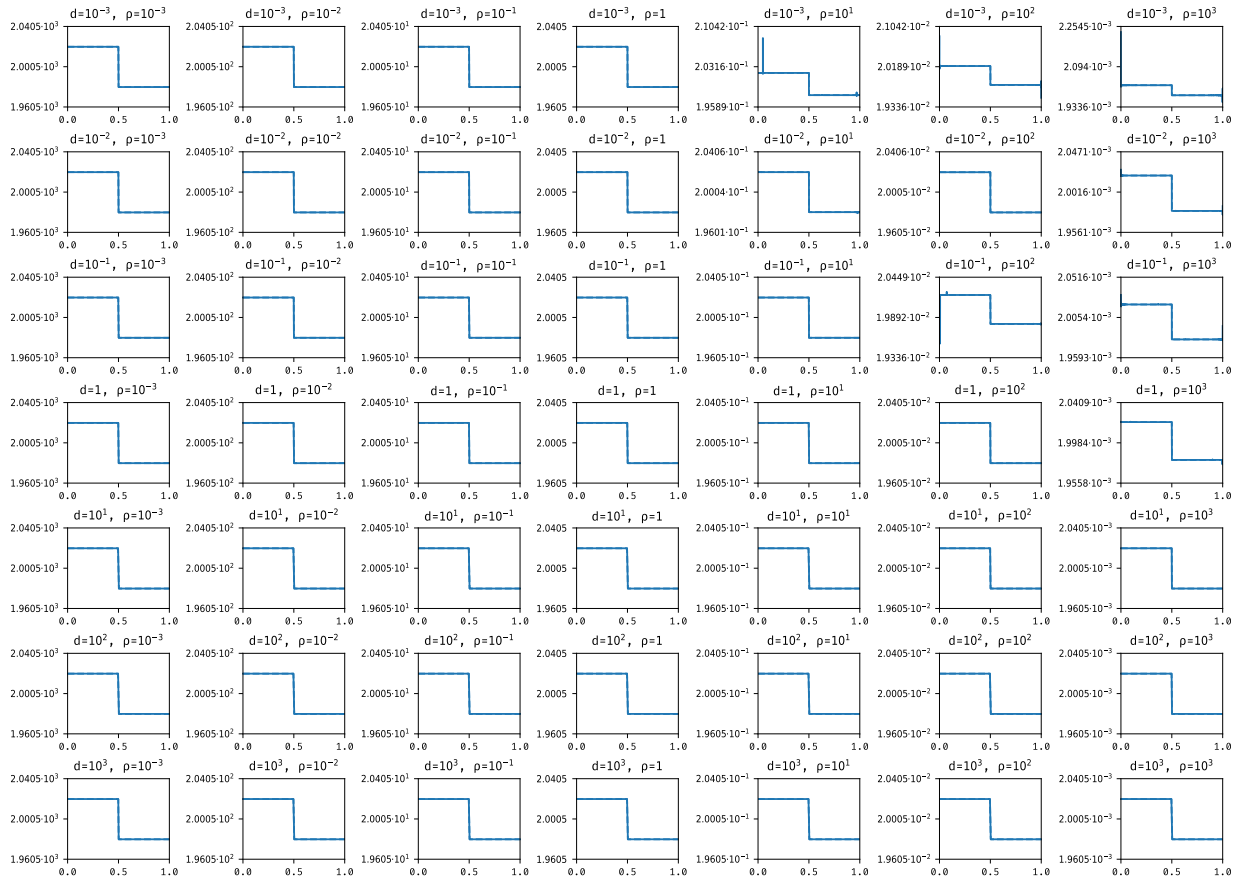


Figure 3: R_{tot} for Heaviside profile, low θ_g value ($\beta = 1$, $\theta_g = 0.01$).

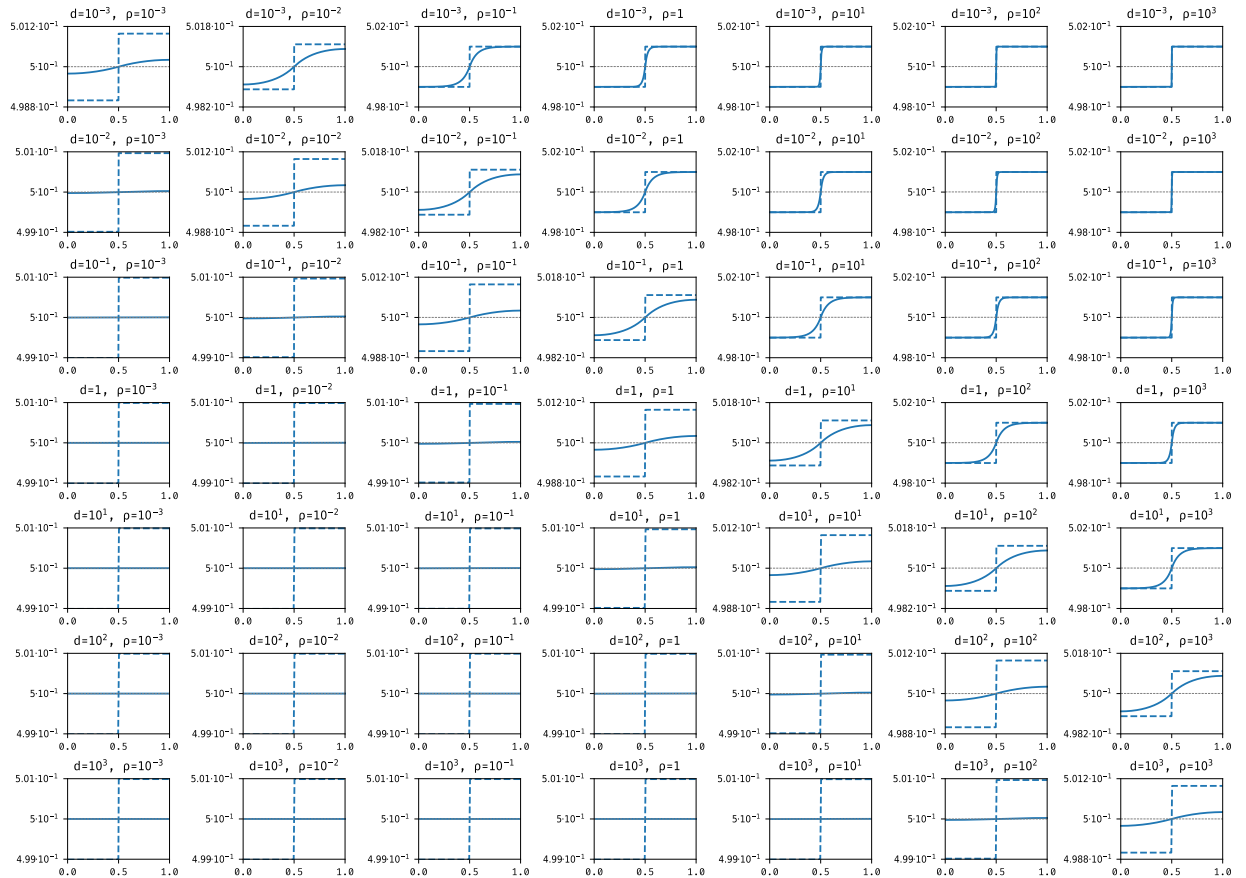


Figure 4: u_2 for Heaviside profile, low θ_g value ($\beta = 1$, $\theta_g = 0.01$).

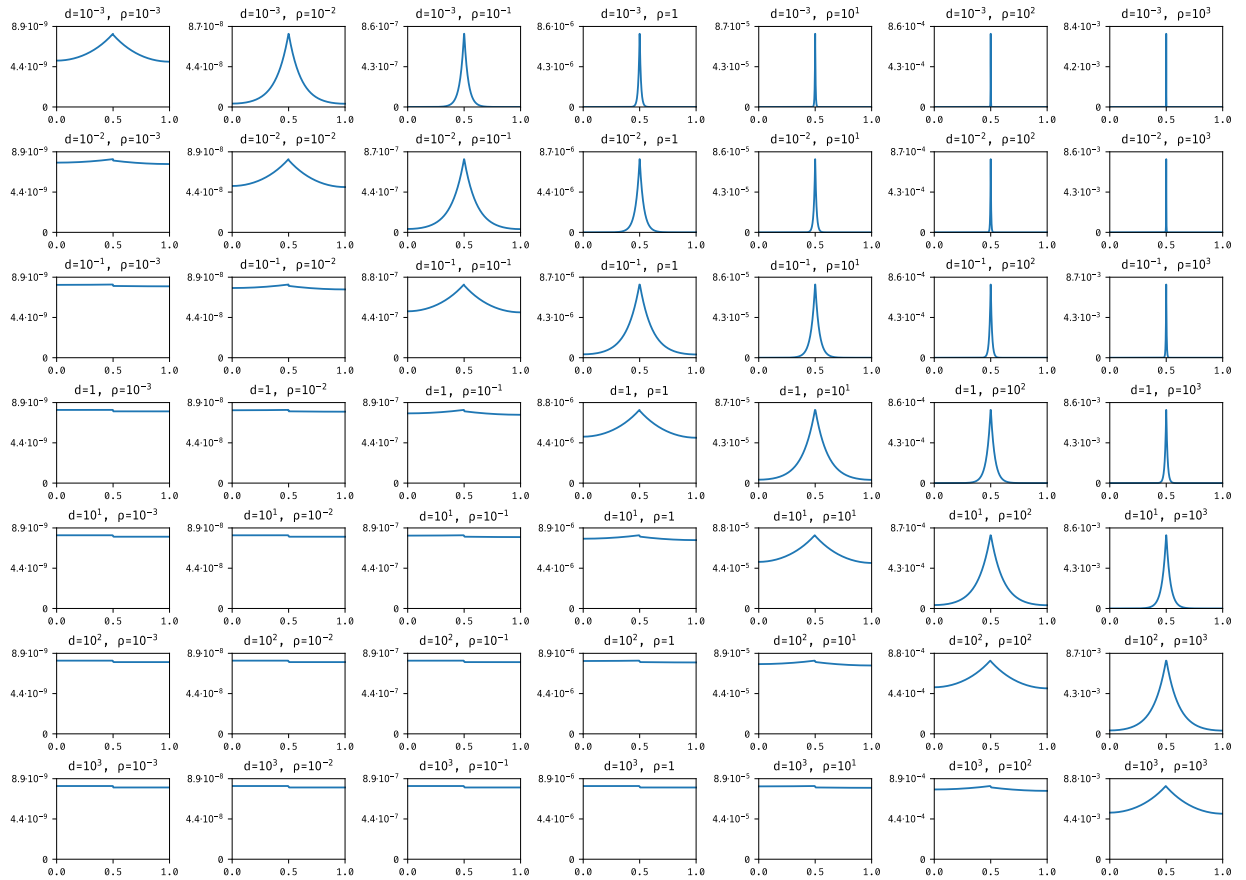


Figure 5: σ_r for Heaviside profile, low θ_g value ($\beta = 1$, $\theta_g = 0.01$).

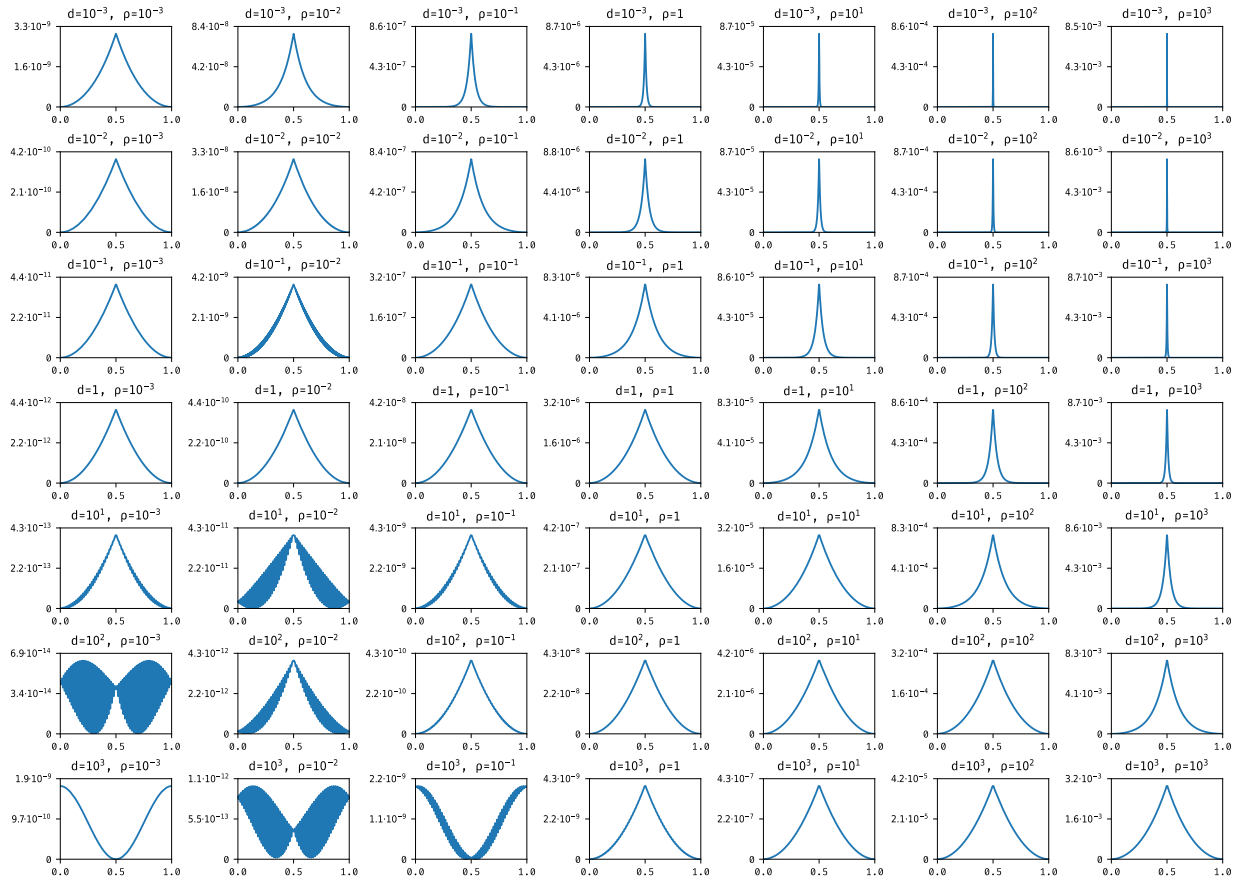


Figure 6: σ_d for Heaviside profile, low θ_g value ($\beta = 1$, $\theta_g = 0.01$).

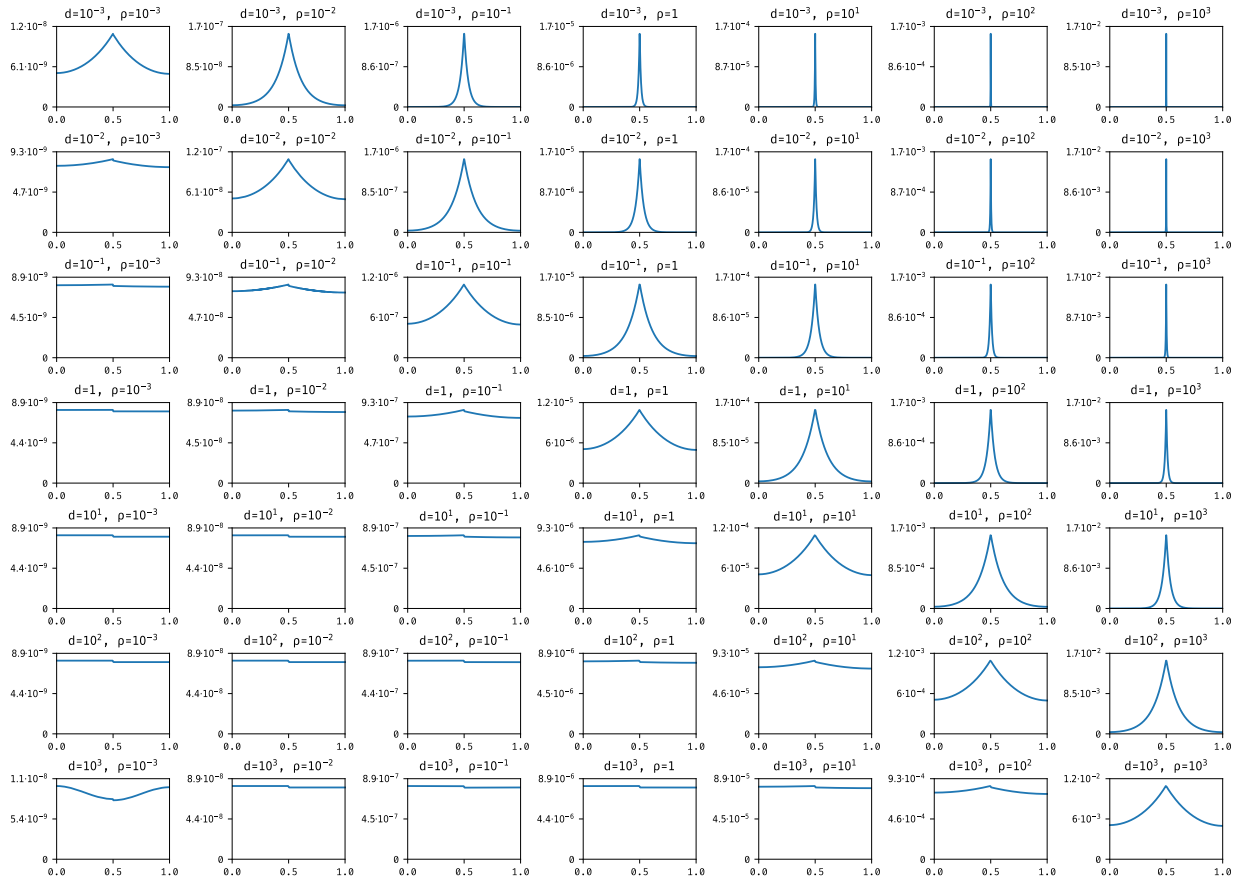


Figure 7: σ_{tot} for Heaviside profile, low θ_g value ($\beta = 1, \theta_g = 0.01$).

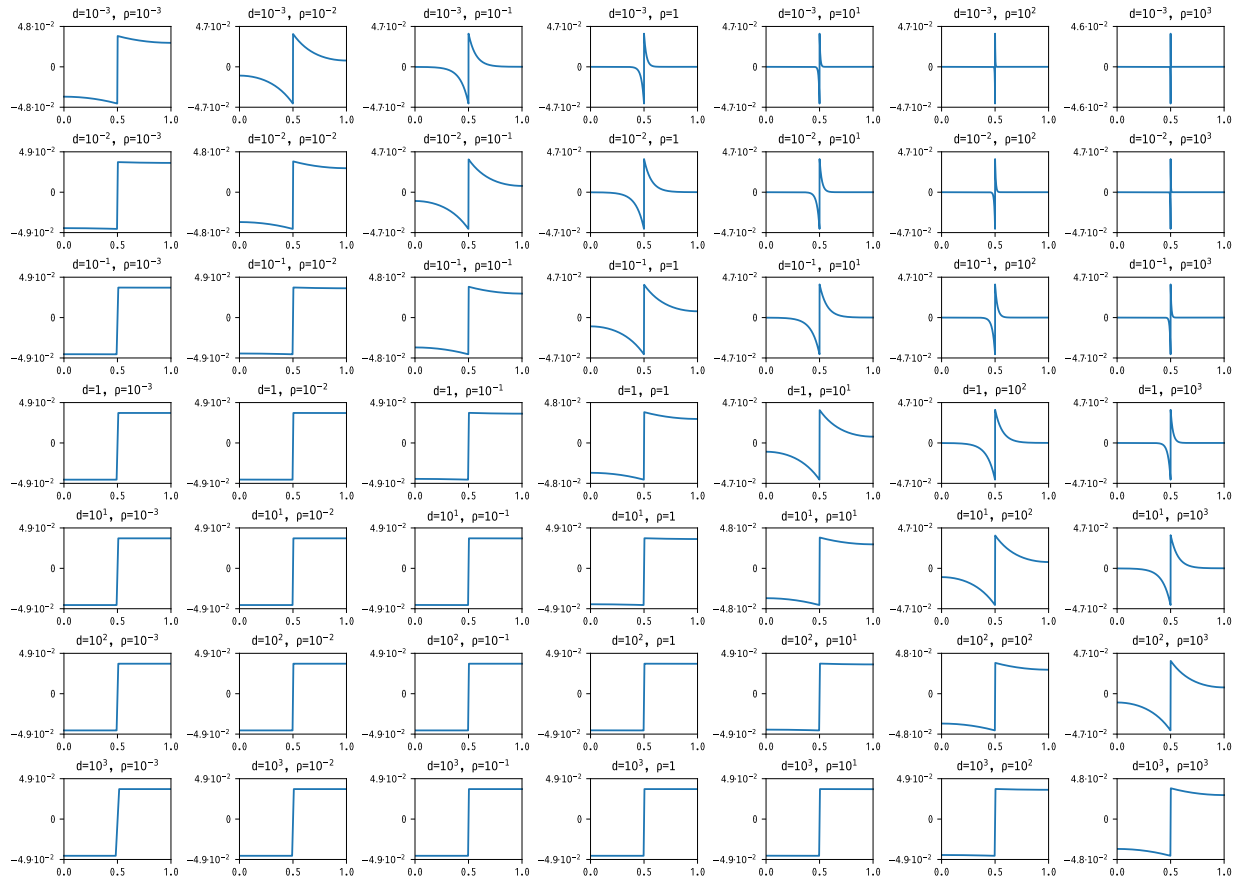


Figure 8: α for Heaviside profile, high θ_g value ($\beta = 1, \theta_g = 0.1$).

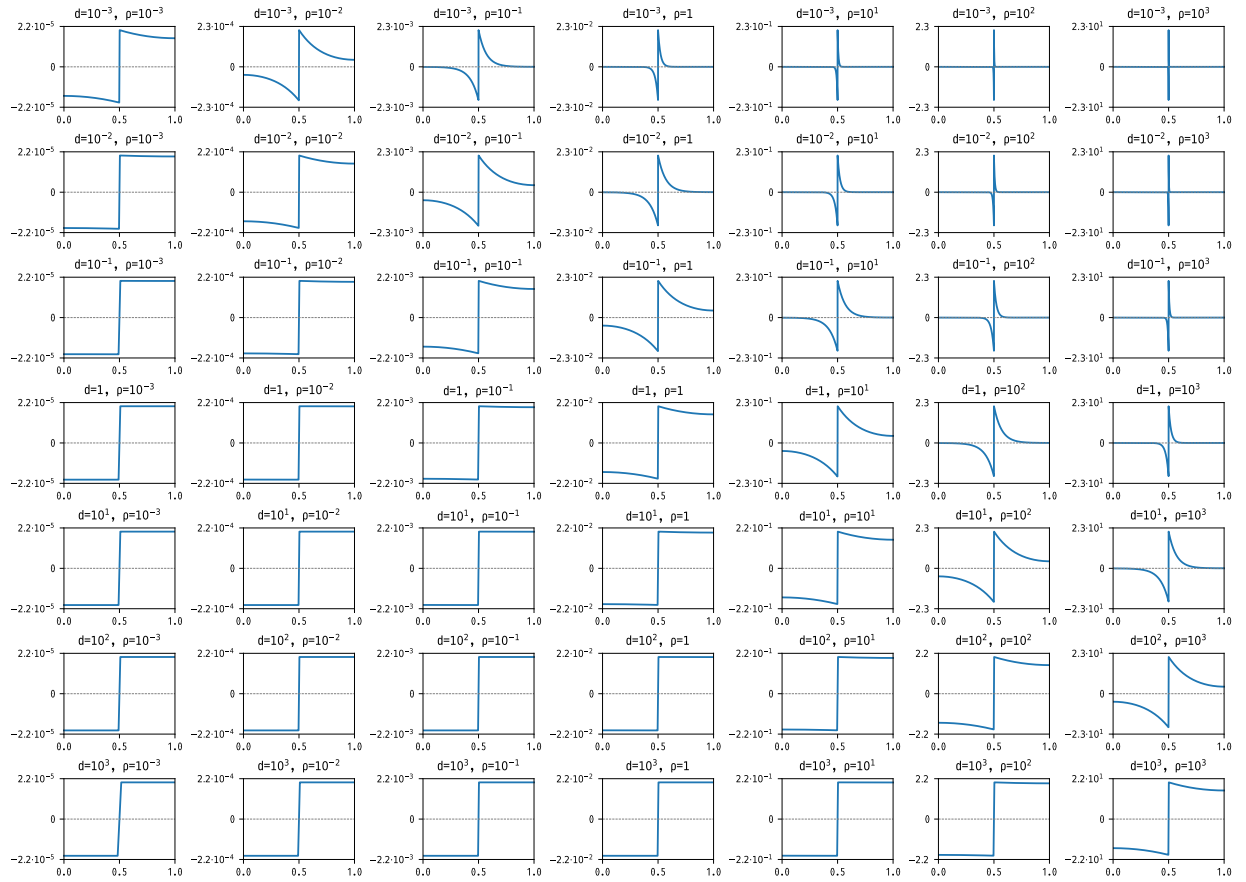


Figure 9: φ for Heaviside profile, high θ_g value ($\beta = 1$, $\theta_g = 0.1$).

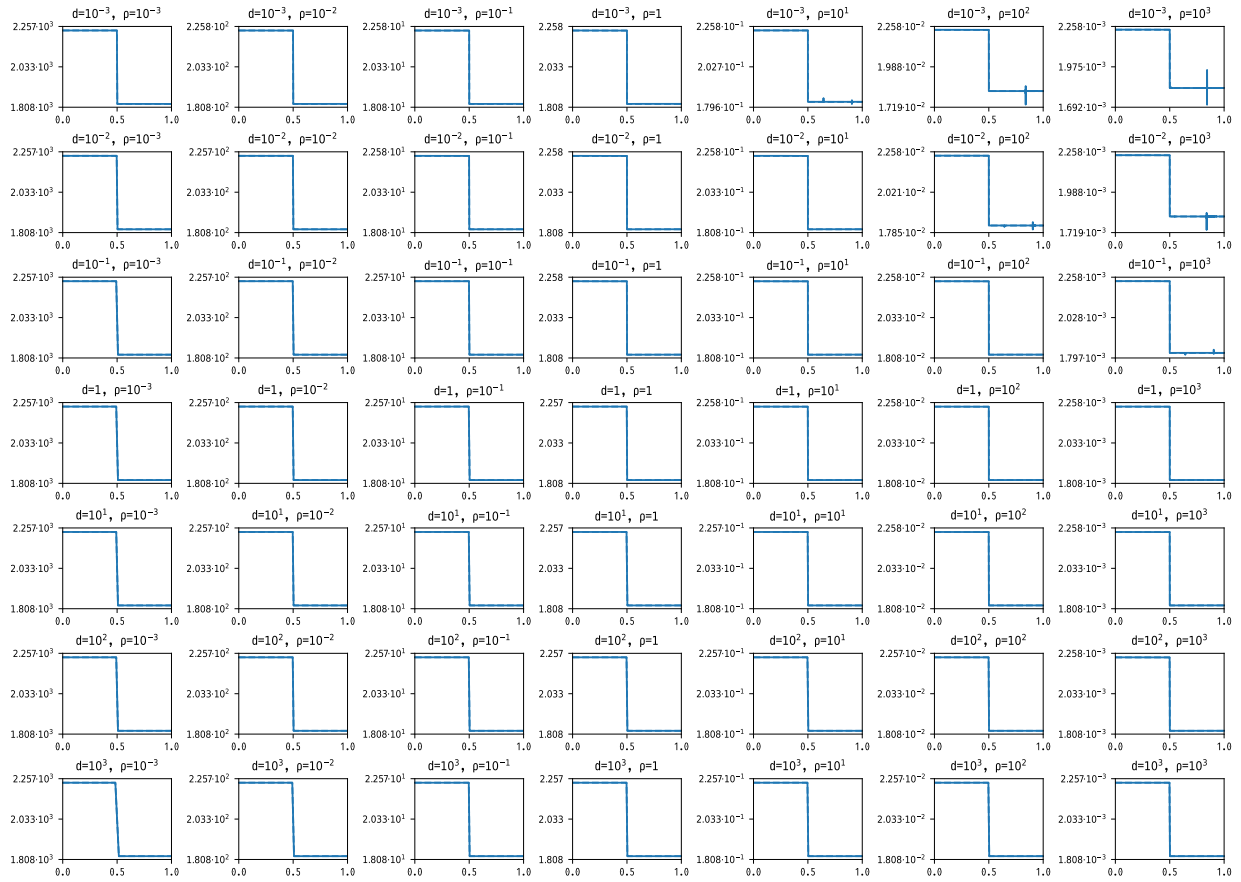


Figure 10: R_{tot} for Heaviside profile, high θ_g value ($\beta = 1$, $\theta_g = 0.1$).

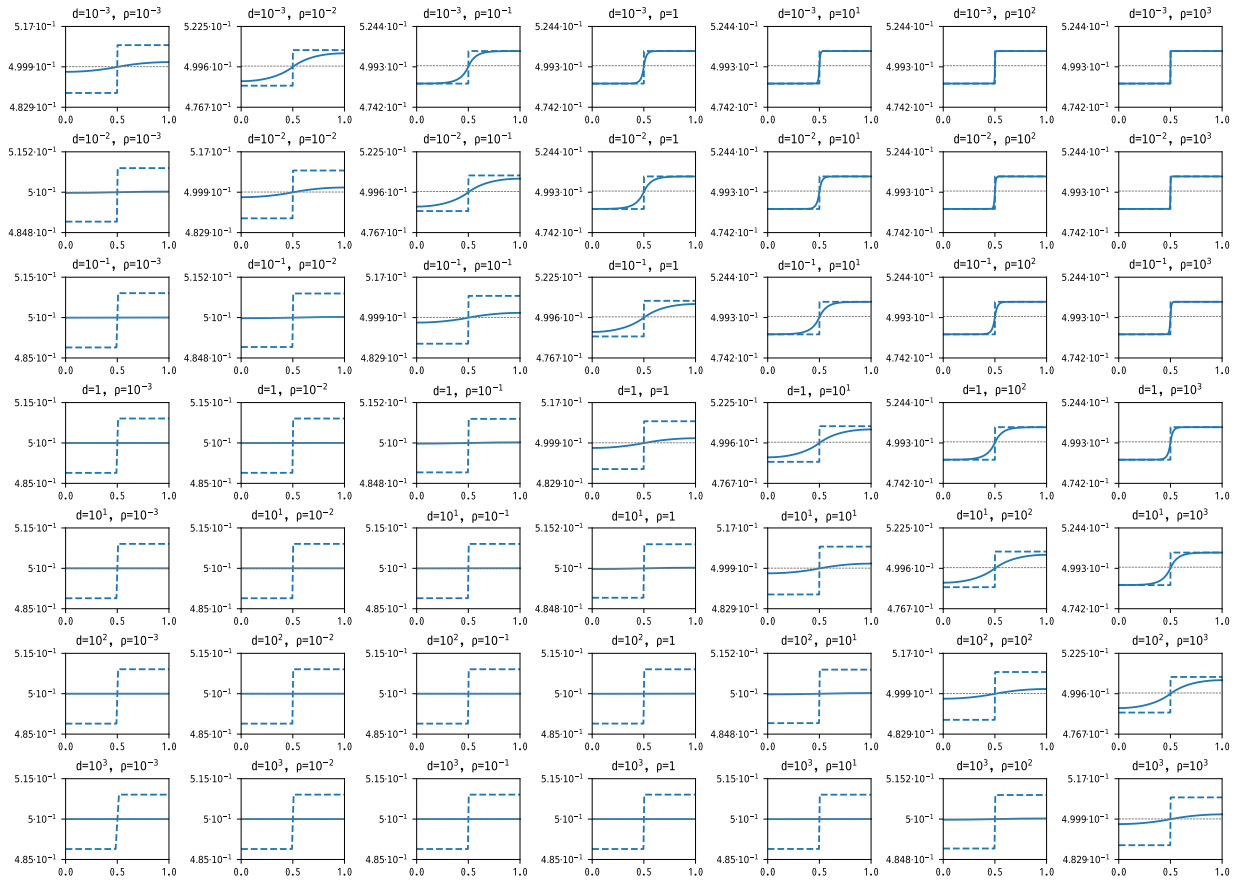


Figure 11: u_2 for Heaviside profile, high θ_g value ($\beta = 1, \theta_g = 0.1$).

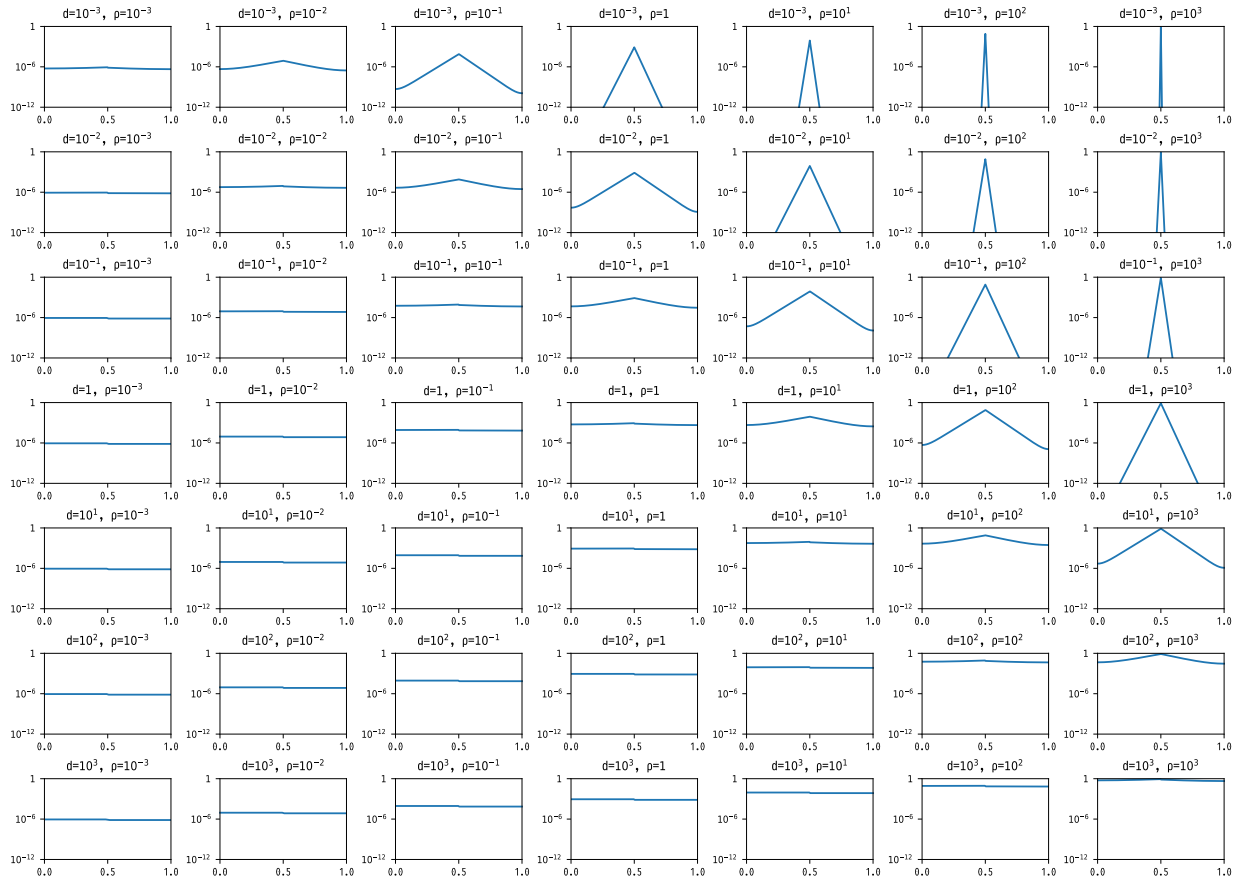


Figure 12: σ_r for Heaviside profile, high θ_g value ($\beta = 1, \theta_g = 0.1$).

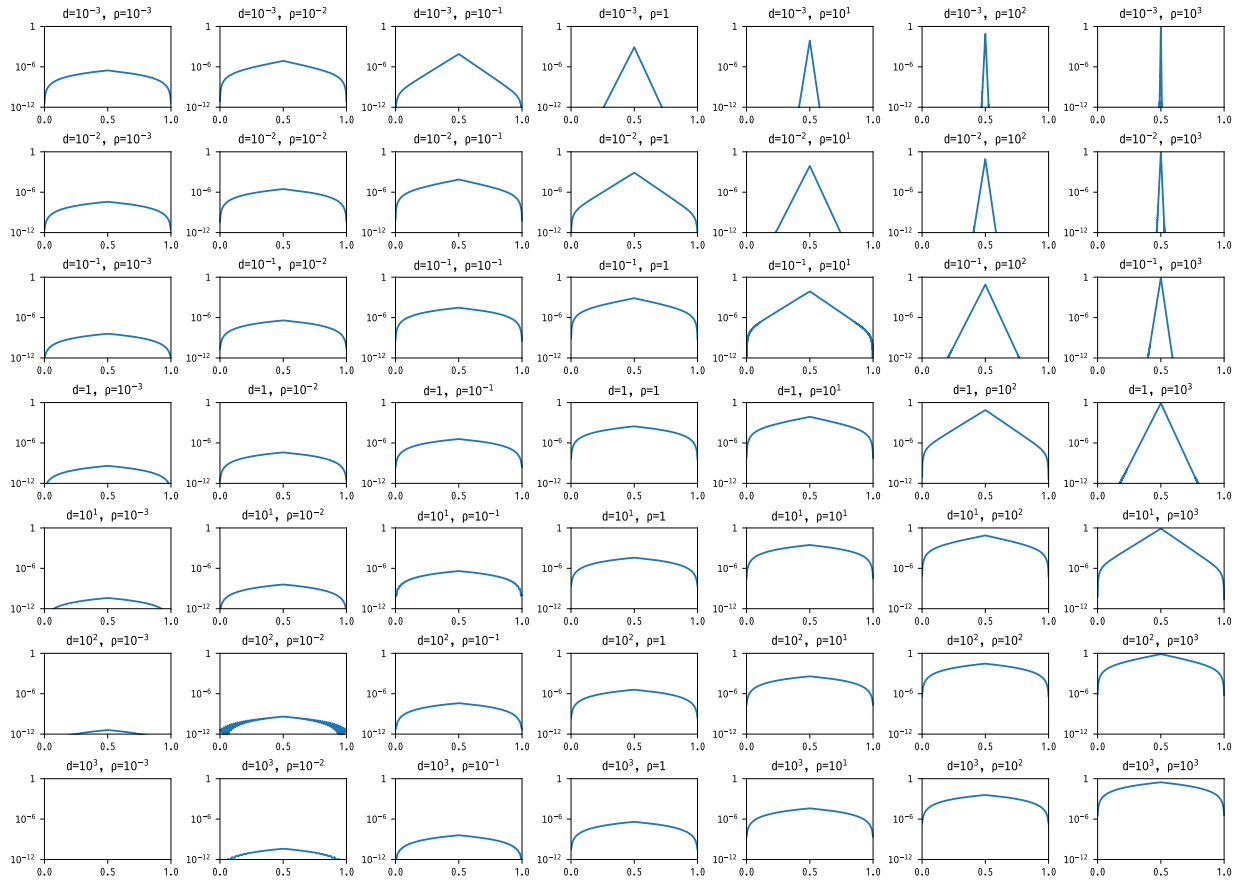


Figure 13: σ_d for Heaviside profile, high θ_g value ($\beta = 1, \theta_g = 0.1$).

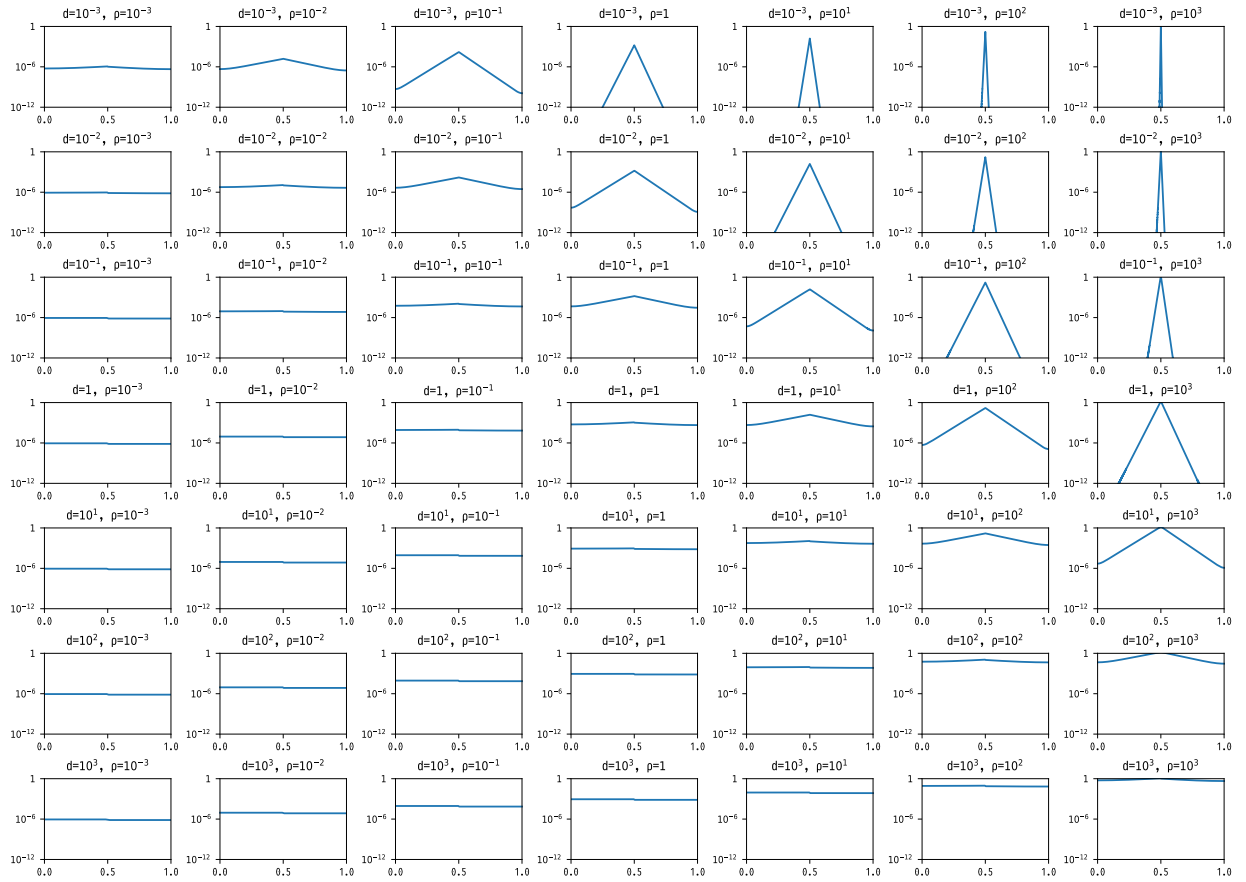


Figure 14: σ_{tot} for Heaviside profile, high θ_g value ($\beta = 1$, $\theta_g = 0.1$).

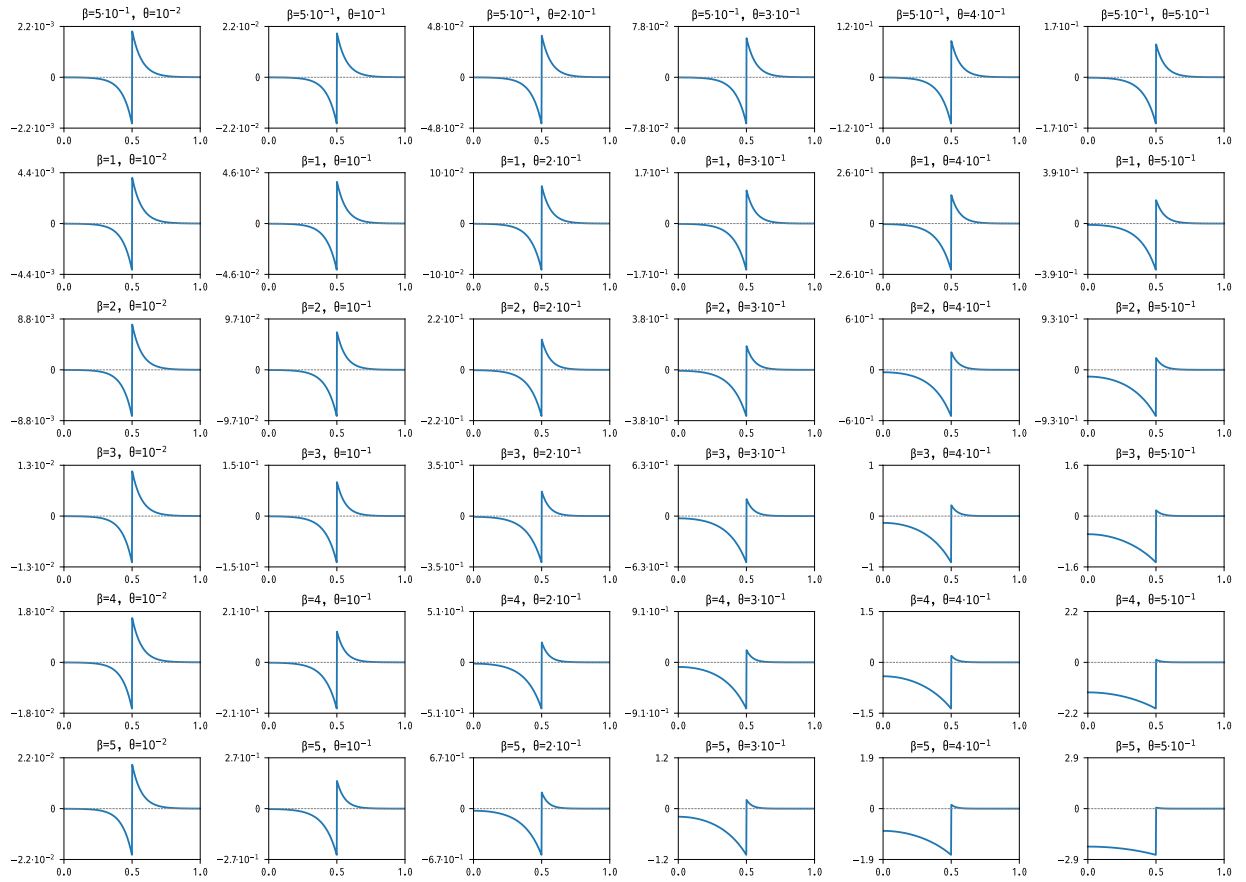


Figure 15: α for Heaviside profile, as a function of β and θ_g ($d = 1$, $\rho = 100$).

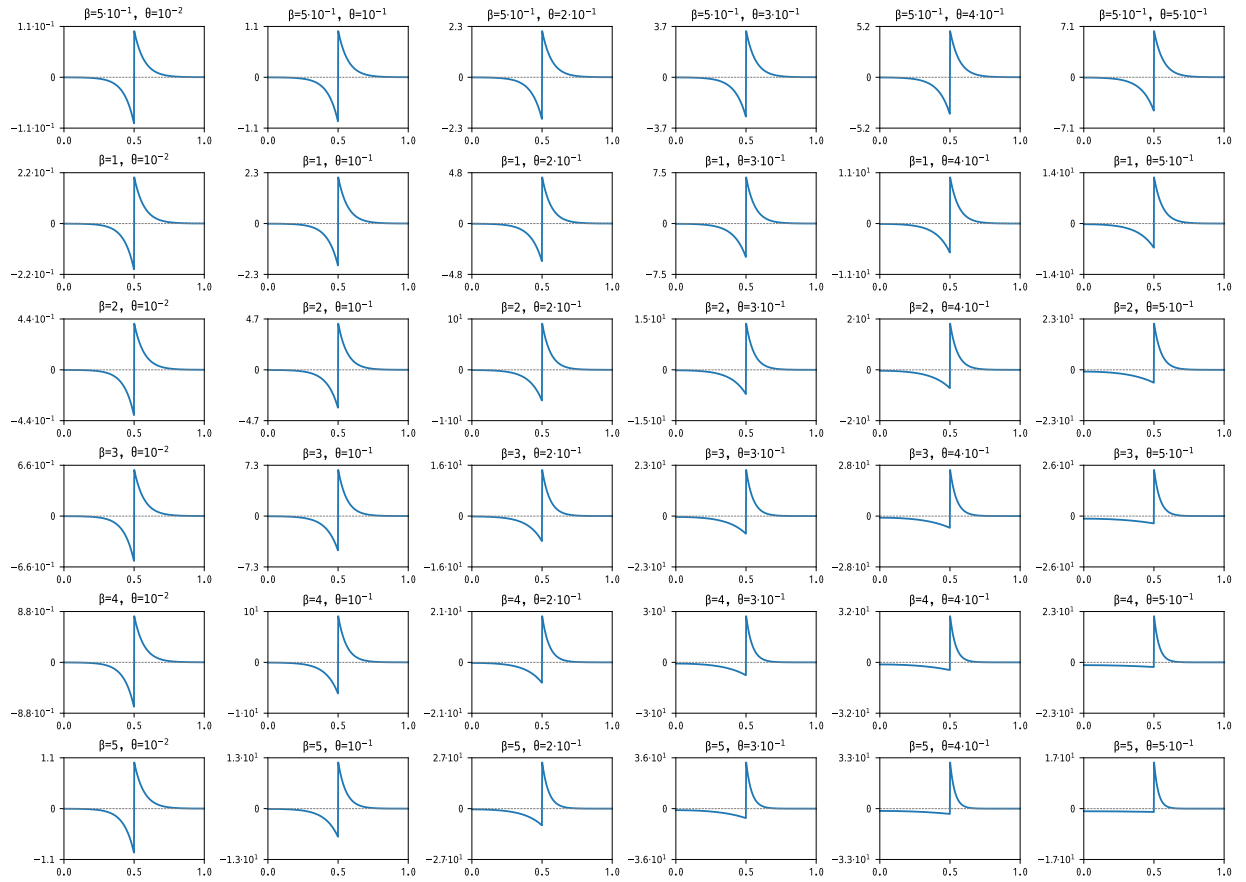


Figure 16: φ for Heaviside profile, as a function of β and θ_g ($d = 1$, $\rho = 100$).

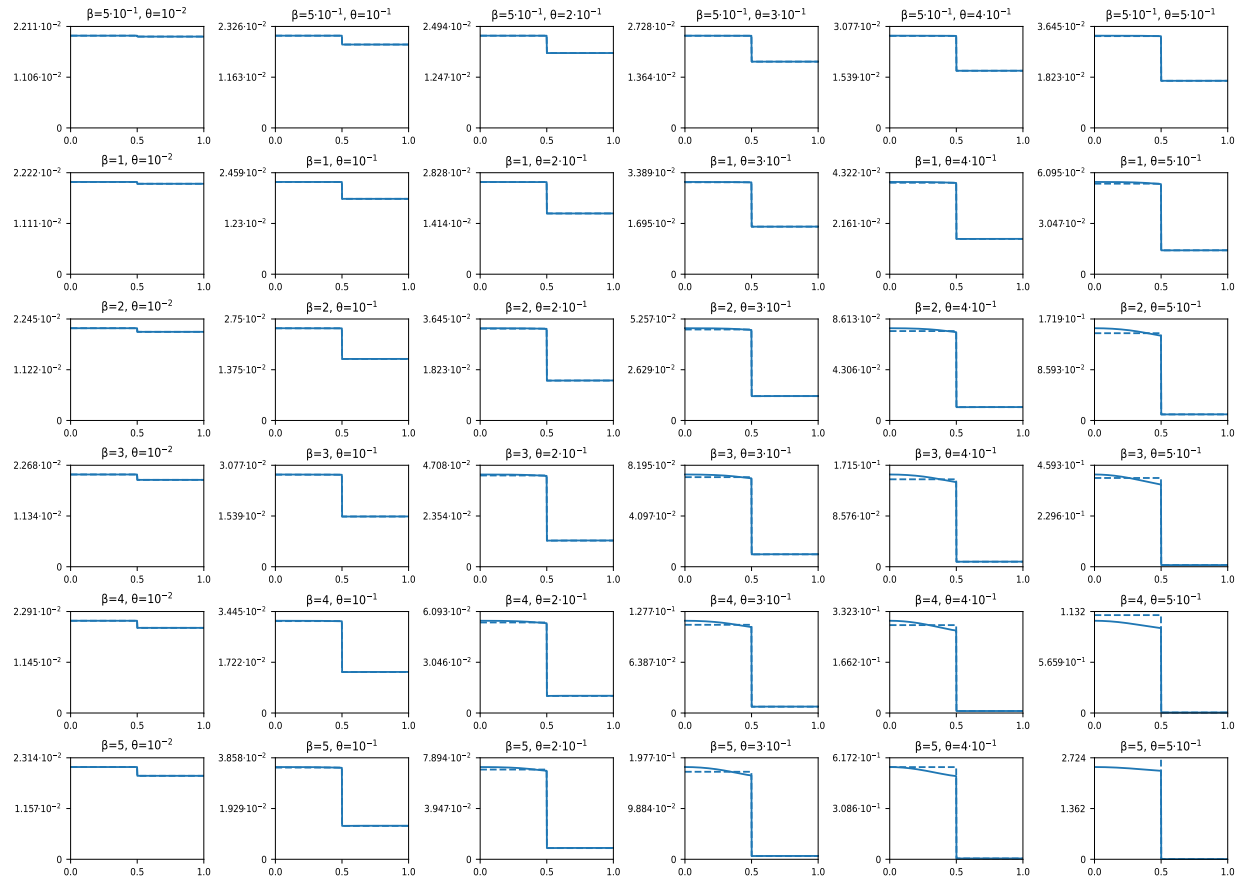


Figure 17: R_{tot} for Heaviside profile, as a function of β and θ_g ($d = 1$, $\rho = 100$).

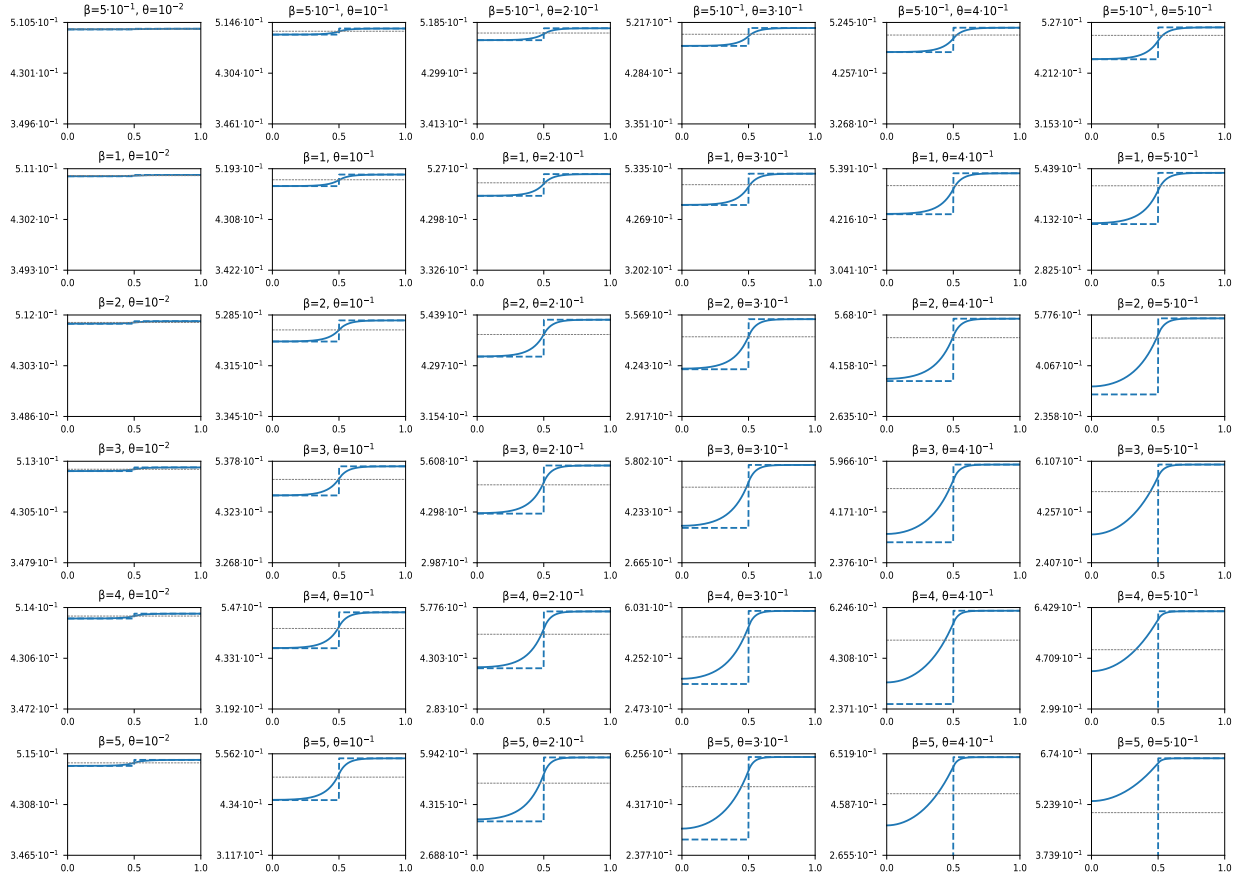


Figure 18: u_2 for Heaviside profile, as a function of β and θ_g ($d = 1$, $\rho = 100$).

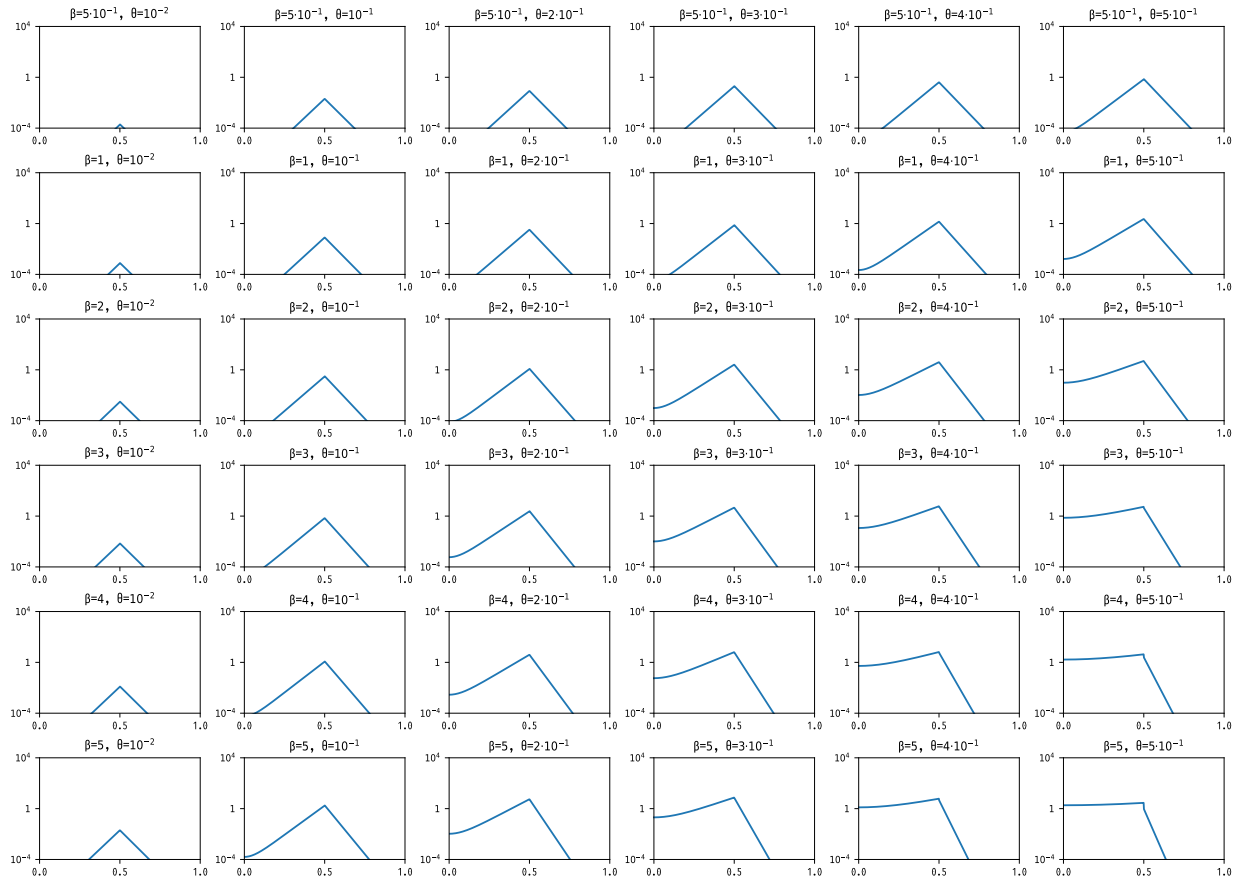


Figure 19: σ_r for Heaviside profile, as a function of β and θ_g ($d = 1$, $\rho = 100$).

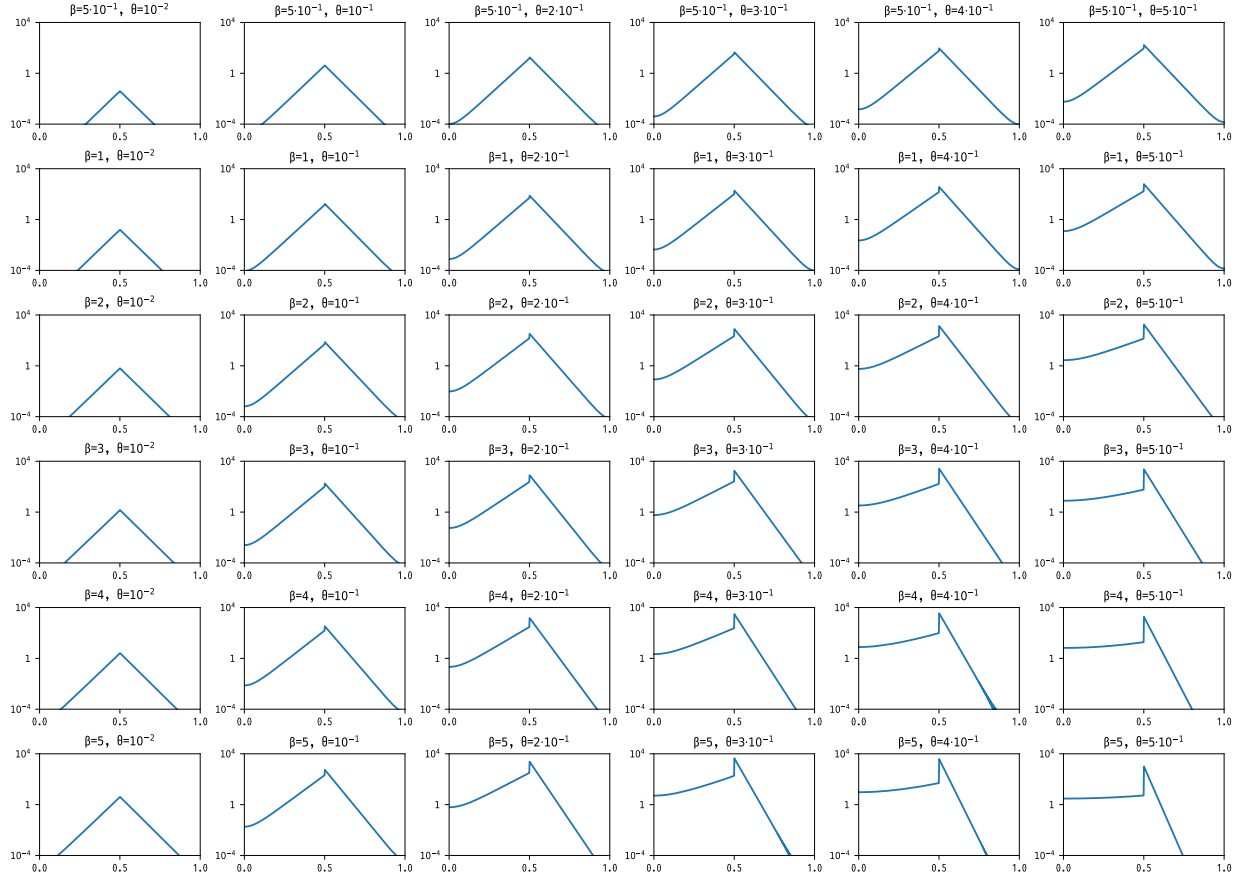


Figure 20: σ_d for Heaviside profile, as a function of β and θ_g ($d = 1$, $\rho = 100$).

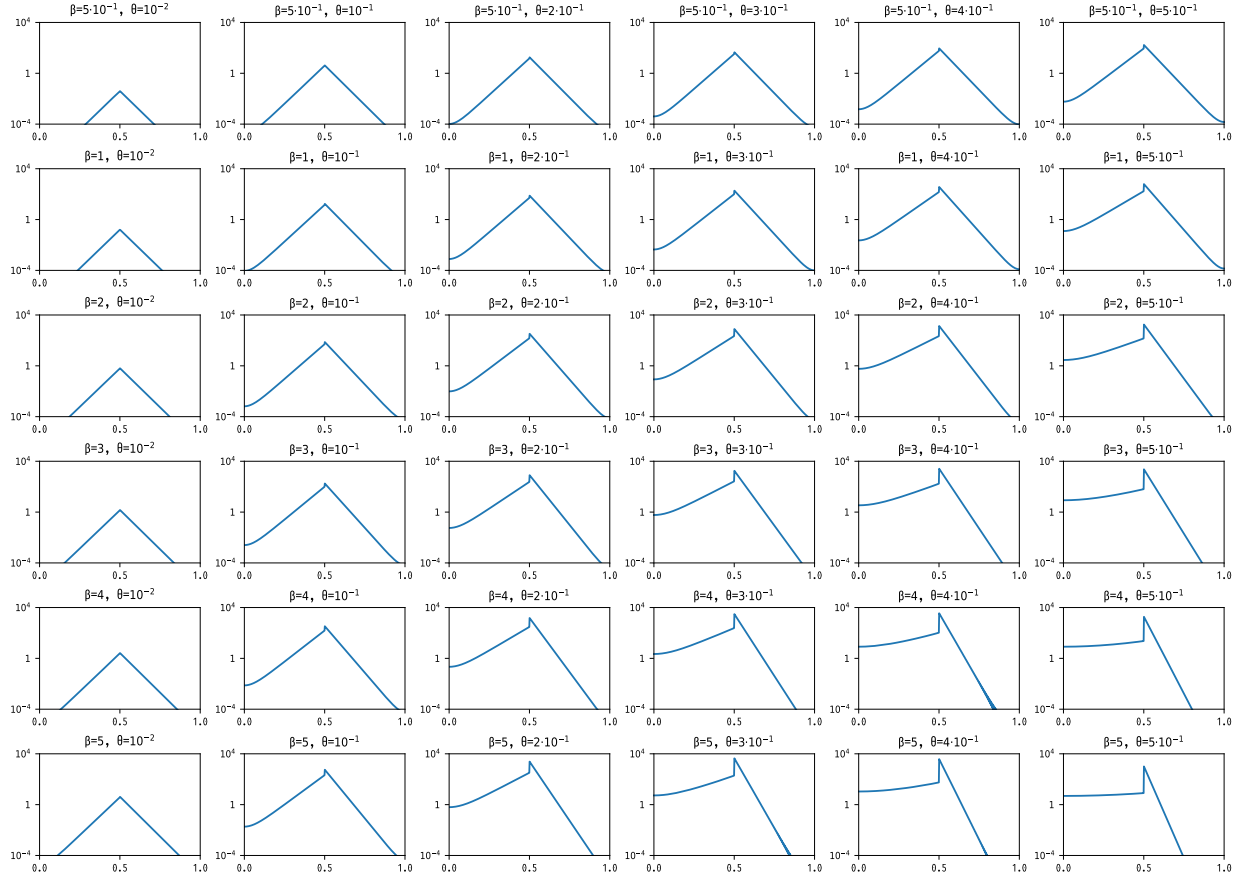


Figure 21: σ_{tot} for Heaviside profile, as a function of β and θ_g ($d = 1$, $\rho = 100$).

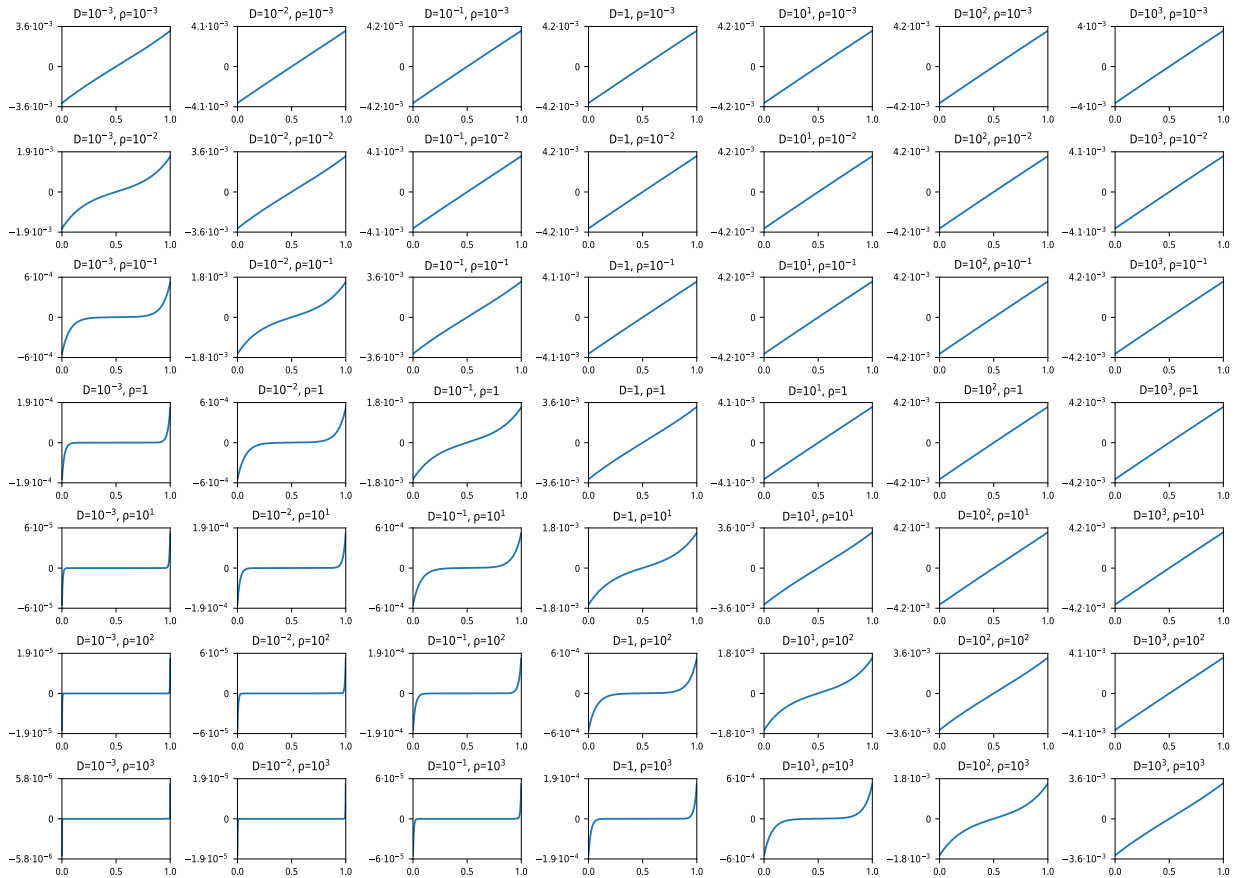


Figure 22: α for Linear profile, low θ_g value ($\beta = 1$, $\theta_g = 0.01$).

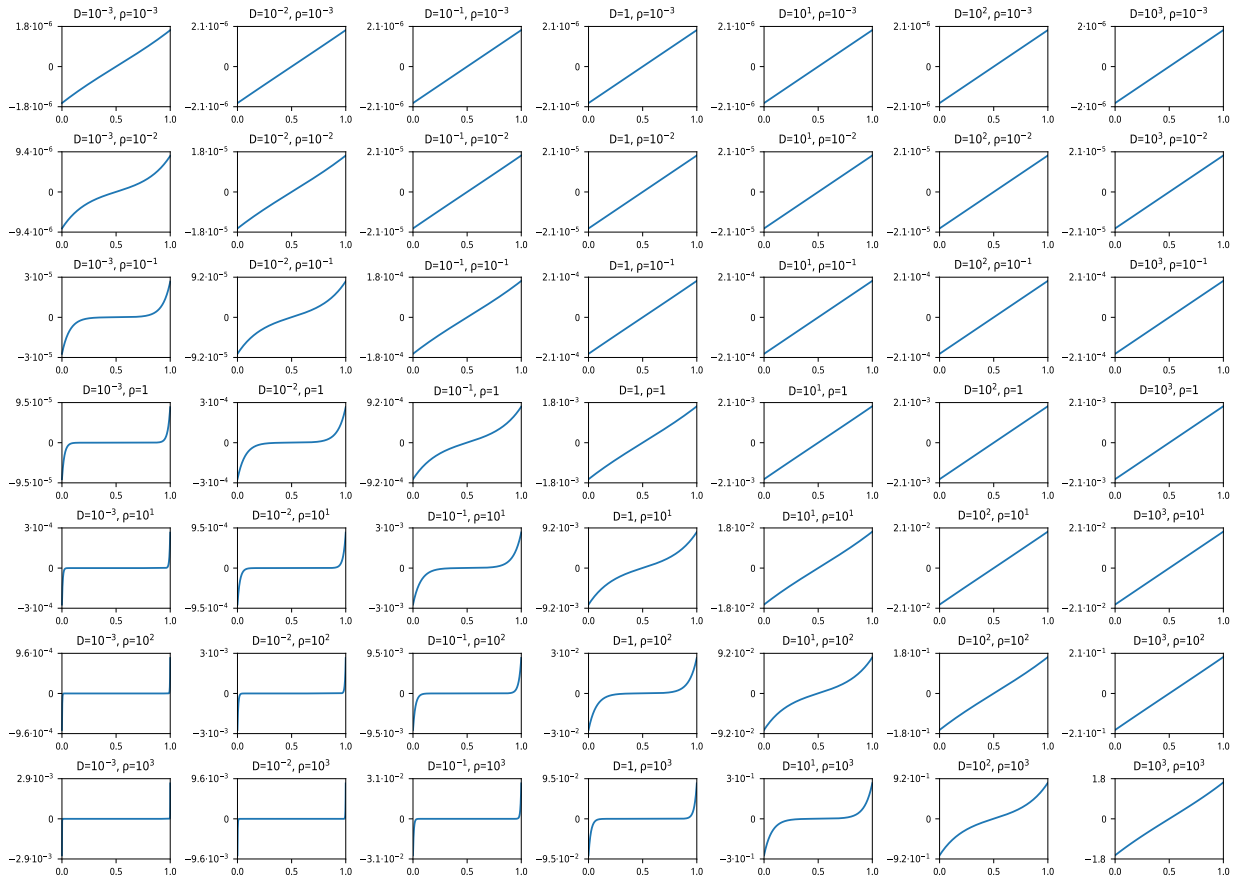


Figure 23: φ for Linear profile, low θ_g value ($\beta = 1$, $\theta_g = 0.01$).

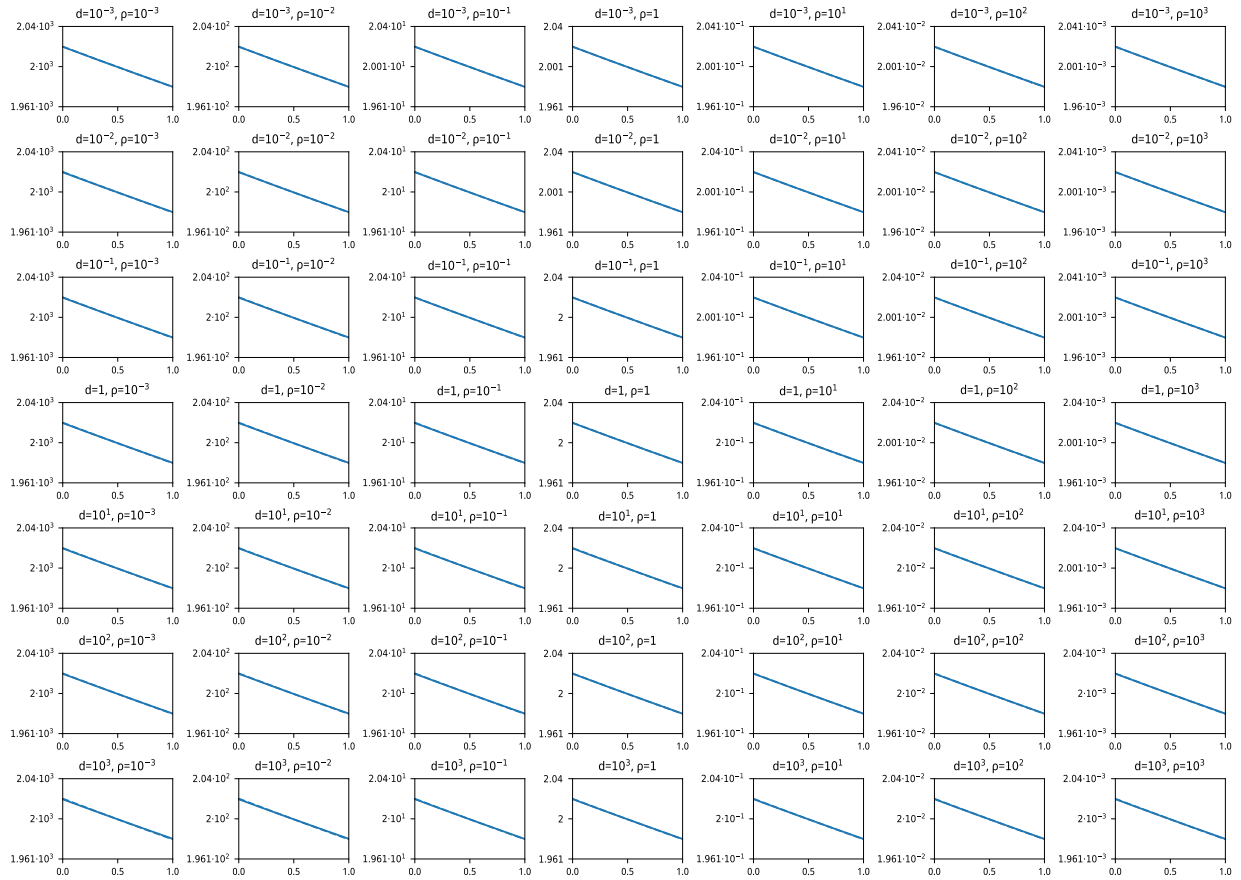


Figure 24: R_{tot} for Linear profile, low θ_g value ($\beta = 1, \theta_g = 0.01$).

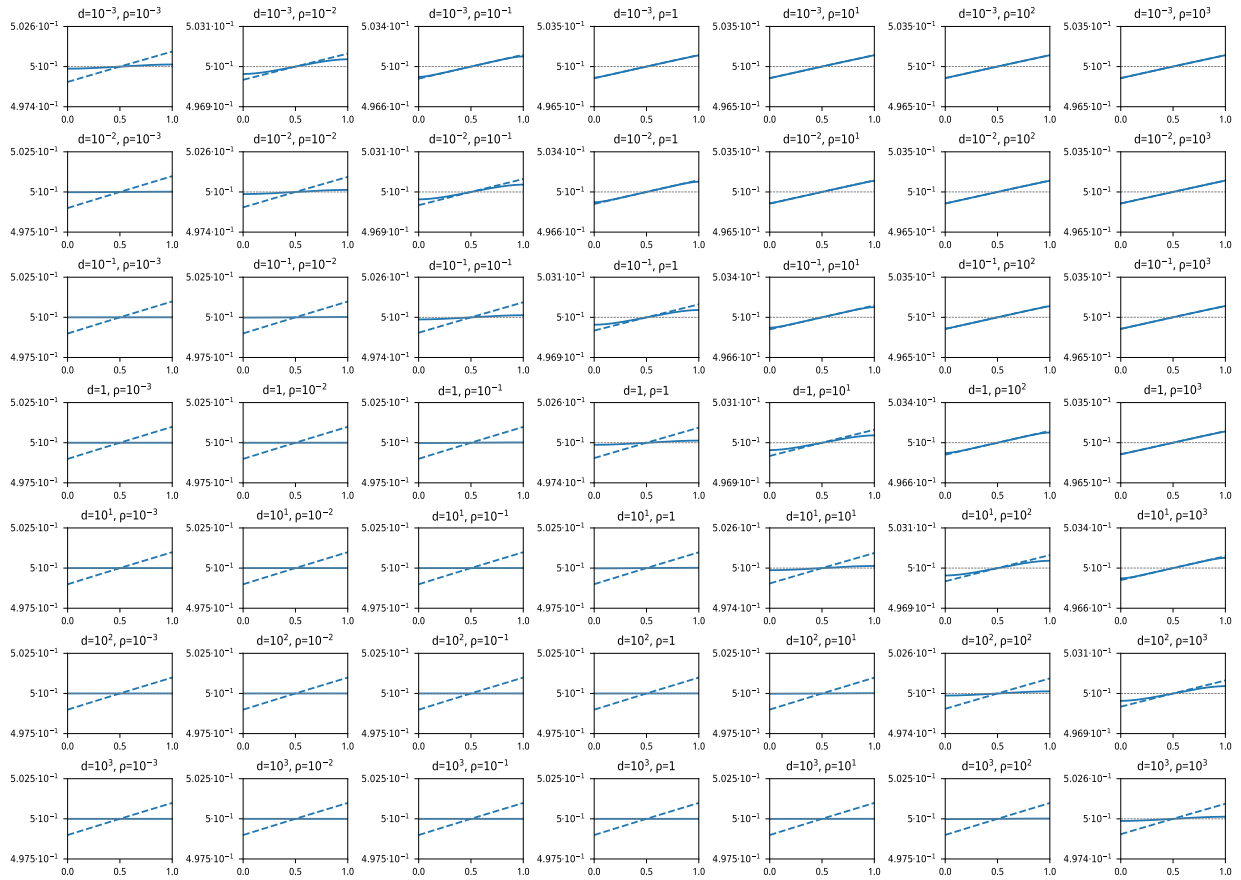


Figure 25: u_2 for Linear profile, low θ_g value ($\beta = 1, \theta_g = 0.01$).

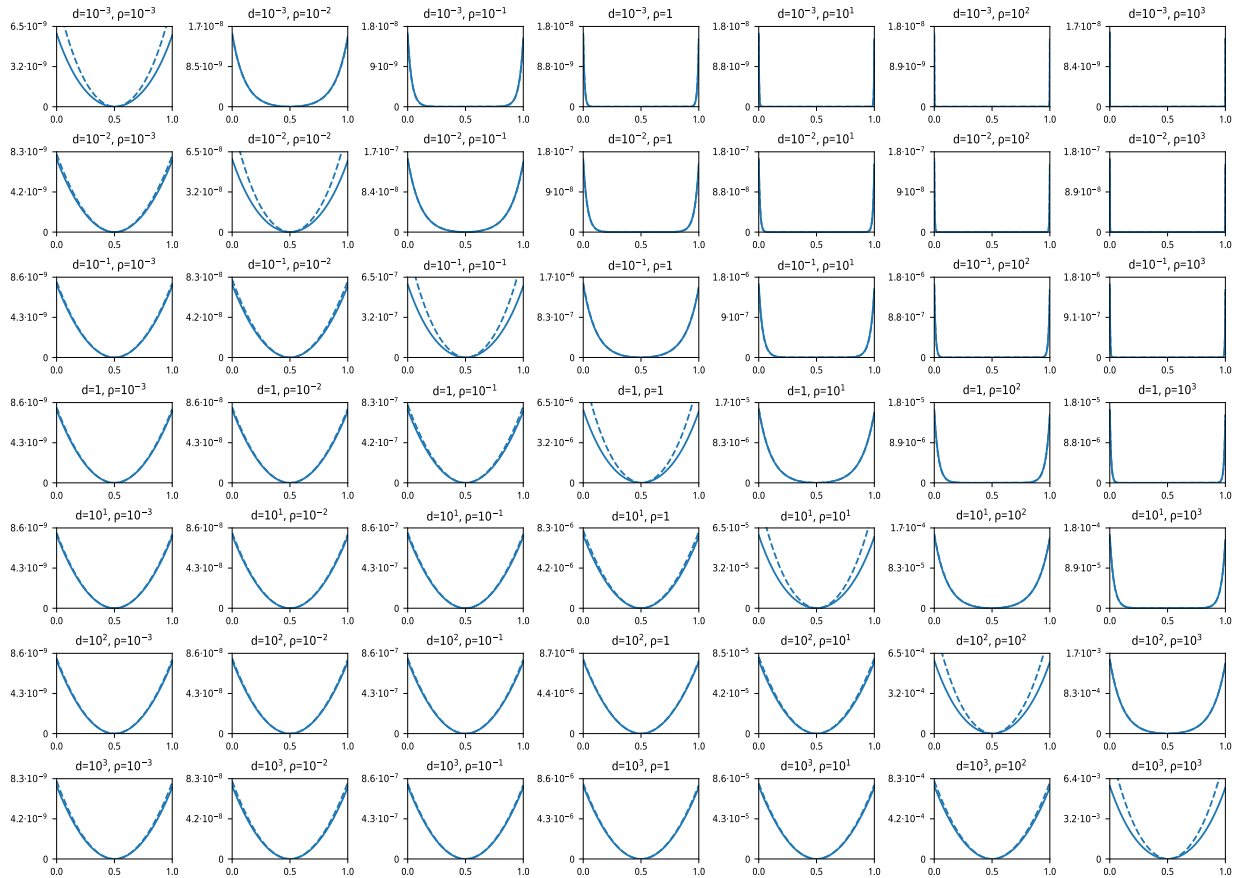


Figure 26: σ_r for Linear profile, low θ_g value ($\beta = 1$, $\theta_g = 0.01$).

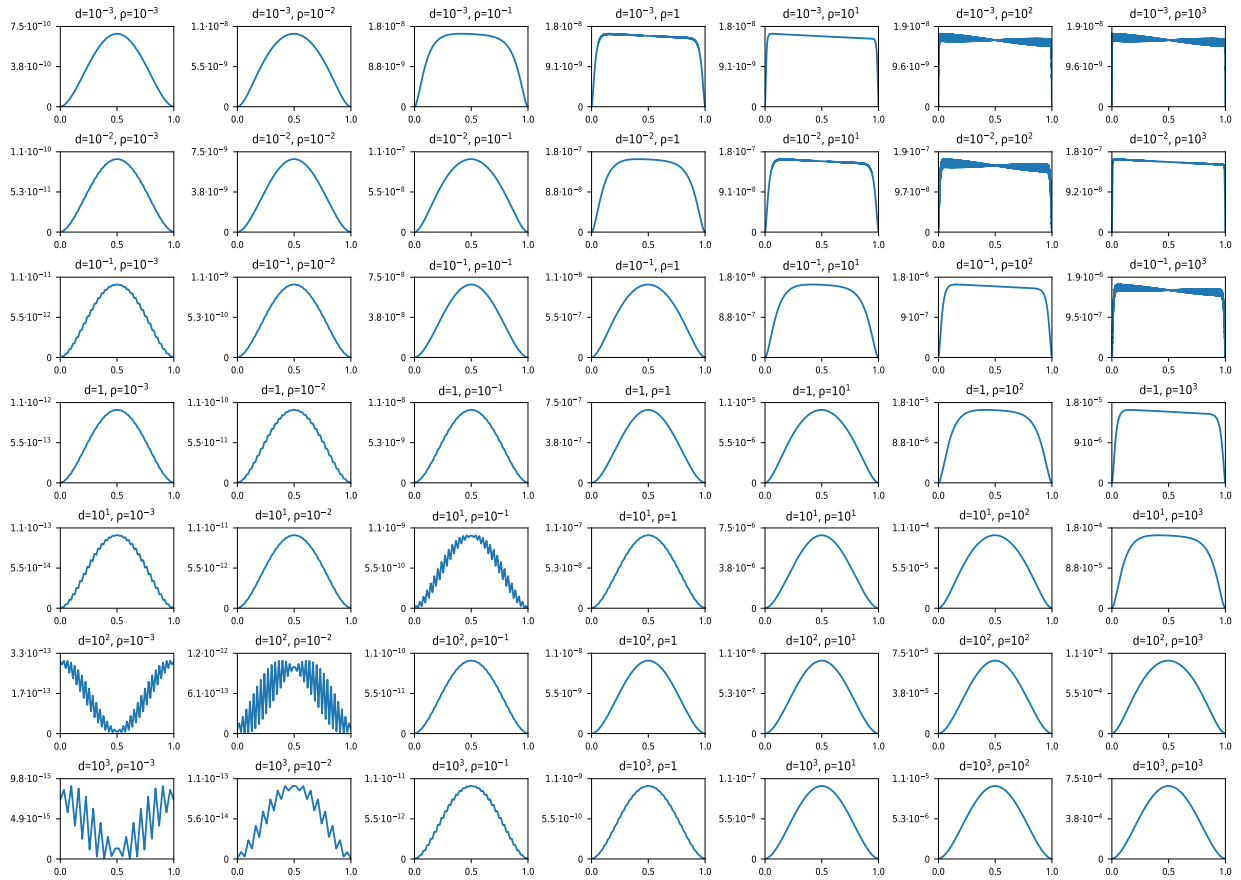


Figure 27: σ_d for Linear profile, low θ_g value ($\beta = 1, \theta_g = 0.01$).

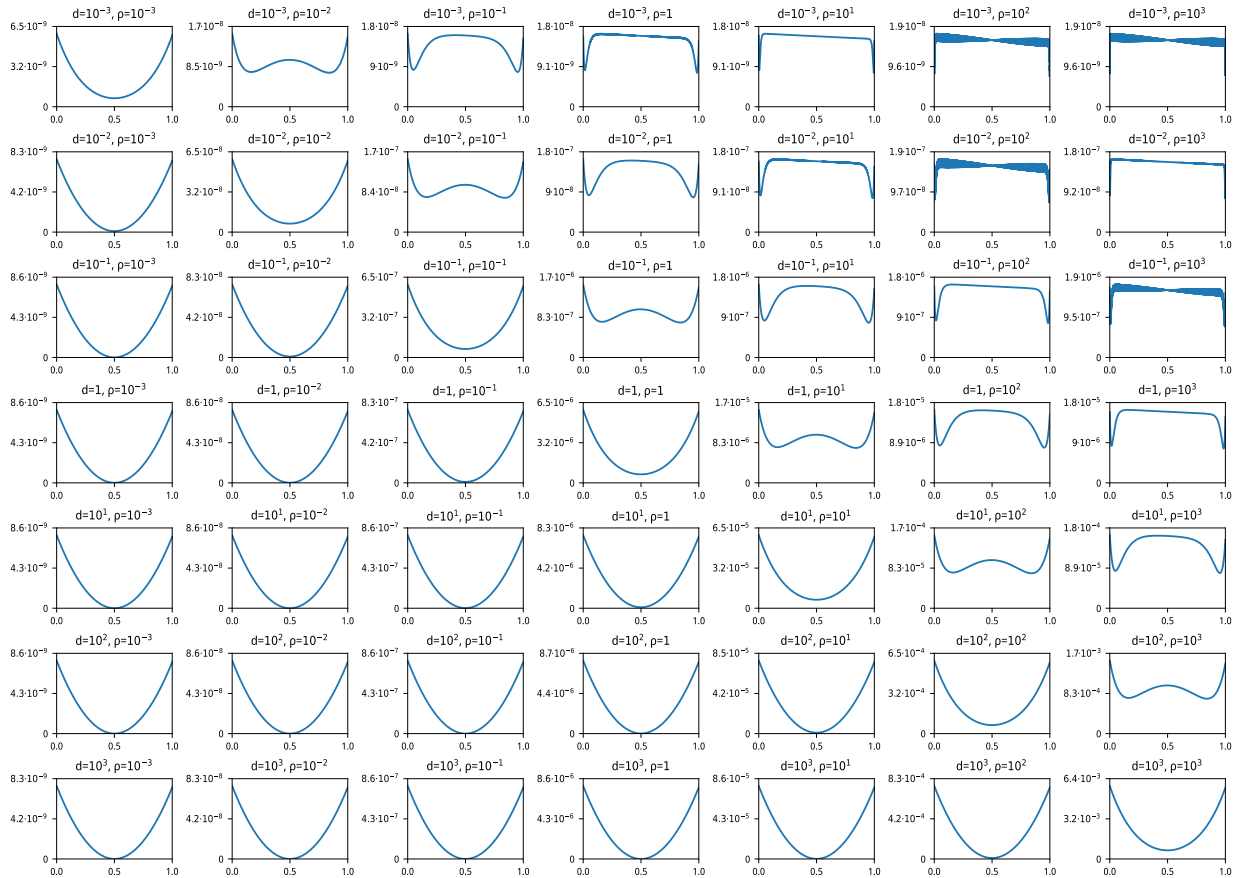


Figure 28: σ_{tot} for Linear profile, low θ_g value ($\beta = 1$, $\theta_g = 0.01$).

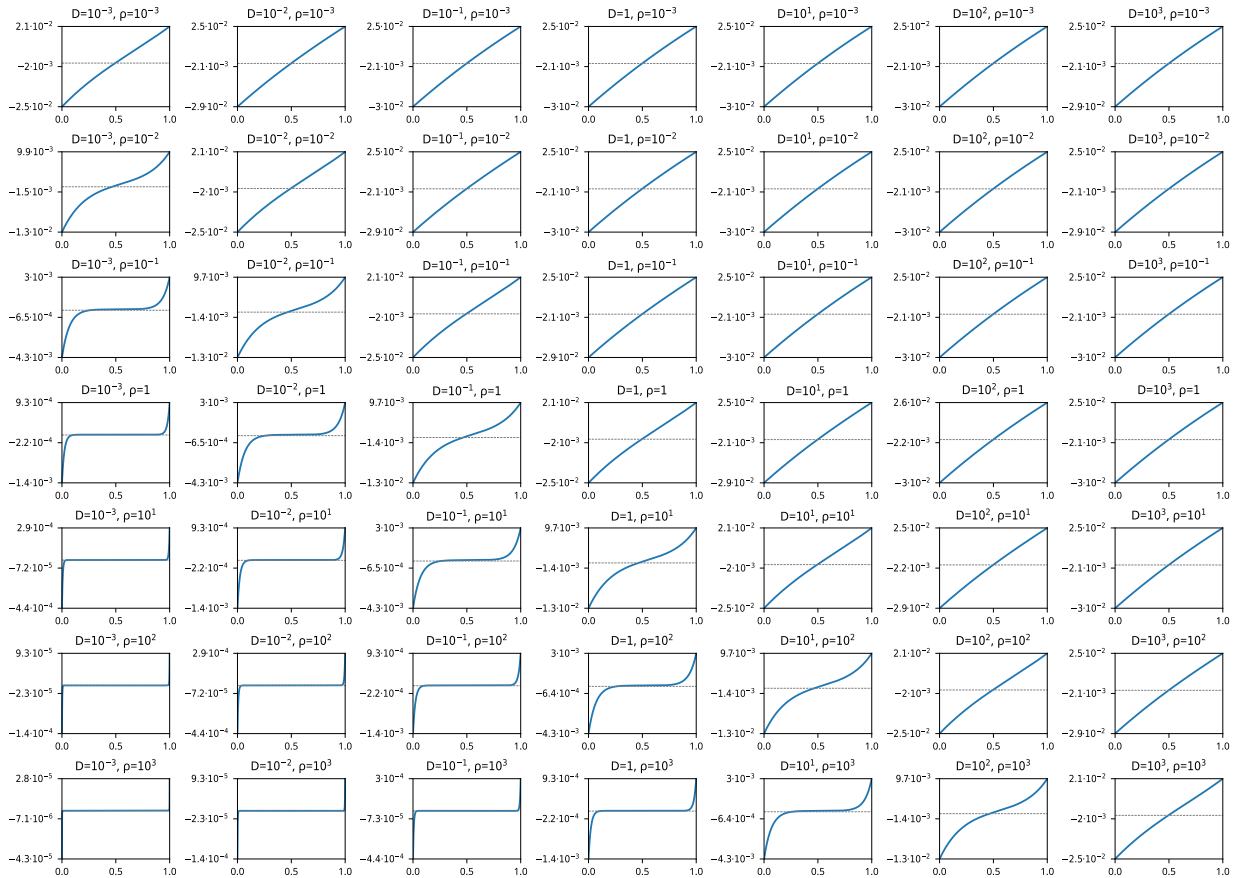


Figure 29: α for Linear profile, high θ_g value ($\beta = 1$, $\theta_g = 0.1$).

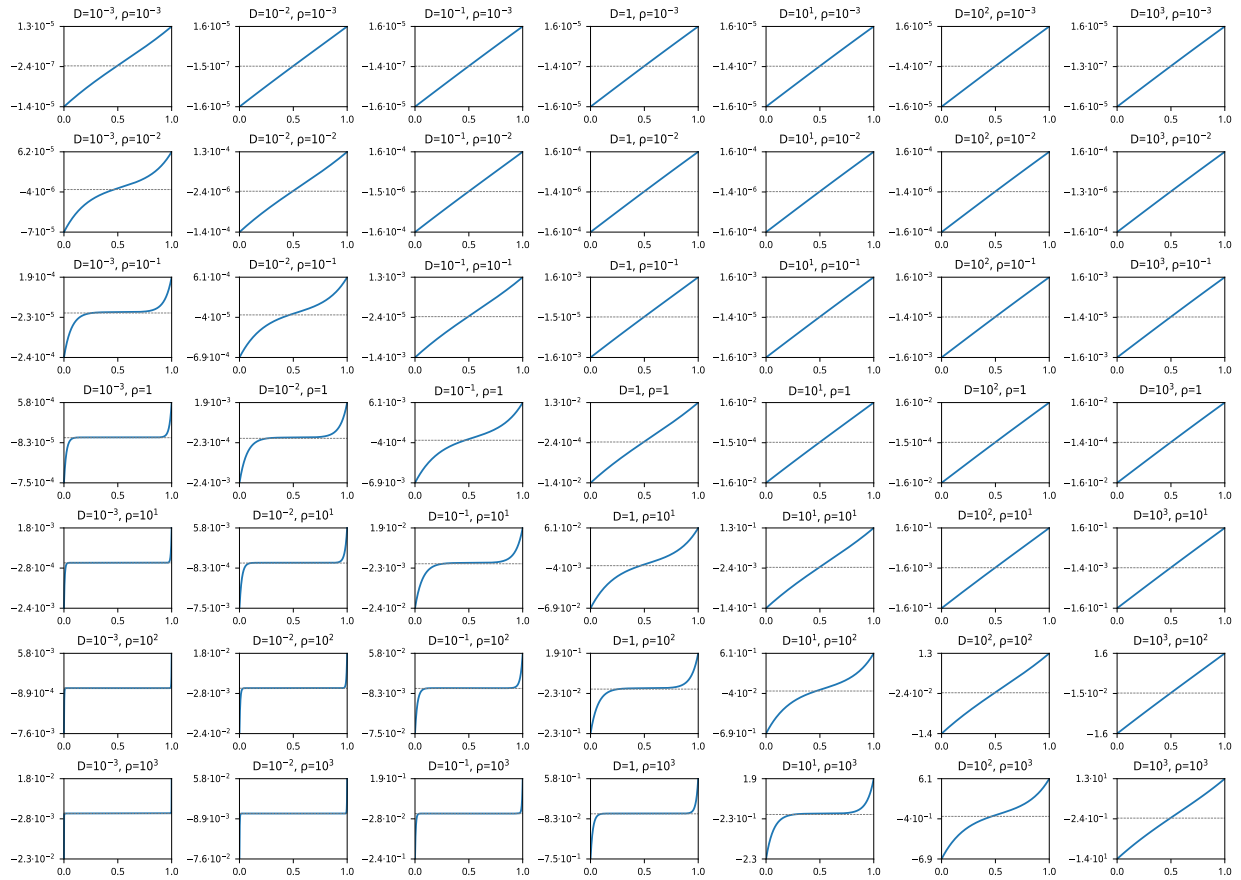


Figure 30: φ for Linear profile, high θ_g value ($\beta = 1$, $\theta_g = 0.1$).

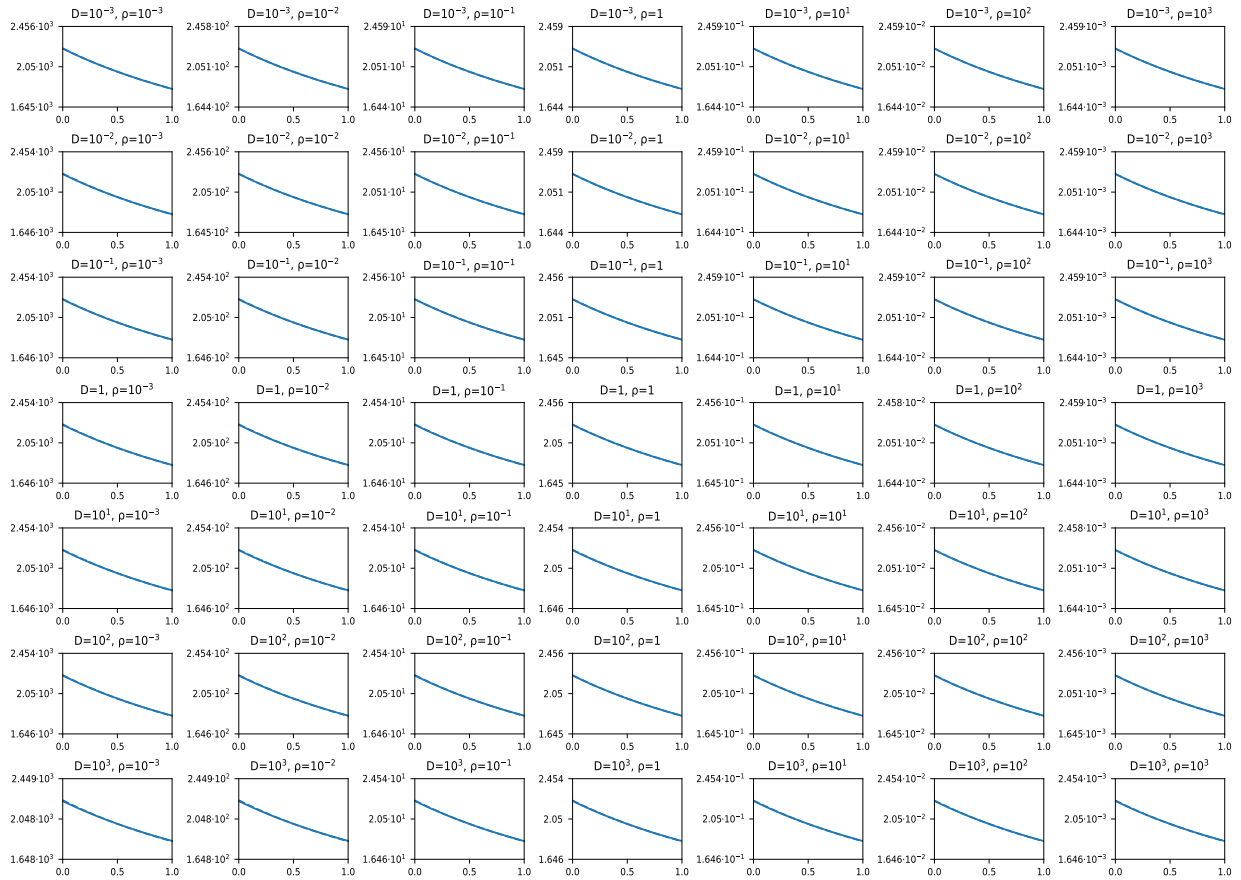


Figure 31: R_{tot} for Linear profile, high θ_g value ($\beta = 1, \theta_g = 0.1$).

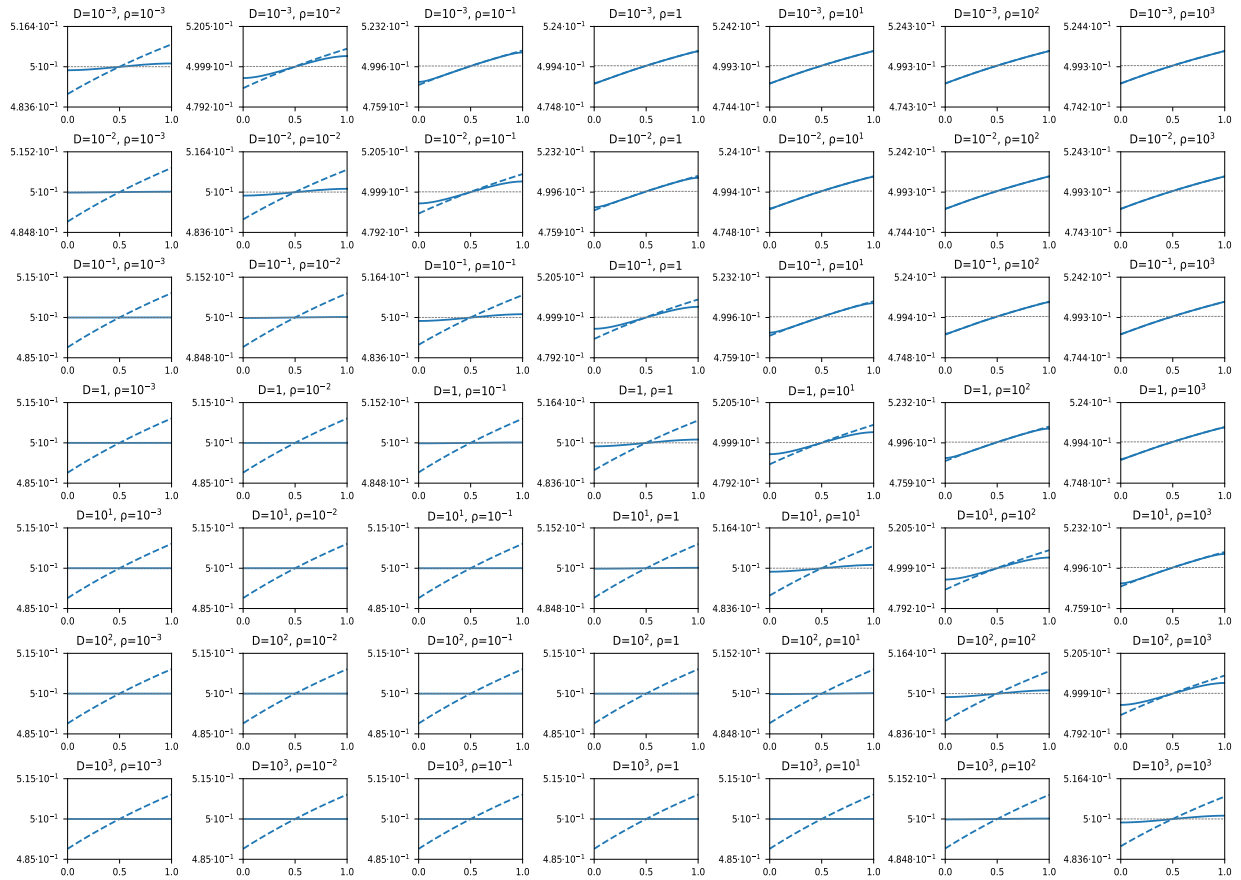


Figure 32: u_2 for Linear profile, high θ_g value ($\beta = 1$, $\theta_g = 0.1$).

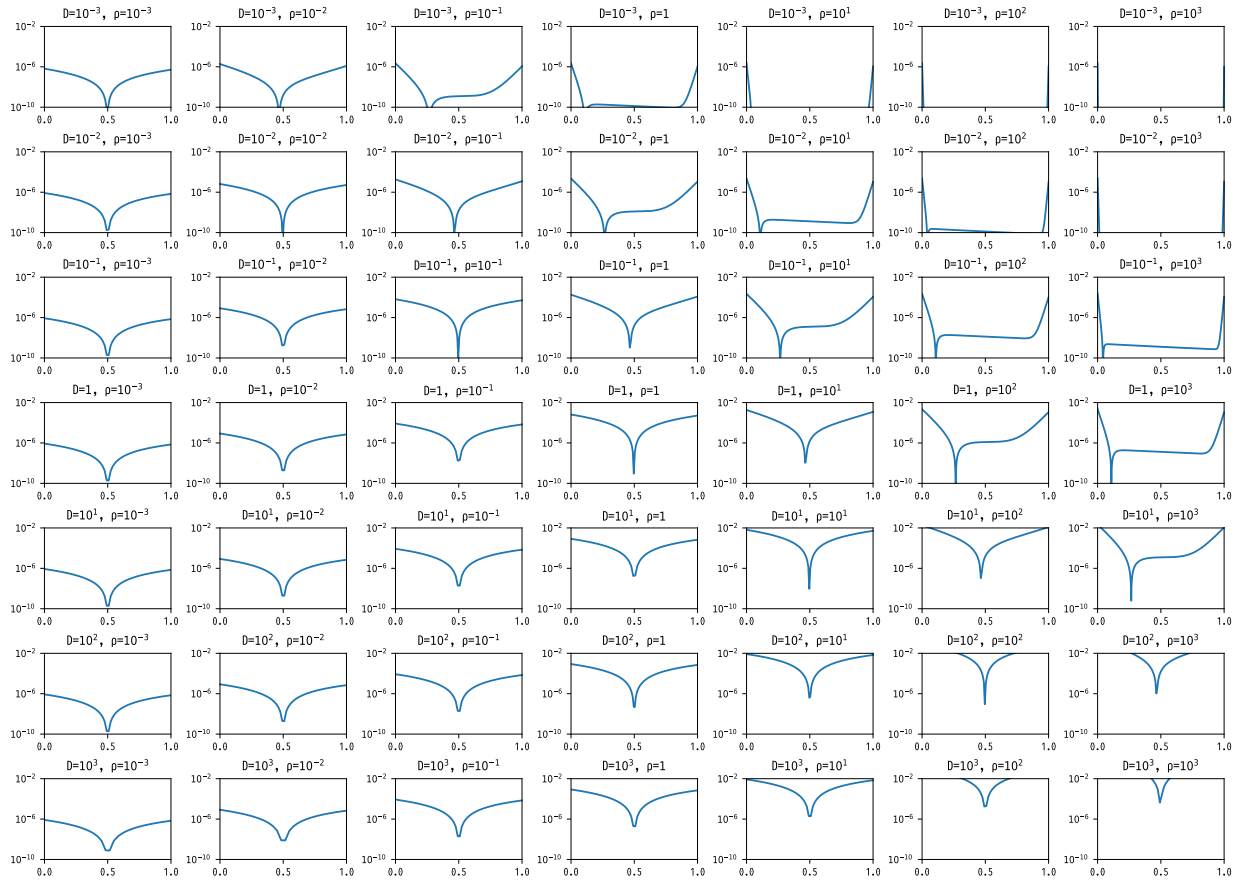


Figure 33: σ_r for Linear profile, high θ_g value ($\beta = 1$, $\theta_g = 0.1$).

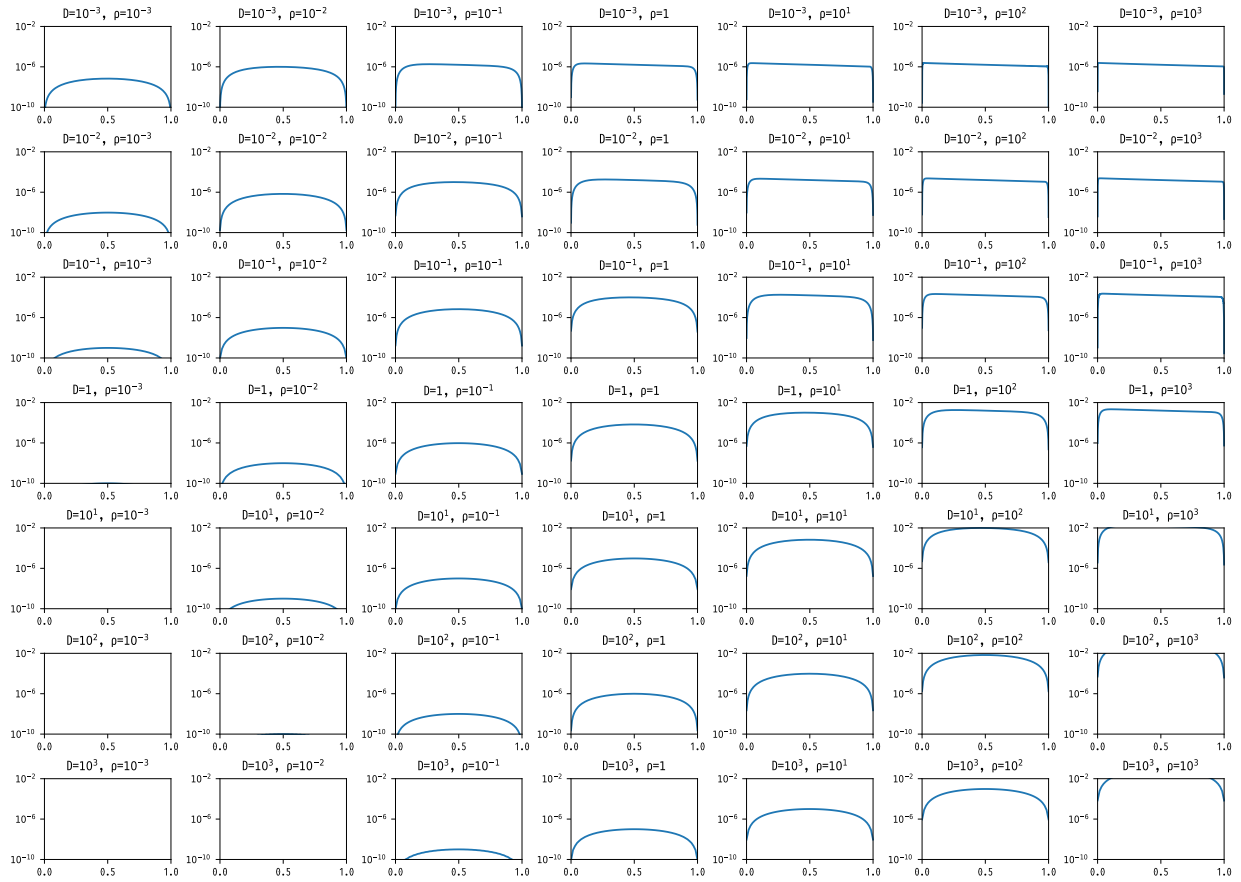


Figure 34: σ_d for Linear profile, high θ_g value ($\beta = 1$, $\theta_g = 0.1$).

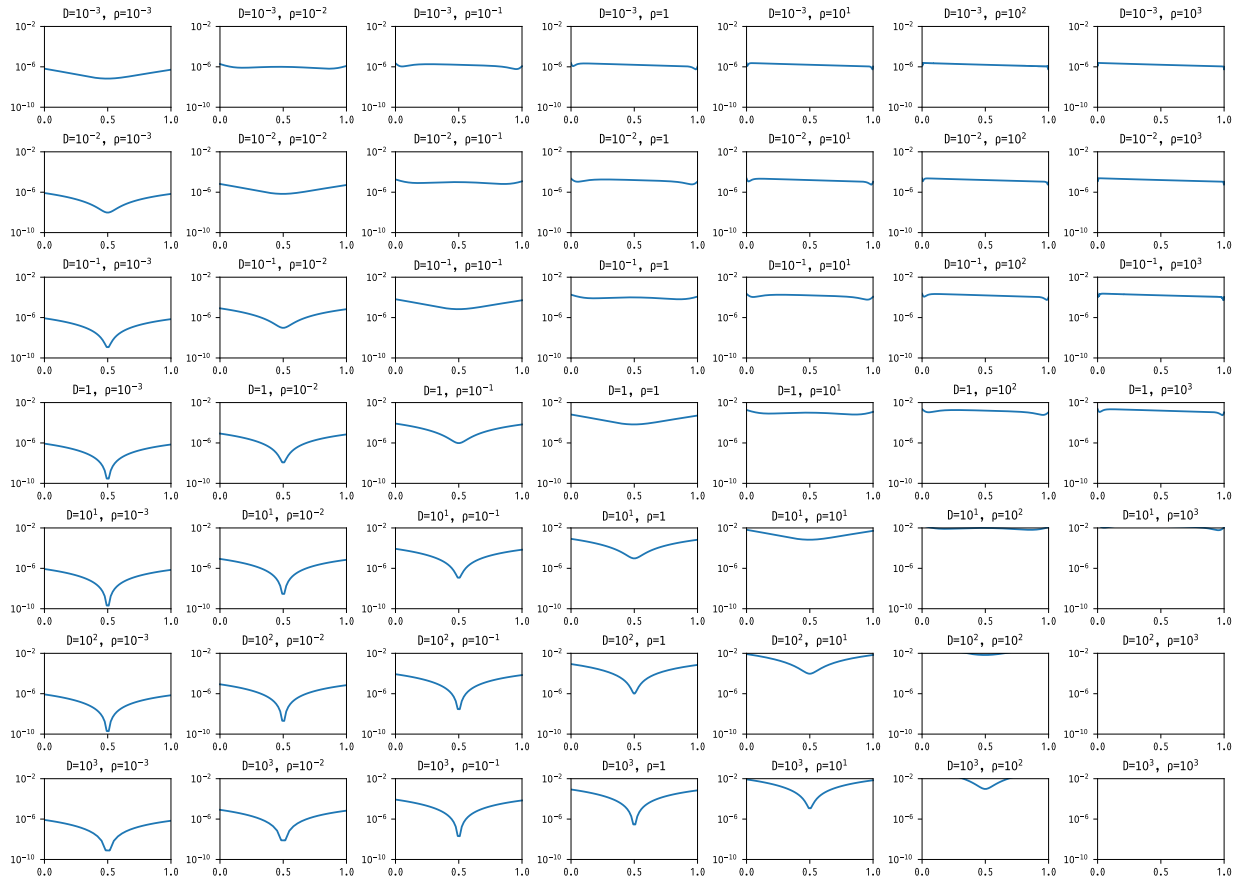


Figure 35: σ_{tot} for Linear profile, high θ_g value ($\beta = 1, \theta_g = 0.1$).

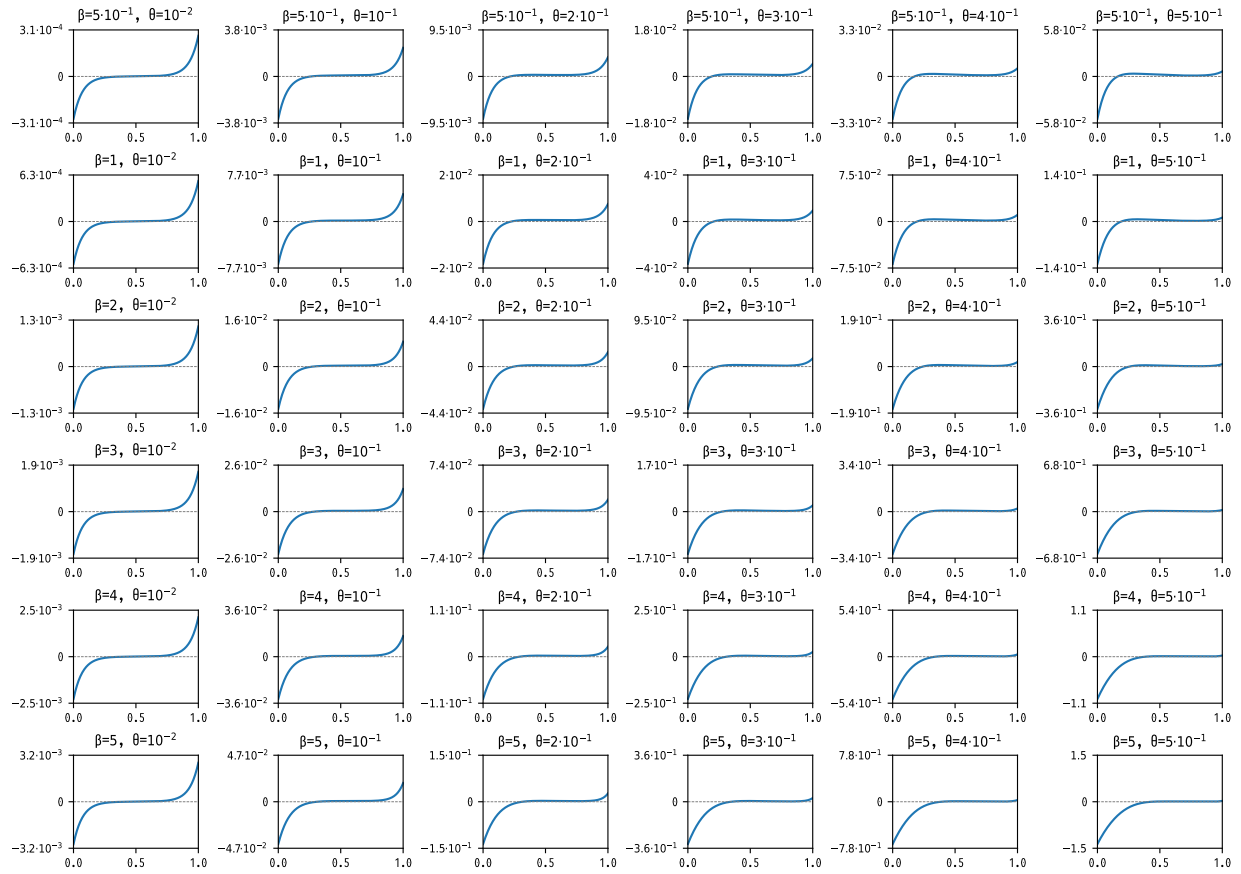


Figure 36: α for Linear profile, as a function of β and θ_g ($d = 1$, $\rho = 100$).

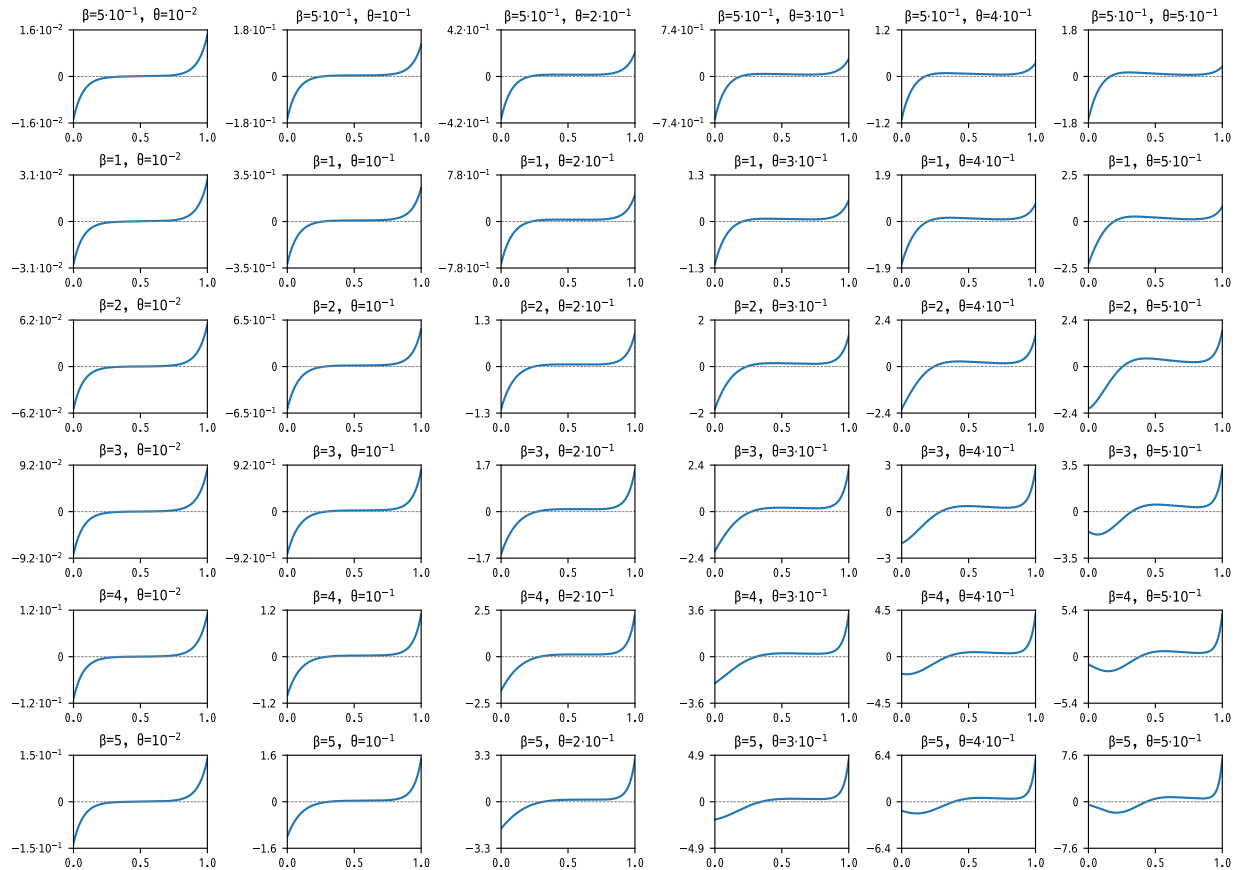


Figure 37: φ for Linear profile, as a function of β and θ_g ($d = 1$, $\rho = 100$).

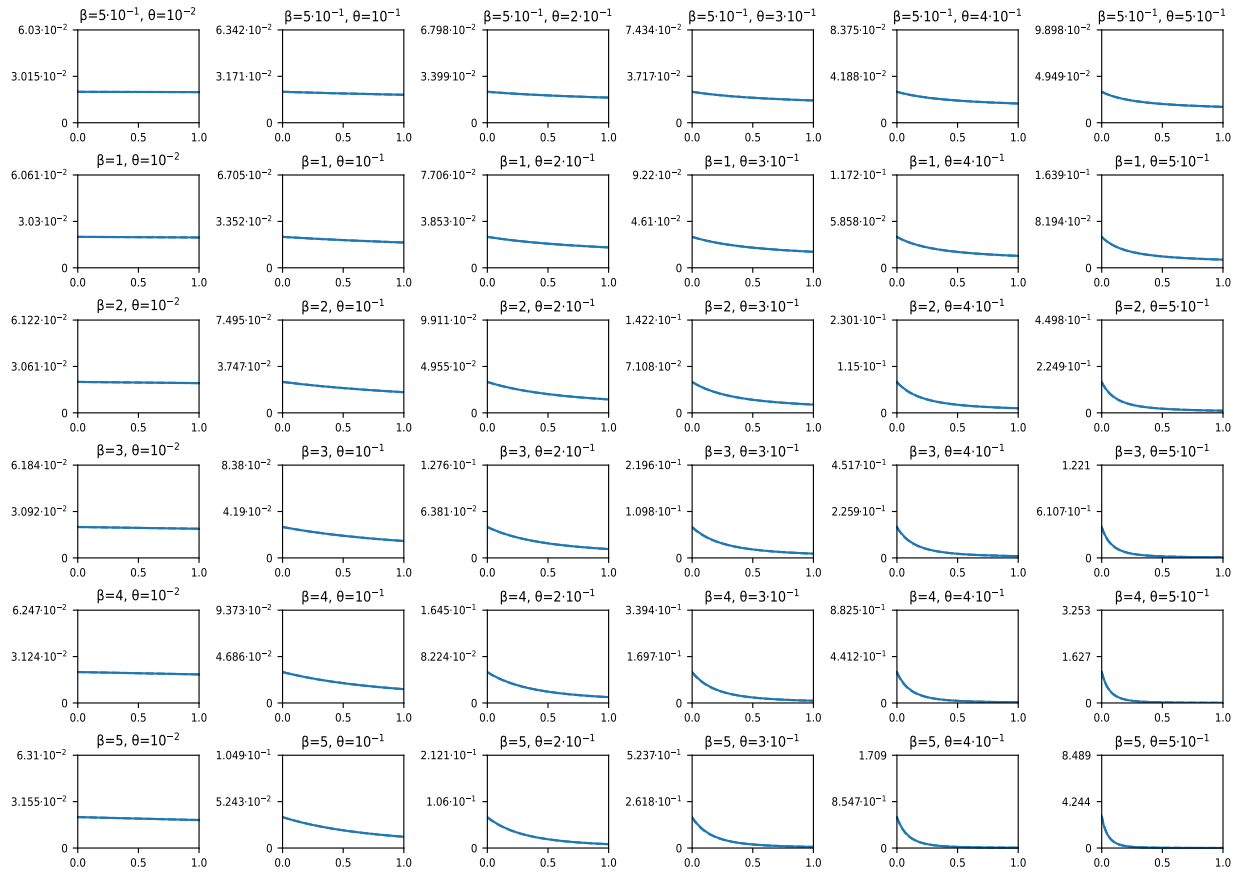


Figure 38: R_{tot} for Linear profile, as a function of β and θ_g ($d = 1$, $\rho = 100$).

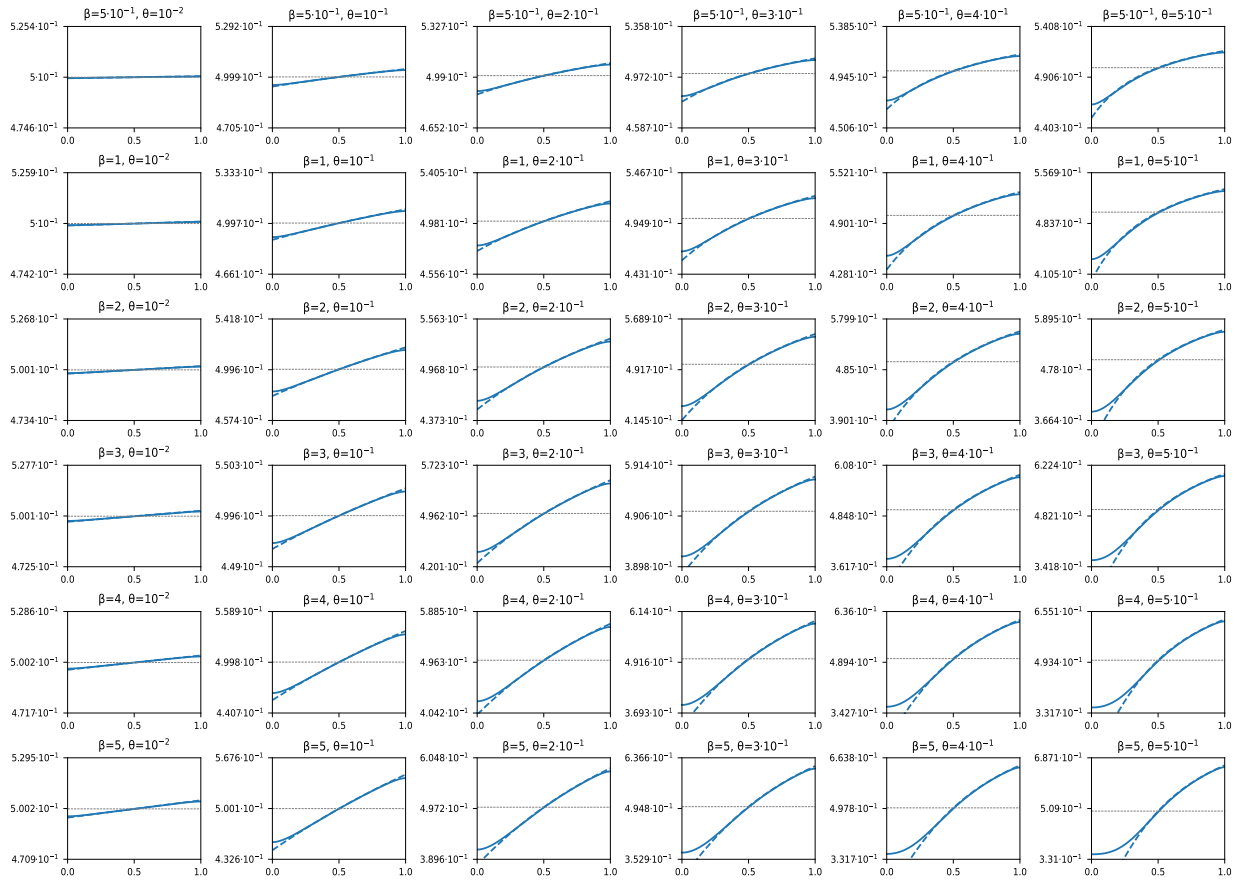


Figure 39: u_2 for Linear profile, as a function of β and θ_g ($d = 1$, $\rho = 100$).

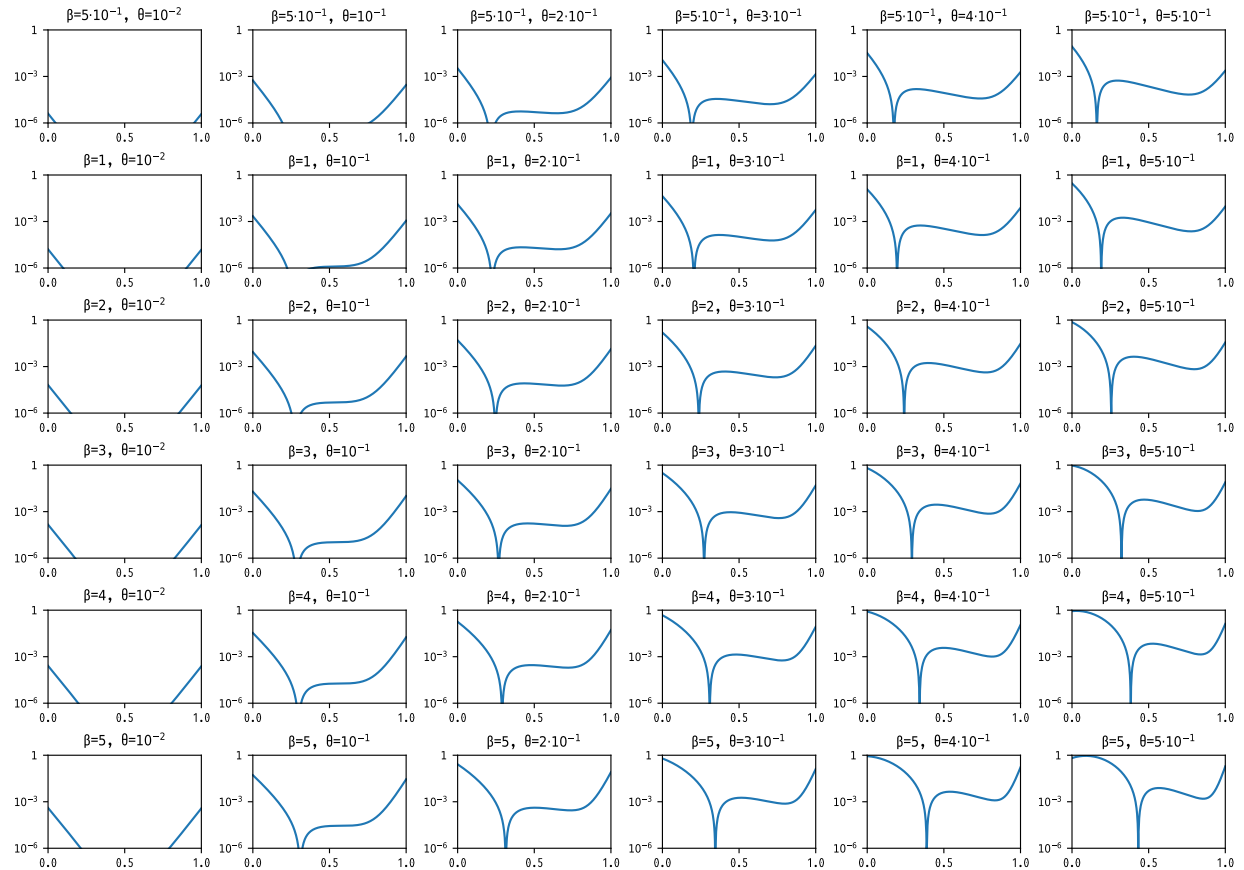


Figure 40: σ_r for Linear profile, as a function of β and θ_g ($d = 1$, $\rho = 100$).

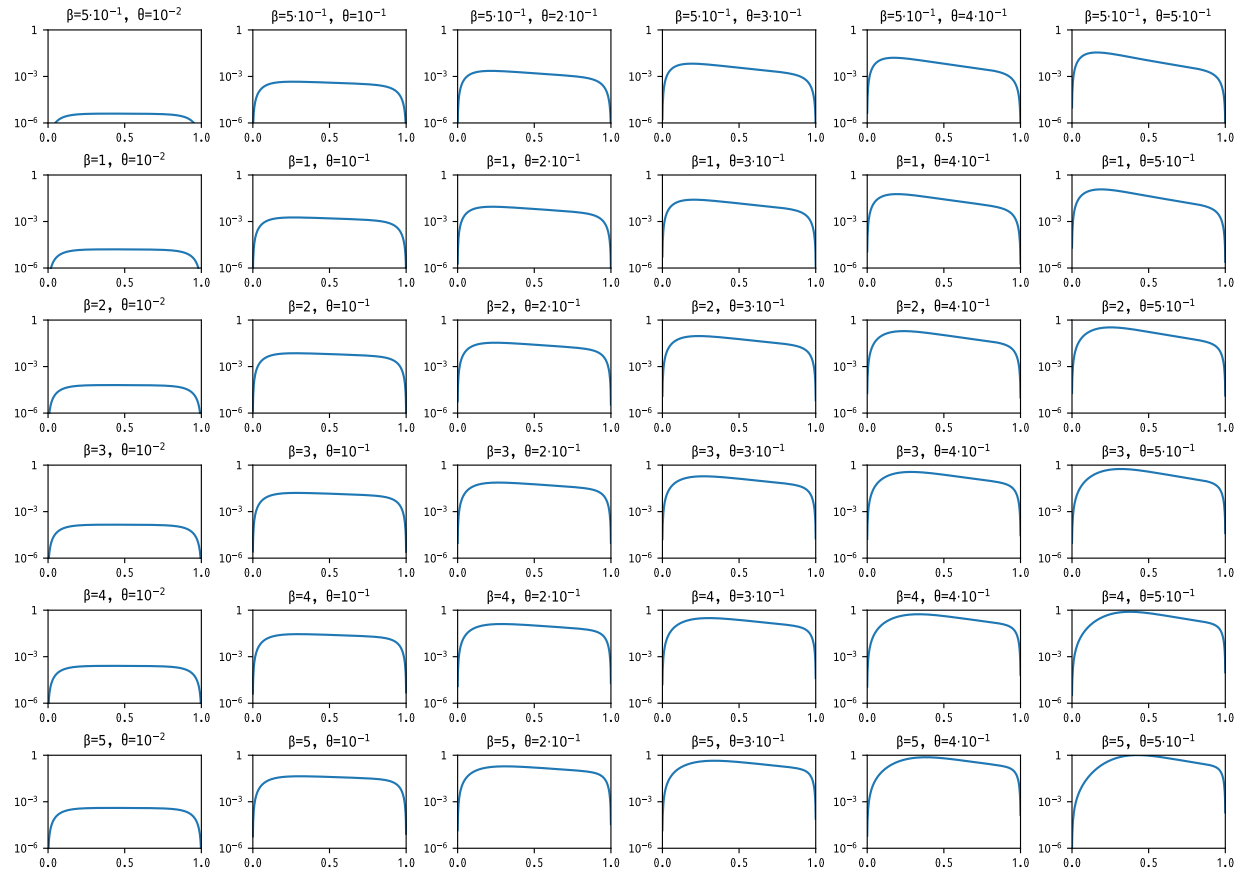


Figure 41: σ_d for Linear profile, as a function of β and θ_g ($d = 1$, $\rho = 100$).

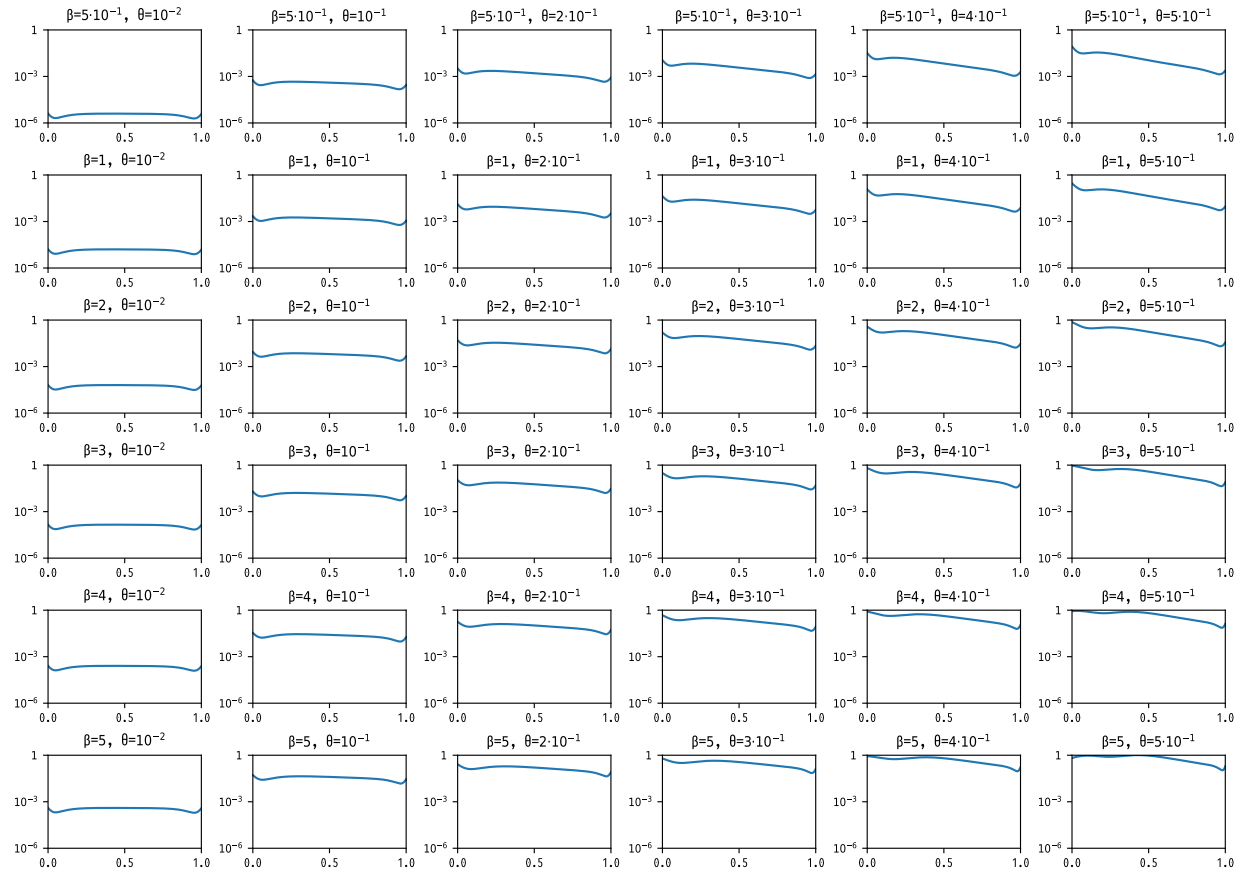


Figure 42: σ_{tot} for Linear profile, as a function of β and θ_g ($d = 1$, $\rho = 100$).